

Structural plasticity of Synaptic Connectivity in the Adult Central Nervous System

Inauguraldissertation

zur

Erlangung der Würde eines Doktors der Philosophie

vorgelegt der

Philosophisch-Naturwissenschaftlichen Fakultät

der Universität Basel

von

Ivan Galimberti

aus Ascona / TI

Basel, 2008

Genehmigt von der Philosophisch-Naturwissenschaftlichen Fakultät
auf Antrag von:

Prof. Dr. Pico Caroni
(Dissertationsleitung)

Prof. Dr. Silvia Arber
(Korreferentin)

Dr. Thomas Oertner
(Externer Experte)

Prof. Dr. Andreas Luthi
(Vorsitz)

Basel, den 22. April 2008

Prof. Dr. Hans-Peter Hauri
(Dekan)

*To my mother
Savina*

TABEL OF CONTENTS	Page
<i>Akwnoledgements</i>	5
<i>Abbreviations</i>	6
1. INTRODUCTION	7
Overview	7
1.1 Synapse formation	8
Target specification	8
Synapse specification	9
Synapse maturation	10
Synapse elimination	10
Synapse stabilization	
1.2 Structural plasticity of axon terminals in the adult	13
Axonal remodeling in the adult	13
Learning-dependent axonal rearrangements	16
Axonal remodeling and aging	17
1.3 The hippocampus: a model system to study learning-related structural plasticity	18
Basic circuits of the hippocampus	19
Hippocampal synaptic plasticity	20
Molecular and structural aspects of hippocampal LTP	21
The mossy fiber projection	22
2. RESULTS	24
2.1 Long-term rearrangements of hippocampal mossy fiber terminal connectivity in the adult regulated by experience	24
Summary	25
Introduction	25
Results	29
Discussion	52

2.2 Spatially predetermined structural plasticity of granule cell subtypes in the hippocampal mossy fiber projection	58
Summary	59
Introduction	59
Results	61
Discussion	75
3. GENERAL DISCUSSION	78
Overview	78
Remodeling of LMTs	78
Regulation of LMT remodeling	79
Hippocampal microcircuits	80
4. MATERIALS AND METHODS	82
Mice and reagents	82
Slice cultures	82
Imaging	83
Immunocytochemistry and histology	84
Analysis of imaging data	84
Electrophysiology	86
Protocols	87
Preparation of organotypic hippocampal slice cultures for long-term live imaging	88
Long-term live imaging of neuronal circuits in organotypic hippocampal slice cultures	105
Staining protocol for organotypic hippocampal slice cultures	115
5. REFERENCES	126
<i>Curriculum vitae</i>	143
<i>Erklärung</i>	147

Acknowledgements

I would like to thank Pico Caroni! You gave me the opportunity to explore nature and to become passionate from neuroscience. You taught and helped me all the time using your intellectual talent. We hoped, wondered, discussed and learned how a little region of the brain is incredibly organized. I will always remember that Friday afternoon when we looked the first mossy fiber projection together..that was the beginning of our great teamwork. Grazie di tutto Pico!

A special thank is for Nadine Gogolla! I enjoyed a lot to work with you. We discovered exiting data and helped each other all the time, this was really a great time! Your friendship helped me a lot to understand different things..as you know..Danke Nadine!

Thanks Yuichi for helping me in developing the project. GRAZIE SAMURAI!

Flavio. It was a pleasure to work with you. Our enthusiasm to explore new territories was a great common feeling...this was short, but intense. Forza Milan!

I would like to thank the members of my thesis committee, Silvia Arber and Thomas Oertner. You followed my PhD during these years and helped me to challenge my data with important observations. Thanks!

Thanks to Andreas Lüthi for participating to the oral exam.

I would like to thank all the other members of the lab that I meet during these 5 years and helped me in different issues:

Vincenzo for introducing me to the slice culture technick..

Alex for helping me in the interpretation of my data..

Lan for giving me very nice EM pictures that were so usefull..

Tami for helping me in the tissue culture room..

San for interesting experiments in slice cultures..

Sudip for different exiting discussions..

Stefan for having always the right antibody at the right moment..

Corinne for performing different PCR reactions..

Smita for being always ready to help me in any occasion..

Claudia for the super protocols of Turin..

Sarah for nice discussions and suggestions..

Kerstin for helping me in screening mice..

Ewa for helping in understanding slice cultures data..

Dominique for challenging me with many questions..

Mike for nice discussions..

Pu for interest comments on my data..

Thanks to the people of the imaging facility! Without your help my results were not be possible! Patrick, Thierry, Aaron, Laurent and Jens.

Grazie Cyril for helping me in different technical issues.

A special thank is to my family! Thanks for the support during these years, without your help this goal would not be possible. Danke Eva! Your love is part of everything..Grazie Tesoro!

Abbreviations

AMPA	α -amino-3-hydroxy-5-methyl-4-isoazolepropionic acid
AMPA-R	AMPA-receptor
BDNF	brain derived neurotrophic factor
CA	corpus ammonis (hippocampal region)
CAM	cell-adhesion molecule
αCaMKII	α calmodulin kinase II
CNS	central nervous system
DCX	doublecortin
DG	dentate gyrus (hippocampal region)
DIV	day in vitro
EE	enriched environment
EPB	<i>en-passant</i> bouton
EPSP-s	evoked postsynaptic potentiation spike
FGF	fibroblast growth factor
GABA	γ -amino butyric acid
GC	granule cell
LH	lateral horn
LMT	large mossy fiber terminal
LMT-C	large mossy fiber terminal complex
LTD	long-term depression
LTP	long-term potentiation
MB	mushroom body
MFT	mossy fiber terminal
NeuN	nuclear marker N
NMDA	N-methyl-D-aspartate
NMDA-R	N-methyl-D_aspartate receptor
NMJ	neuromuscular junction
NO	nitric oxygen
PKA	protein kinase A
PKC	protein kinase C
PN	projection neuron
PSD-95	postsynaptic density protein-95
STDP	spike-timing-dependent plasticity
TB	terminaux bouton
Wnt	composite from the gene names <i>Wingless</i> and <i>Int-1</i>

1. Introduction

Overview

Neuroscience aims at understanding how we perceive, move, think, and remember using trillions of neurons. Every day our brain receives massive amounts of electrical and chemical signals that are processed through connected networks of neurons, which must be built with high specificity in order to produce meaningful and predictable information. Neurons transmit these signals to one another at specialized sites called synapses. These are excitatory or inhibitory, and accordingly increase or decrease neuronal responses. Thus, synapse development, maturation and dynamic is crucial in establishing proper functional neuronal circuits. In recent years it has become clear that synapses can be produced and dismantled even in the adult brain. As a consequence, dendritic spines and axonal boutons can appear and disappear throughout life. This neuronal remodeling is called “structural plasticity” and might be fundamental to learning, memory and cognition.

In this introduction I describe some of the key components that are important to deal with structural plasticity of axon terminals in the adult. I will first start by explaining how synapses form during development, a process likely to also be relevant to how “mature synapses” might form in the adult brain. I will then report on what is known about axonal structural plasticity in the adult, and finally introduce the hippocampus as a model system to study structural plasticity.

1.1 SYNAPSE FORMATION

Synapse formation is a complex process that occurs over a protracted period of development. It involves five main stages: target specification, synapse specification, maturation, elimination and stabilization. Multiple molecules influence not only when and where synapses form, but also synaptic specificity and stability.

Target specification

The first step in synapse formation is target recognition. Axons from different brain regions have to grow into their respective target fields and produce synaptic contacts with the correct cell type. For example, retinal ganglion cell axons traverse long distances from the eye into the lateral geniculate nucleus of the thalamus before synapsing onto thalamic cell dendrites (Schatz 1996 and 1997). Similarly, motor neuron axons from the ventral horn of the spinal cord traverse long distances to innervate muscle fibers (Sanes & Lichtman 2001). Many studies showed that molecules including netrins, semaphorins, and ephrin A are important to guide axons to their target fields. For example, netrins and semaphorins affect the orientation of axonal growth cones through local gradients (Bagri & Tessier-Lavigne 2002, Tessier-Lavigne 1995). As soon as axons have reached their target zones, they can arborize within these regions using members of the Wnt, fibroblast growth factor (FGF) and neurotrophin (e.g BDNF) families. Wnt and FGF molecules induce axon arborisation and accumulation of recycling synaptic vesicles in innervating axons (Scheiffele 2003). BDNF can promote regional axon-and dendrite arborisations by regulating directly the density of synaptic innervation (Alsina et al. 2001).

Synapse specification

The second step in synapse formation starts when axons have innervated their target fields and need to recognize the correct cell type to synapse with. In the phase of recognition, several classes of Cell-Adhesion Molecules CAMs have been shown to be implicated. For example, barrel field pyramidal cells and septal granule cells in the somatosensory cortex express N-cadherin and cadherin 8, and their corresponding thalamic inputs as well, which lead to a reciprocal recognition (Gil et al. 2002). This indicates that functionally connected groups of neurons express molecules that help them to come in contact preferentially, and suggests that synapse specification is predetermined within neuronal circuits. Once axons have recognized their correct cell type, they start to induce synaptic contacts. Different classes of molecules are capable of directly induce various aspects of synapse induction. These include Narp and Ephrin B1, two secreted proteins that cluster subsets of postsynaptic proteins, and SynCAM and Neuroligin, two CAM that can trigger the formation of presynaptic boutons (Biederer et al. 2002, Dalva et al. 2000, O'Brien et al. 1999, Scheiffele et al. 2000). The result is the molecular assembly of the synaptic junction through the delivery of pre- and postsynaptic components, which define a fully functional synapse. In presynaptic assembly, synapse assembly involves the appearance of scaffold proteins of the active zone, such as Piccolo, Bassoon and RIM, as well as components of the synaptic vesicle exocytotic machinery including syntaxin, SNAP25, and N-type voltage-gated calcium channels (Shapira et al. 2003). In postsynaptic assembly, synapse assembly involves the recruitment of scaffolding proteins of the PSD-95 family, as well as NMDA-type and AMPA-type glutamate receptors (Sans et al. 2000, Washbourne et al. 2002, Petersen et al. 2003). At this point synapses are ready to sense electrical and chemical signals, and can undergo maturation (Figure 1).

Synapse maturation

The third step in synapse formation is the maturation of developing synapses by expanding their sizes and changing their functional properties. For example, in the first month of cortical development terminal enlargements are correlated with a two- to threefold increase of synaptic vesicles per terminal (Vaughn 1989). Furthermore, in hippocampal neurons, glutamatergic synapses initially form on filopodia or dendritic shafts that develop over time into dendritic spines (Fischer et al. 1998). In parallel, as hippocampal synapses mature, the probability of transmitter release decreases, and the reserve pool of vesicles increases. In addition, the expression of the “adult” NR2A subunit of the NMDA receptors replaces the “young” NR2B subunit, mediating a decrease in hippocampal NMDA current duration (Sorra & Harris 2000, Bolshakov & Siegelbaum 1995). Interestingly, many developing brain regions exhibit “silent synapses”, which lack surface AMPA receptors and therefore are characterized by functional NMDA but not AMPA currents (Isaac et al. 1997). These synapses can insert AMPA receptors due to NMDA activation, increasing their size and synaptic efficacy, and can represent a repertoire of activity dependent synapses recruited upon special input.

Synapse elimination

The fourth step in synapse development is synapse elimination, which runs in parallel to synapse maturation. Synapse elimination decreases the initial number of synapses formed in early postnatal life, which is far greater than the number retained in adulthood. Interestingly, pruning of synapses has been shown to be activity-dependent, and appears to be critical in the formation of proper neuronal circuits. A nice example involves the climbing fibers that arise from the inferior olivary nucleus, which form multiple synapses with a single Purkinje cell. Initially, Purkinje cells are innervated by a nest of climbing fibers that contact the soma, and initially synapse onto finger-like perisomatic spines and later onto thorns, which are large spines located on the proximal dendrites (Laxson & King 1983 and Larramandi & Victor 1967). Soon thereafter, only one climbing fiber

remains in contact, and all the others are eliminated. The result is that each Purkinje cell is innervated by a single climbing fiber (Crepel et al. 1971). This process of eliminating perisomatic spines, supernumary climbing fibers and thorns is thought to be activity dependent, and result from a competition between different afferents. A similar process occurs during the formation of the neuromuscular junction, where motor neurons from the spinal cord innervate muscles (Sanes & Lichtman 1999), and during the formation of ocular dominance columns in the visual cortex (LeVay et al. 1980). In the mature brain, synapse elimination is also occurring, and probably is an important mechanism for removing inappropriate or ineffective connections. Recent studies have shown that activity regulates synapse elimination and synapse formation in the mature barrel cortex, an area that receives sensory input from the whiskers (Knott et al. 2002, Trachtenberg et al. 2002). Taken together, these studies demonstrate that patterned activity plays a fundamental role in synapse formation and elimination in both young and adult animals, and that activity related synapse turnover is crucial to fine-tune networks.

Synapse stabilization

The last step in synapse formation involves synapse stabilization, which mainly reflects stabilization of synaptic proteins via ubiquitination. Studies at the *Drosophila* neuromuscular junction have shown that local applications of proteasome inhibitors induce a rapid strengthening of synaptic transmission owing to a 50 % increase in the number of synaptic vesicles released (Aravamudan & Broadie 2003, Speese et al. 2003). In addition, in the vertebrate hippocampus, activity-dependent internalization of homologous AMPA receptors is regulated by ubiquitination (Colledge et al. 2003). These data indicate that ubiquitination of synaptic proteins is activity-dependent and crucial for synapse stability.

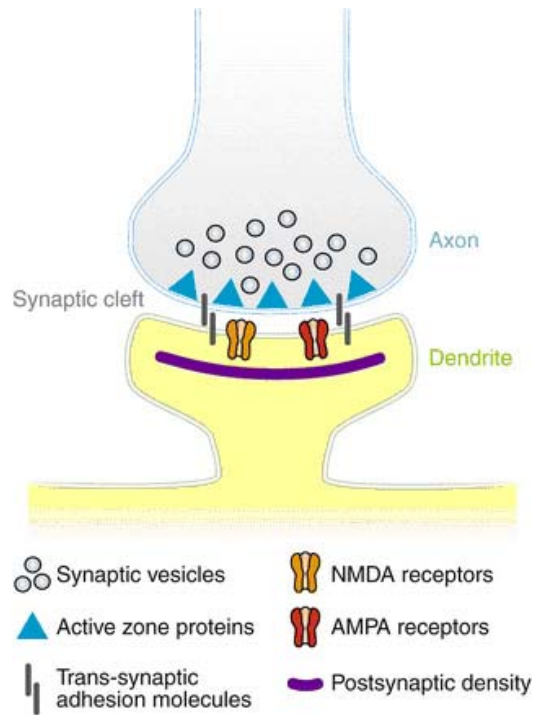


Figure 1. Basic elements of CNS glutamatergic synapses (modified from McAllister et al. 2007)

Outlook

Since “synapse turnover” is happening in the adult, it is plausible that aspects involved in developmental synapse formation also regulate structural plasticity. For example, Cell Adhesions Molecules might control cell type recognition, molecules of the Wnt and FGF families might promote new neuronal growth, and activity might promote the maturation of new synapses. However, to understand how structural plasticity leads to new synaptic contacts, we first need to understand where and under what circumstances it is occurring. For example, not every neuron might undergo structural plasticity, and remodeling might preferentially involve neuronal and synapse subtypes. Accordingly, it is important to determine whether structural plasticity might preferentially take place at certain neuronal subtypes, and whether structural plasticity within the same neuron might also be subcompartmentalized.

1.2 STRUCTURAL PLASTICITY OF AXONAL TERMINALS IN THE ADULT

modified from Nadine Gogolla, Ivan Galimberti and Pico Caroni,
Current Opinion in Neurobiology 2007, 17: 516-524

Structural plasticity of axons beyond developmental circuit assembly processes, and in the absence of physical lesions, is a recent discovery, and an exciting addition to the plasticity repertoire of mammalian brains. The late discovery reflects the advent of novel tools to deal with the overwhelming complexity of axonal arborisation patterns in the brain and the need to repeatedly image identified axons *in situ* over time periods ranging from days to months (Caroni 1997, Feng et al. 2000, Brecht et al. 2004 and Svoboda & Yasuda 2006). Such repeated live imaging analysis of identified axons has proven indispensable in order to adequately document the occurrence of structural plasticity processes in axons under physiological conditions.

Although the surface has just been scratched so far, it is already clear that these novel aspects of brain plasticity can potentially match the functional impact of long-term plasticity mechanisms at pre-existing synapses. Thus, as we discuss below, structural plasticity of axons provides neuronal circuits with plasticity mechanisms that complement functional modifications of pre-existing circuitry, and might be qualitatively different from them. This is mainly due to the different time scales of the phenomena (seconds to hours, versus days to weeks), to the larger spatial scale of the modifications (axons can sample synaptic territories ranging in the tens and even hundreds of microns), and to the fact that structural plasticity can persistently modify the local architecture of microcircuits in both quantitative and qualitative ways (Galimberti et al. 2006)

Axonal remodeling in the adult

Direct studies of the structural plasticity of axons in the adult have become possible because of the advent of genetic methods to selectively label very few neurons at any given time *in vivo*, achieving what can be viewed as ‘live Golgi stains’(Caroni 1997, Feng et al. 2000, Brecht et al. 2004) and to microscopy techniques allowing imaging of fluorescent samples several hundred microns deep into neural tissue (Svoboda & Yasuda 2006). In this chapter, we highlight recent live imaging studies of axonal plasticity and

mention some of the more compelling evidence from behavior–anatomy correlative studies.

Recent studies have measured structural plasticity of axonal branches and boutons *in vivo*, using two-photon microscopy of GFP-labeled axons in mouse and monkey cortex. De Paola *et al.* (De Paola et al. 2006) found that axons belonging to different types of neurons can exhibit distinct structural plasticity properties in adult mouse barrel cortex. In thalamocortical afferents the majority of EPBs persisted (5% turnover in one week; 15% turnover in one month), and remodeling was due to elongation and retraction of side-branches (up to 150 μm excursions within four days; comparable total numbers of side-branches were stable or dynamic). Layer VI axons were rich in highly plastic TBs (20% turnover in one week; 50% turnover in one month; 70% turnover in one and a half months). Layer V-II/II neurons had comparatively low contents of TBs and moderately plastic EPBs (10% turnover in one week, 20% turnover in one month). Appearance/disappearance events for bouton populations were generally matched, suggesting that the plasticity led to no significant net changes in total synapse numbers (Berardi et al. 2004). Significantly, the boutons could be subdivided into stable and dynamic subpopulations, with many stable boutons persisting for at least nine months (Berardi, N et al. 2004). Stettler *et al.* (Stettler et al. 2006) investigated axon branching and bouton dynamics in primary visual cortex of adult Macaque monkeys and found that a subset of TBs and EPBs appear and disappear every week. Turnover values for layer II/III pyramidal neuron axons were 7% in one week, 14% in two weeks for EPBs, and about twice that value for TBs (See also scheme of Figure 2).

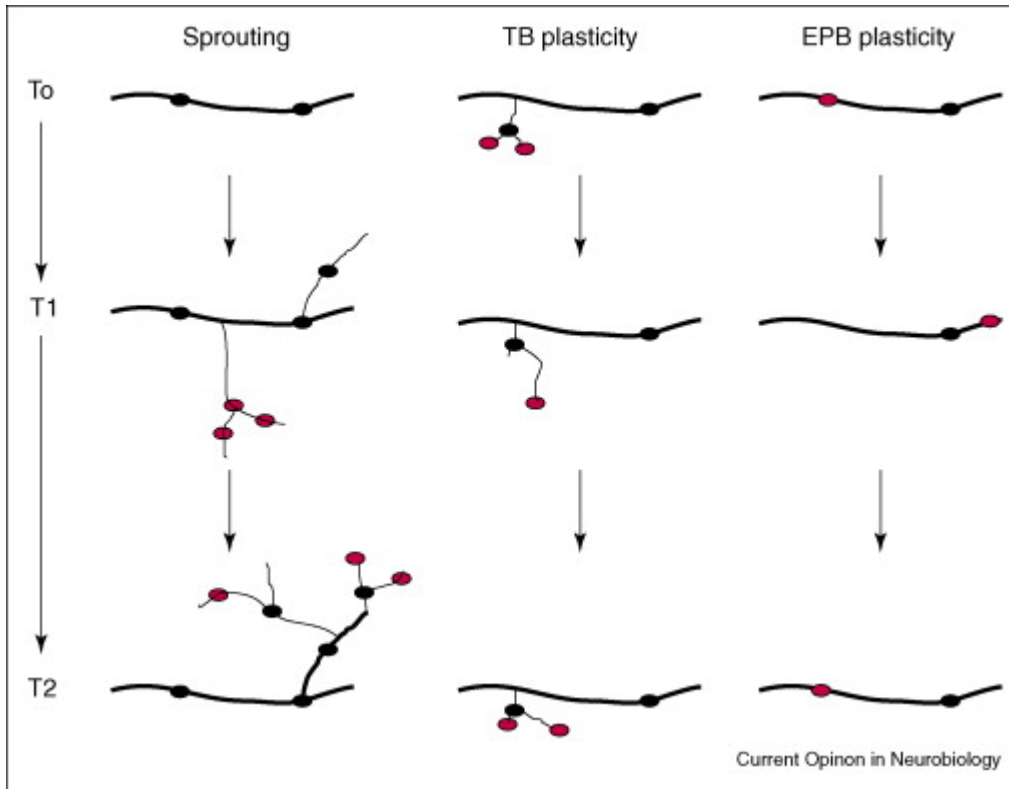


Figure 2. Sampling scales of axonal structural plasticity.

Side-branch sprouting mediates sampling of postsynaptic territories ranging tens and hundreds of micrometers away from the original axon branch, whereas *en-passant* bouton (EPB) plasticity is confined to the territory covered by pre-existing axon branches. Terminal bouton (TB) plasticity can sample many tens of micrometers but might not lead to the establishment of stable new circuitry. Stable boutons are in black, dynamic boutons in red. Sprouts are ‘guided’ (i.e. stabilized) by new stable boutons. Axonal processes can be stable (thick lines) or dynamic (thin lines). The schematic indicates the state of an axonal segment at three successive time points (To, T1, T2), separated by about 10–15 days.

Does presynaptic appearance/disappearance reflect a complete turnover of synapses? If dendritic spines and axonal boutons rearrange by producing and dismantling synaptic contacts, one would expect that the appearance/disappearance values of new spines and boutons would be balanced. Indeed, reported spine and presynaptic bouton turnover values in adult neocortex fall within comparable ranges (De Paola et al. 2006, Stettler et al. 2006, De Paola et al. 2003, Holtmaat et al. 2006, Lee et al. 2006 and Majewska et al. 2006); but see reference (Xu et al. 2007), suggesting that entire synaptic structures might appear and disappear in many cases. However, balanced presynaptic and postsynaptic remodeling is not always the rule, and a recent study has suggested that dendritic spines

might turn over more readily than axonal boutons (Majewska et al. 2006). One possible interpretation of these findings is that the extra spines might not go on to form functional synapses and might be lost within about a day from their initial appearance. On a similar vein, recent results in mouse neocortex showed that spine growth can precede synapse formation and that an active zone can appear as late as four days after the initial outgrowth (Knott et al. 2006). In addition, new spines can contact pre-existing presynaptic boutons to form multi-spine boutons. Perhaps not surprisingly, the latter process is the predominant pathway when dendrites of new hippocampal granule cells form synapses with pre-existing perforant path axons in the adult hippocampus (Toni et al. 2007). Besides in such special cases, the particular mechanisms of synapse turnover in the adult are in most cases unclear, and simultaneous imaging of presynaptic and postsynaptic elements will be necessary in order to investigate the rules leading to presynaptic-driven synaptogenesis versus postsynaptic-driven synaptogenesis in the adult CNS.

Learning-dependent axonal rearrangements

Structural remodeling might underlie aspects of learning and memory by rearranging synaptic contacts within local microcircuits, and possibly also through the assembly or dismantling of entire parts of local circuits. Although these possibilities have not been investigated extensively yet, the available evidence suggests that this might indeed be the case. For example, spatial learning was reported to promote an expansion of mossy fiber terminals in the CA3 region of the rodent hippocampus (Ramírez-Amaya et al. 1999 and Holahan et al. 2006). Furthermore, housing mice in an enriched environment led to an increased local complexity of hippocampal mossy fiber terminal complexes in stratum lucidum (Galimberti et al. 2006). Parallel pharmacological studies provided evidence that similar rearrangements in organotypic slice cultures depend on synaptic activity and transmitter release from mossy fiber terminals, suggesting that experience might regulate persistent local changes of connectivity in the mossy fiber projection (Galimberti et al. 2003). As mentioned in the previous chapter, learning of a new skill might produce axonal projection shifts, possibly including the assembly of new local circuits. In one suggestive example, London taxi drivers were found to have on average larger posterior

hippocampi than non-taxi drivers, suggesting that overtraining for a complex spatial task can increase neuropil volumes in a brain region specifically involved in navigational skills (Maguire et al. 2000). In a further example, monkeys trained for a new complex motor behavior involving the hand exhibited substantial rearrangements of receptive fields in motor cortex and increased synaptic densities specifically in the expanded areas within a time period of four to eight days (Kleim et al. 2002). These observations suggest that new experience can produce predictable and persistent alterations in axonal connectivity in the adult CNS. However, the mechanisms involved and the functional roles of these remodeling processes remain to be determined. For example, it is not clear how ‘spontaneous’ presynaptic bouton turnover relates to large scale experience related alterations in connectivity, how experience impacts on structural plasticity, and whether the structural changes directly encode new information or mainly facilitate its acquisition.

Axonal remodeling and aging

Axonal remodeling decreases from young adulthood to middle age in mice. Thus, in young mice axonal branches in the parasympathetic submandibular ganglion underwent significant rearrangements over several weeks, whereas rearrangements were reduced and axonal branches were recognizable for many months and up to years in older mice (Gan et al. 2003). In addition to a general reduction in structural plasticity, age seems to produce gradual and long-lasting alterations in the connectivity of certain circuits. Thus, when mice of increasing age were compared, most hippocampal mossy fiber terminals shrunk, while 5–8% of them expanded gradually along pyramidal cell dendrites, suggesting the existence of sustained age-related shifts in the organization of a major axonal projection in the hippocampus (Galimberti et al. 2006). These initial observations raise the possibility that, along with a general decrease in plasticity with increasing age, life stages might be accompanied by their characteristic local circuit architecture properties.

1.3 THE HIPPOCAMPUS: A MODEL SYSTEM TO STUDY LEARNING-RELATED STRUCTURAL PLASTICITY

Learning is the process by which we acquire knowledge about the world, while memory is the process by which that knowledge is encoded, stored and later retrieved. Many important behaviors are learned. We learn the motor skills that allow us to master our environment, and languages that enable us to communicate what we have learned to other generations. Different recruitments of brain regions are important for different elaborations of learning and memory. For example the hypothalamus, the amygdala and related structures are essential for *emotional* dependent learning and memory. However, neocortical association areas (the prefrontal, limbic, and parieto-occipital-temporal cortices), the parahippocampal region (which includes parahippocampal, perirhinal, and entorhinal cortices) and the hippocampus are involved in *explicit* (declarative) learning and memory, and systems that include the neostriatum and cerebellum mediate *procedural* learning and memory (the acquisition of motor skills and habits).

Explicit memory can be classified as *episodic* (a memory for events and personal experience) or *semantic* (a memory for facts). We use episodic memory when we recall that we saw the first snow of winter yesterday or that we heard the Queen's *Show must go on* several months ago, whereas we use semantic memory to store and recall object knowledge. Nevertheless, all explicit memories can be expressed in declarative statements, such as "Last spring I visited my grandfather at his country house" (episodic knowledge) or "iron is heavier than water" (semantic knowledge). The hippocampus is one of the brain regions that plays an important role in episodic learning and memory in animals and humans. Electrophysiological recordings and molecular imaging studies in animals, as well as MRI imaging studies in humans provided correlative evidence that episodic learning and memory involves hippocampal activity (Vazdarjanova et al. 2004, Guzowski et al. 2001, Gabrieli et al. 1997 and Henke et al. 1997). In addition, recent data revealed that there is structural plasticity in hippocampal principal neurons, and suggested that remodeling of hippocampal circuits might underly an important aspect of episodic learning and memory (Muller et al. 2002, De Paola et al. 2003 and Galimberti et

al. 2006). Therefore, the hippocampus is an attractive system to understand how structural plasticity might relate to learning and memory.

Basic circuits of the hippocampus

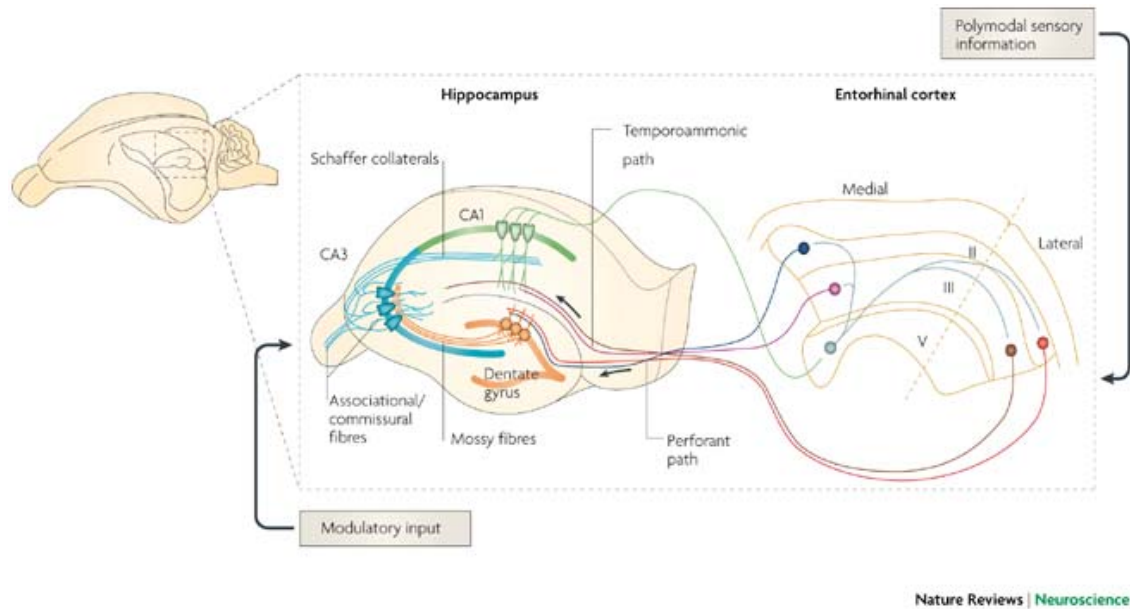


Figure 3. Basic anatomy of the hippocampus (modified from Guilherme et al. 2008)

The major input to the hippocampus is carried by axons of the perforant path, which convey polymodal sensory information from neurons in layer II and III of the entorhinal cortex. In parallel, afferents of cholinergic and serotonergic neurons provide a modulatory input to different hippocampal cell types. Layer II afferents from the lateral and medial enthorhinal cortex make excitatory synaptic contacts with the outer and middle third of dentate gyrus granule cells dendritic trees, respectively. Granule cells initiate the trisynaptic loop (granule cells-CA3 and-CA1 pyramidal neurons) by projecting through the mossy fibers to the proximal apical dendrites of CA3 pyramidal cells. CA3 pyramidal cells project to ipsilateral CA1 pyramidal cells through schaffer collaterals, and to contralateral CA3 pyramidal cells through commissural connections. Other layer II afferents from lateral enthorhinal cortex innervate directly the distal apical dendrites of CA3 pyramidal cells. Layer III afferents from medial and lateral enthorhinal cortex innervate the distal apical dendrites of CA1 pyramidal cells. The output of the hippocampus are afferents of CA1 pyramidal cells that project to layer V of the

enthorinal cortex, which convey this information back to polymodal association areas of the neocortex (Amaral & Lavenex 2007). The three major subfields of the hippocampus (DG, CA3 and CA1) have a laminar organization in which the cell bodies are tightly packed with afferent fibers terminating on selective regions of the dendritic tree. The hippocampus is also home of a rich diversity of inhibitory interneurons (see Figure 3 and Amaral & Lavenex 2007 for more details).

Hippocampal synaptic plasticity

The most famous example of hippocampal synaptic plasticity is long-term potentiation LTP, which was first identified in the hippocampus and is believed to represent an important mechanism of learning and memory (Bliss & Lomo 1973 and Bliss & Gardner-Medwin 1973, Gruart et al. 2006 and Whitlock et al. 2006). For example, in the CA1 area of the hippocampus, LTP occurs when schaffer collaterals receive high-frequency electrical stimulation that induces an enhancement of synaptic transmission with CA1 pyramidal cells. The opposing process to LTP is long-term depression LTD, in which synaptic transmission is weakened by low-frequency stimulation (Dudek & Bear 1992). LTD might serve as a learning mechanism in its own right, or might be a means of ensuring homeostatic stability by preventing an increase in overall activity in potentiated networks. Other forms of activity-dependent hippocampal plasticity have been found, including, EPSP-spike (E-S) potentiation, spike-timing-dependent plasticity STDP, depotentiation and de-depression (Dan & Poo 2004, Staubli & Lynch 1990 and Montgomery & Madison 2002). In spite of much progress in studying plasticity, we still have no clear picture of how synaptic plasticity in extensive networks of cells leads to storage and recall of information. In 1949 Donald Hebb proposed the “neurophysiological postulate”:

“When an axon of a cell A excites cell B and repeatedly or persistently takes part in firing it, some growth process or metabolic change takes place in one or both cells so that A’s efficiency as one of the two cells firing B is increased”

This idea, together with the discovery of LTP, led to the synaptic plasticity and memory (SPM) hypothesis (Martin et al. 2000), which might currently represent the predominant view by a majority of neuroscientists as to the relationship between synaptic plasticity and learning:

Activity-dependent synaptic plasticity is induced at appropriate synapses during memory formation, and is both necessary and sufficient for the information storage underlying the type of memory mediated by the brain area in which that plasticity is observed.

Molecular and structural aspects of hippocampal LTP

In the hippocampus, the mechanisms underlying LTP are not the same in all subfields. For example in the mossy fiber pathway LTP is nonassociative and presynaptic, whereas in the schaffer collateral pathway it is associative and postsynaptic. The induction of LTP in the CA1 region depends on four postsynaptic factors: postsynaptic depolarization, activation of NMDA receptors, influx of Ca^{2+} , and activation by Ca^{2+} of several second-messenger systems in the postsynaptic cell. Initially, high-frequency stimulation of schaffer collaterals leads to glutamate release from presynaptic terminals that bind AMPA receptor channels. This triggers the depolarization of the postsynaptic membrane and relief from the Mg^{2+} dependent blockade of the NMDA channels. Ca^{2+} flow through the NMDA channel and the resulting rise of Ca^{2+} in the dendritic spine triggers Ca^{2+} dependent kinases e.g. $\alpha\text{CaMK II}$ and PKA. αCaMKII and PKA phosphorylate AMPA receptor-channels and increase their sensitivity to glutamate. In addition, new AMPA receptor-channels are added to synaptic junctions and retrograde messengers e.g. NO act on protein kinases in the presynaptic terminal to initiate an enhancement of transmitter release that contributes to maintain LTP. Therefore, LTP in the schaffer collateral pathway is associative and postsynaptic-dependent. This synaptic efficacy over several hours is supposed to involve the activation of gene transcription and protein synthesis (West et al. 2002). Some of the proteins that are synthesized, e.g. BDNF, can also lead to structural changes (Poo 2001). Indeed, there is evidence that induction of LTP leads to changes in the number and shape of spines (Nikonenko et al. 2002, Yuste & Bonhoeffer 2001 and Mueller et al. 2002). For example, induction of LTP in hippocampal slices leads to the formation of new spines and its inhibition with an NMDA receptor antagonist

(AP5) prevents this structural change (Engert & Bonhoeffer 1999). In contrast to LTP, LTD reduces the diameter of spine heads (Zhou et al. 2004). Similar changes in spine and bouton morphology and number have also been found in different brain areas after learning (Bailey & Kandel 1993 and Geinisman et al. 2001). These results suggest that structural plasticity contributes to the modulation of synaptic transmission, and represents an anatomical trace of learning-related synaptic plasticity.

The mossy fiber projection

When Ramón y Cajal initially observed dentate gyrus granule cells axons at the light microscopic level, he saw the appearance of mossy-like structures and therefore called them “mossy fibers”. Later it became clear that this mossy appearance was due to the existence of giant terminals that were called large mossy fiber terminals (LMTs). Mossy fibers project through the dentate hilus and CA3 area of the hippocampus and have more than one terminal type: LMTs, small filopodial extensions that emanate from LMTs, and en-passant varicosities epVs. Small filopodial extensions and epVs target GABA-containing interneurons along the entire projection. However, LMTs are specialized to target mossy cells and CA3 pyramidal neurons (Acsady et al. 1998 and Henze et al 2000). Mossy cells are excitatory interneurons of the dentate hilus that project in the inner third of the granule cells dendritic tree. This projection is called *ipsilateral associational-commissural projection* and reinforces mossy fibers synaptic plasticity providing feed forward excitation. In the CA3 area, mossy fibers run in two main bundles, the main projection and the infrapyramidal projection. The main projection runs entirely along the stratum lucidum, whereas the infrapyramidal projection runs first within the proximal extent of stratum pyramidale, to cross over to stratum lucidum in the CA3a region. At the end of CA3, mossy fibers make a turn temporally and project for 1-2 mm longitudinally towards the temporal pole of the hippocampus (Amaral & Lavenex 2007). CA3 pyramidal neurons make synaptic contacts with LMTs using specialized spine-clusters called “thorny excrescence clusters”, and each CA3 pyramidal cell has been estimated to be contacted by 30-50 different LMTs from distinct mossy fibers (Henze et al. 2000).

The mossy fiber projection represents a particularly advantageous system to study the structural plasticity of an axon that is involved in episodic learning and memory. The fact that each mossy fiber exhibits a sparse excitatory connectivity along CA3, with 10-15 LMTs at 80-150 μm intervals, suggests that LMTs might establish contacts with some degree of spatial selectivity. In addition, individual LMTs can elicit action potentials in postsynaptic pyramidal cells, and they do exhibit structural plasticity (Reid et al. 2001, Henze et al. 2002, De Paola et al. 2003 and Galimberti et al. 2006).

2. RESULTS

2.1. LONG-TERM REARRANGEMENTS OF HIPPOCAMPAL MOSSY FIBER TERMINAL CONNECTIVITY IN THE ADULT REGULATED BY EXPERIENCE

Ivan Galimberti^{1,2}, Nadine Gogolla^{1,2}, Stefano Alberi³, Alexandre Ferrao Santos²,
Dominique Muller³, and Pico Caroni²

¹Equal contribution

²Friedrich Miescher Institut, Maulbeerstrasse 66, CH-4058 Basel, Switzerland

³CMU, University of Geneva, Geneva, Switzerland

Neuron

2006 (Vol. 50: 749-763)

SUMMARY

We investigated rearrangements of connectivity between hippocampal mossy fibers and CA3 pyramidal neurons. We find that mossy fibers establish 10-15 local terminal arborization complexes (LMT-Cs) in CA3 exhibiting major differences in size and divergence in adult mice. LMT-Cs exhibited two types of long-term rearrangements in connectivity in the adult: progressive expansion of LMT-C subsets along individual dendrites throughout life, and pronounced increases in LMT-C complexities in response to enriched environment. In organotypic slice cultures, subsets of LMT-Cs also rearranged extensively and grew over weeks and months, altering the strength of preexisting connectivity, and establishing or dismantling connections with pyramidal neurons. Differences in LMT-C plasticity reflected properties of individual LMT-Cs, not mossy fibers. LMT-C maintenance and growth were regulated by spiking activity, mGluR2-sensitive transmitter release from LMTs, and PKC. Thus, subsets of terminal arborization complexes by mossy fibers rearrange their local connectivities in response to experience and age throughout life.

INTRODUCTION

Sustained rearrangements of synaptic connections can provide mechanisms to alter connectivity in neuronal circuits, and encode experience in the brain (Lichtman and Colman, 2000; Poirazi and Mel, 2001; Chklovskii et al., 2004). It is well established that local rearrangements of circuitry driven by experience play prominent roles in the fine-tuning of neuronal circuits during postnatal development (Lichtman and Colman, 2000; Linkenhoker and Knudsen, 2002; Gan et al., 2003; Linkenhoker and Knudsen, 2005). In contrast, although there is abundant evidence for pronounced physiological plasticity in the adult, evidence that structural rearrangements of circuitry also take place in the adult has been scarce (but see Knott et al., 2002). Recent *in vivo* time-lapse imaging studies in neocortex have reported appearance and disappearance of postsynaptic dendritic spine subpopulations, and shown that the frequency of these events can be influenced by sensory experience (Lendvai et al., 2000; Trachtenberg et al., 2002; Holtmaat et al., 2005). These remodeling events were more frequent in younger mice, but turnover was also detected in older adults (Holtmaat et al., 2005; Lee et al., 2006; but see Zuo et al.,

2005). In addition, a study using long-term organotypic hippocampal slice cultures showed that subsets of presynaptic terminals can undergo comparable balanced turnover, and that the extent of this turnover is again enhanced by synaptic activity (De Paola et al., 2003). Finally, recent studies of adult mouse barrel and visual cortex have provided evidence for such structural plasticity of presynaptic terminals *in vivo* (De Paola et al., 2006; Stettler et al., 2006). However, these studies imaged groups of either pre- or postsynaptic elements within small regions of neuropil, and could thus not assign complete sets of synapses by individual identified presynaptic neurons to their postsynaptic targets. Consequently, it has remained unclear to what extent synapse rearrangement processes in the adult produce net alterations in the numbers of synaptic connections between identified synaptic partners. For the same reasons, it has also remained unclear whether, and under what circumstances, repeated rearrangement processes can lead to incremental shifts of connectivity in the adult. To address these questions, we looked for simple and well-characterized circuitry that had been implicated in experience-related anatomical plasticity, and which was accessible to large-scale repeated imaging during long periods of time.

The mossy fiber projection by dentate gyrus granule cells onto hippocampal pyramidal neurons in CA3 (Johnston and Amaral, 1998; Henze et al., 2000) is an attractive system to investigate patterns of synaptic connection rearrangements on a comprehensive scale. First, most of the mossy fiber projection in CA3 is lamellar with respect to the hippocampal long axis, and exhibits stereotype and simple relationships with respect to the number of its postsynaptic partners. Each mossy fiber establishes 10-15 large mossy fiber terminals (LMTs) at 80-150 μm intervals along its projection in CA3 that can be unambiguously identified anatomically (Johnston and Amaral, 1998). The average number of distinct mossy fiber inputs per pyramidal neuron in CA3 has been estimated at about 30-45 (Henze et al., 2000), suggesting that the probability for random pairs of mossy fibers to synapse onto the same pyramidal neuron is very low. These low synapse numbers stand in sharp contrast to the very high degree of connectivity among pyramidal neurons in CA3, and from CA3 to CA1. Second, mossy fibers in stratum lucidum establish well-characterized and powerful excitatory synaptic connections with pyramidal

cells through LMTs, and with inhibitory interneurons through en-passant varicosities and LMT filopodia (Acsady et al., 1998; Geiger and Jonas, 2000; Reid et al., 2001; Henze et al., 2002; Engel and Jonas, 2005; Nicoll and Schmitz, 2005). The latter provide efficient feed-forward inhibition, and mediate the predominant outcome of mossy fiber activation when these spike at low frequencies (Lawrence and McBain, 2003; Mori et al., 2004). In contrast, mossy fibers elicit increasing excitation of CA3 pyramidal neurons when firing at higher frequencies (Geiger and Jonas, 2000; Henze et al., 2002; Mori et al., 2004). As a consequence, and probably depending on spiking frequency, one or a small number of converging LMTs can be sufficient to elicit action potentials in a postsynaptic pyramidal cell, assigning a major instructional role to this synapse in triggering network activity in the hippocampus (Henze et al., 2002). In addition, postsynaptic spiking induced by LMTs also serves as a powerful trigger to induce LTP at co-active weaker associational synapses onto the distal sections of the same pyramidal neuron dendrites (Kobayashi and Poo, 2004). A third key feature is that individual mossy fibers only fire rarely during hippocampal recruitment (sparse code), suggesting that small ensembles of co-active granule cells as such convey information to the hippocampal network, and that the precise outcome of the firing for each of these cells might be functionally important (Johnston and Amaral, 1998; Henze et al., 2002).

Several lines of evidence have implicated the mossy fiber projection in anatomical plasticity related to experience. Neuroanatomical analyses using Timm staining in mice and rats have suggested that mossy fiber projection sizes are correlated to performance in hippocampal-dependent tasks (e.g. Schopke et al., 1991; Pleskacheva et al., 2000), and that experience can lead to significant alterations in the size of the mossy fiber projection (Schwegler et al., 1991; Ramirez-Amaya et al., 2001). Furthermore, long-term stress can lead to reductions in spatial learning performance and in the average density of mossy fiber synapses as determined by electron microscopy, and these impairments can be reversed through training for spatial tasks (McEwen, 1999; Sandi et al., 2003). Finally, independent studies have revealed that the dendrites and dendritic spines of CA3 pyramidal neurons are particularly sensitive to stress-inducing treatments and stress-related hormones (e.g. McEwen, 1999), suggesting that both the pre- and postsynaptic

elements of mossy fiber synapses are subject to experience-related anatomical plasticity in the adult. Taken together, these findings from distinct species and experimental approaches support the notion that the mossy fiber projection and its LMT synapses in CA3 provide a promising system to investigate persistent rearrangements of synaptic circuitry influenced by experience in the adult brain.

Here we exploited transgenic mice expressing membrane-targeted GFP in only few neurons (*Thy1-mGFP^s*) (De Paola et al., 2003), and high-resolution imaging to investigate the connectivity of LMTs in fixed mouse tissue and organotypic slice cultures. We find that LMTs are highly heterogeneous in vivo and in slice cultures, and that many of them are connected through 10-200 μm processes to “satellite LMTs” that can contact distinct pyramidal neurons in CA3. LMTs are thus components of local presynaptic terminal arborization complexes (LMT-Cs) by mossy fibers, exhibiting varying degrees of divergence with respect to their local targets in CA3. We then show that LMT-Cs exhibit pronounced long-term rearrangements in the adult. We provide evidence for two distinct types of rearrangements: 1) a life-long gradual growth of the largest LMT-Cs along pyramidal cell dendrites; 2) a dramatic increase in the complexity of many LMT-Cs in mice housed in an enriched environment. We finally show that subsets of LMT-Cs exhibit comparable rearrangements and growth over weeks and months in slice cultures, that these anatomical rearrangements reflect functional rearrangements in the local connectivity of LMT-Cs with pyramidal neurons, that heterogeneities in plasticity and growth reflect local properties of individual LMT-Cs, and that LMT-C maintenance and growth are regulated by synaptic activity, mGluR2-sensitive transmitter release from LMTs, and PKC. Taken together, these results demonstrate the existence of sustained local rearrangements of connectivity by defined terminal arborization structures regulated by activity in the adult.

RESULTS

Divergence and convergence of LMT complex connectivities onto pyramidal neurons

As a prerequisite to investigate the anatomical plasticity of LMTs, we analyzed their morphologies and connectivities, using *Thy1-mGFP^s* transgenic mouse lines expressing membrane-targeted GFP in only few neurons (DePaola et al., 2003), high-resolution light microscopy of perfused brain tissue, and 3D image processing. The degree of anatomical resolution conferred by the mGFP marker allowed us to provide views of hippocampal LMTs at a very high level of overall organization and resolution (Fig. 1). We found that in addition to core terminal regions with filopodia adjacent to the main axon, which had been described in previous studies, LMTs frequently exhibited processes of 10-200 μm in length, which emerged from the core LMT and terminated at “satellite LMTs” (Fig. 1A, Suppl. Fig. 1; range of 0-5 satellites per LMT; depending on age, 38% (2.5 months), 58% (6 months), and 70% (16 months) of all LMTs exhibited satellites; see Fig. 3C). Like core LMTs, satellites were larger than 2.5 μm in diameter, exhibited filopodia, and contacted pyramidal neurons (see below). To rule out the possibility that some of the structures might be due to the mGFP marker itself, we also acquired images from mice expressing cytosolic YFP (*Thy1-cYFP^s*) (Feng et al., 2000). Although the resolution was substantially inferior, the cytosolic marker revealed the same types of subcomponents and arrangements, including core regions and satellites, as detected with the mGFP marker (Suppl. Fig. 1B). For the sake of clarity, we therefore introduce the term “LMT complex” (LMT-C) to designate a local presynaptic terminal arborization structure consisting of a core LMT, its filopodia, its satellite LMTs, and their filopodia. Accordingly, mossy fibers establish 10-15 LMT-Cs in CA3, and some of these LMT-Cs exhibit satellites.

A comparison among large sets of LMT-Cs within small regions of hippocampus revealed pronounced variations among these presynaptic terminal complexes, which ranged from small core terminal regions to very large and highly complex structures consisting of LMTs with multiple subunits, and of several satellites (Fig. 1; see also Figs. 2A, 2C, 3C). Reconstruction of three LMTs from serial EM sections of non-transgenic

hippocampi provided independent evidence that individual LMTs can consist of multiple interconnected subunits (Suppl. Fig. 2). The very large sizes of some LMT-Cs, and the presence of satellites at many of them suggested that many of these terminal structures might establish synaptic contacts with more than one postsynaptic CA3 pyramidal neuron. Indeed, a detailed analysis provided clear evidence of individual LMT-Cs in contact with more than one CA3 pyramidal neuron (Fig. 1A, Suppl. Videos 1, 2). This was not only true for the different LMTs belonging to an LMT-C, but also for large individual LMTs (Fig. 1A). In addition to this unexpected local divergence of the outputs by one LMT-C onto distinct pyramidal neurons, we also found clear evidence for extensive convergence of distinct LMT-C inputs onto individual thorny excrescence clusters (Fig. 1B).

We conclude that LMT-Cs are local terminal arborization structures of mossy fibers exhibiting dramatic differences in their sizes, complexities, and divergence onto CA3 pyramidal neurons in adult mice.

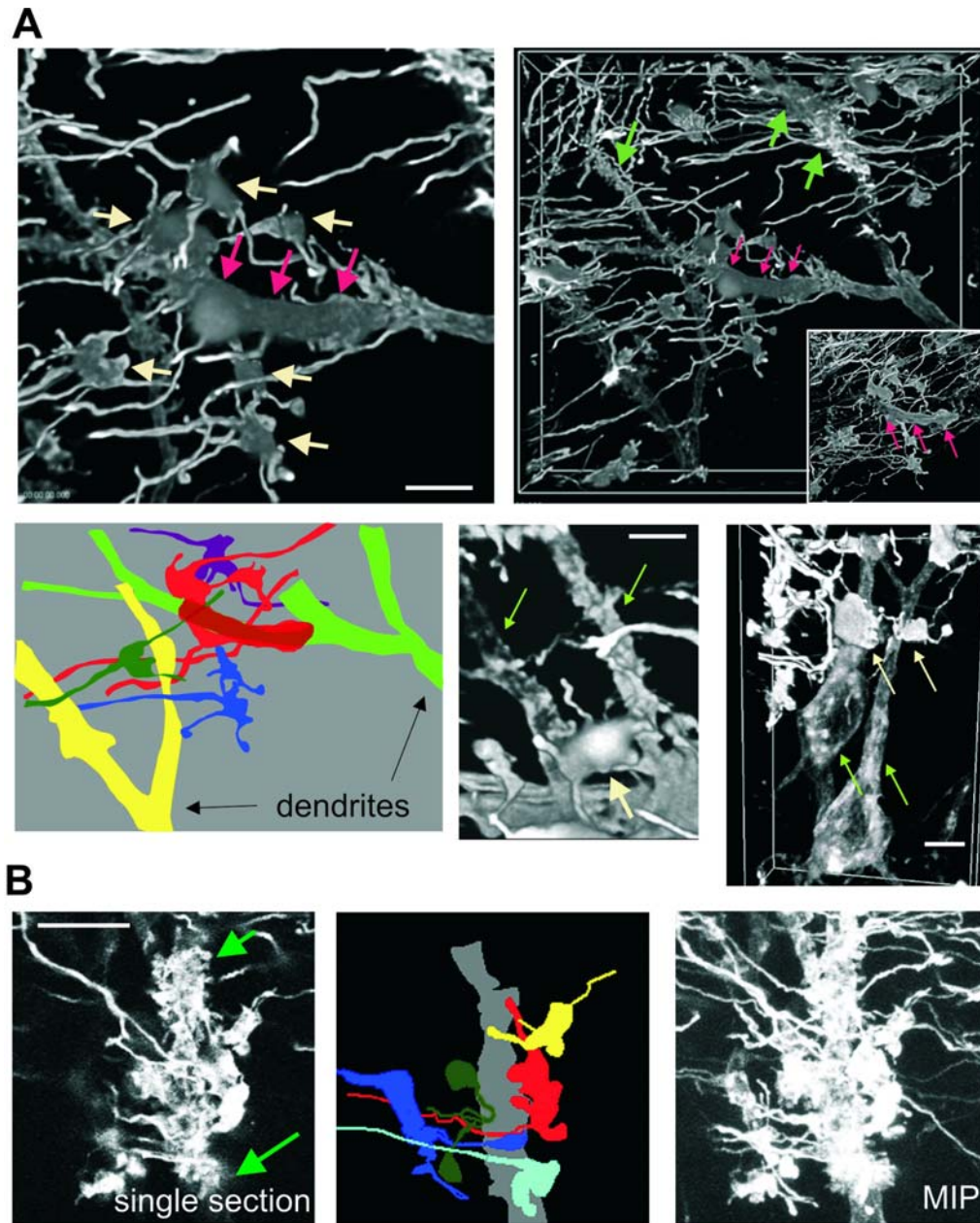
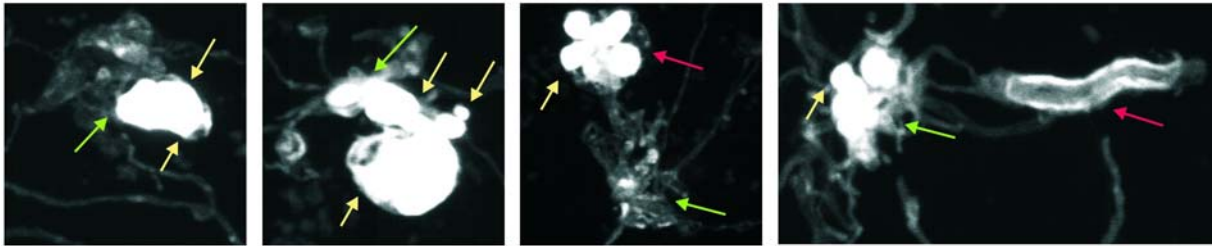
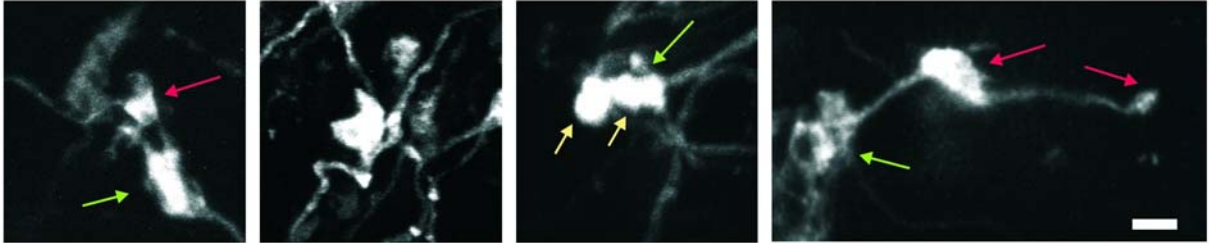


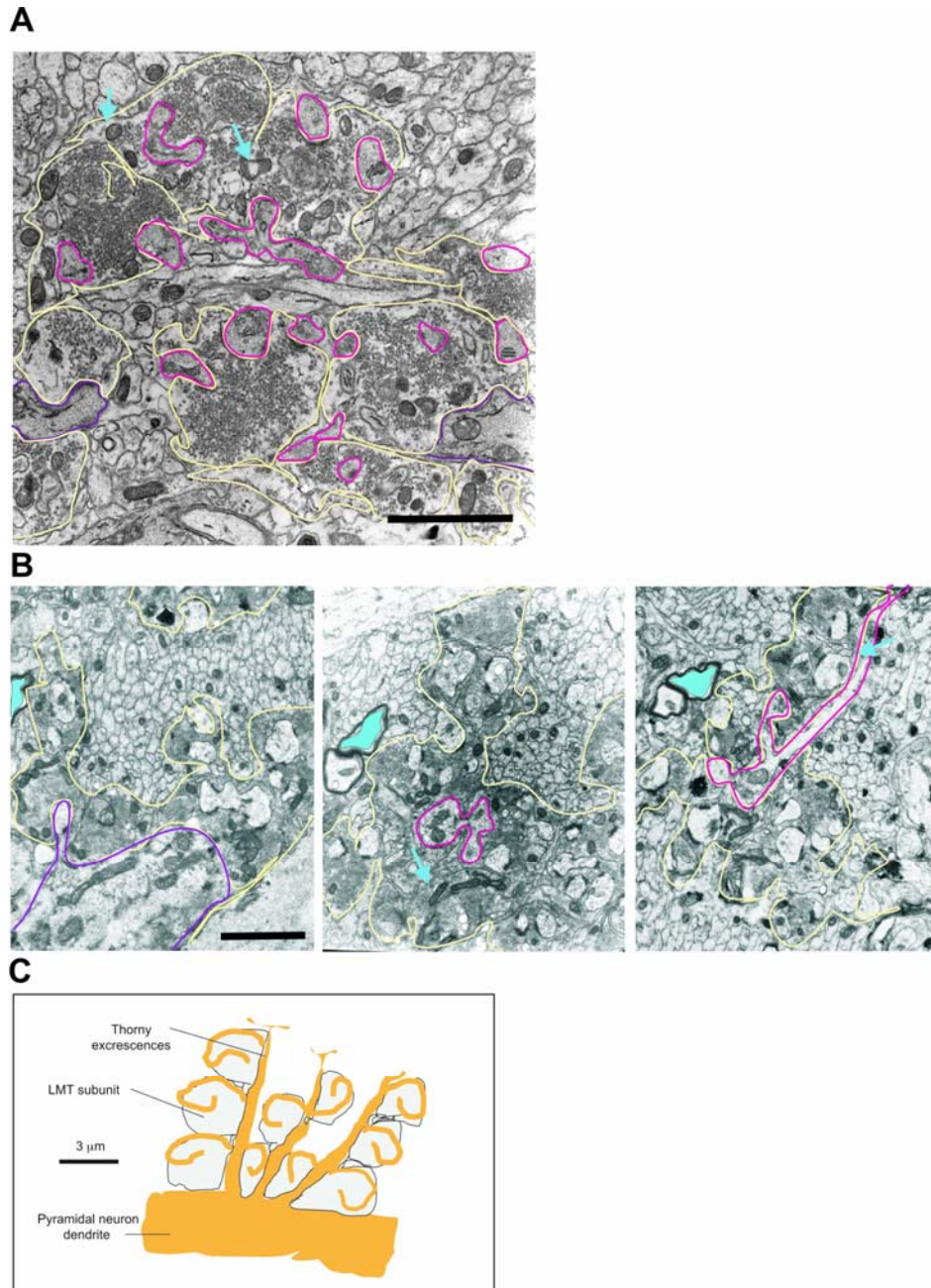
Figure 1. Divergence and convergence of LMT-C connectivity onto pyramidal neurons in CA3.

A: Complexity and divergence of LMT-Cs. Individual mossy fibers and pyramidal neurons in CA3a/b (6-months *Thy1-mGFP^s* mouse); Imaris volume projections (high-intensity mode acquisition). Upper panel, left: cream arrows: LMTs, red arrows: one LMT covering a long segment of pyramidal neuron dendrite. Upper panel right: lower magnification image of field shown on the left. Green arrows: two examples of thorny excrescence clusters. The inset shows the same field, but seen from behind (mirror image to facilitate orientation); proximal sections were excluded to reveal the dendrite-facing surface of the elongated LMT (red arrow). Lower panel left: camera lucida drawing of CA3 field shown above. LMTs belonging to the same complex (3D-analysis) are in the same color. Lower panels center and right: Examples of LMT-Cs (cream arrows) each contacting two distinct pyramidal neurons (green arrows); right: LMT and one satellite (to the right).

B: Convergence of LMT-Cs belonging to distinct mossy fibers at the same thorny excrescence cluster of a pyramidal neuron dendrite in CA3 stratum lucidum (2.5-months *Thy1-mGFP^s* mouse). Left: single confocal section (green arrows delineate the outline of the thorny excrescence cluster); center: camera lucida drawing, including LMTs from 5 distinct mossy fibers converging onto the thorny excrescence cluster; right: MIP of stacks including the cluster and its mGFP-positive LMT inputs. The LMT-Cs belonging to the dark blue and green mossy fibers both include satellites, and converge on a second dendrite on the left. Bars: 5 μm . □

A**B**

Supplementary Figure 1. Comparison of LMT-Cs in vivo, as visualized using *Thy1-mGFPs* or *Thy1-cYFPs* mice. Image settings (MIP of raw data) comparable to those shown in Fig. 2A for LMT-Cs in slice cultures. Arrows: original LMT (green; next to mossy fiber), satellites (red), beady subunits (yellow). A: Examples of LMT-Cs in 15 Mo, *Thy1-mGFPs* mice. Note how the LMT structures are comparable to those detected in slice cultures. B: Examples of LMT-Cs in 4 Mo, *Thy1-cGFPs* mice. Note how complex arrangements, including beaded subunits and satellites are also visualized with cytosolic YFP. Bar: 5 μ m.



Supplementary Figure 2. Ultrastructural analysis of complex LMTs.

Electron micrographs of CA3a LMTs in 3 months wild-type mice. Blue arrows: regions where connection between subunits is included in the section. A: A complex LMT consisting of multiple interconnected subunits (cream outlines; verified by consecutive sections). Note arrangement of many thorny excrescences (red outlines) around the edge of LMT subunits. B: Serial sections of one complex LMT. Outlines: interconnected subunits (cream), base of dendrite (violet, left panel) and examples of postsynaptic thorns interconnecting LMT subunits (red); for orientation, a myelinated axonal profile is filled in blue. C: Partial reconstruction of LMT complex shown in (B). The schematic is based on 65 consecutive sections, and outlines the main topographic relationships included in the sections (axonal elements in blue, dendritic elements in yellow); it indicates the arrangement of thorny excrescence main branches (three of them), and their secondary branches extending around the edges of LMT subunits, but does not include tertiary side-branches into LMT subunits and their synaptic complexes. LMT subunits were interconnected along thorn main branches. Bars: 2 μ m.

Life-long expansion of hippocampal LMT subsets along pyramidal dendrites

We next wondered whether the dramatic complexities and differences among LMT-Cs are present to a similar extent throughout life, or whether LMT-Cs might undergo systematic alterations with maturation and during adulthood. A comparison of LMTs from the same regions of hippocampal CA3, but from mice of different ages, revealed clear differences in the size distributions of these presynaptic terminal structures, and a selective shift to larger sizes with increasing age (Fig. 2A-C). The mGFP construct labeled mossy fibers and LMT-Cs with remarkable and comparable homogeneity throughout life (Suppl. Fig. 3), arguing against the possibility that these LMT size shifts might reflect systematic distortions of the imaging data set. Interestingly, the shifts in LMT sizes did not affect all LMT size groups equally: while a large fraction (50-80%, depending on the age) of LMTs was relatively small (volumes equivalent to 1-3 subunits of 3 μm diameter) at any age, the remaining LMTs shifted to larger sizes, and the average sizes of the largest 5-10% among them grew dramatically with age (Fig. 2B). Remarkably, this gradual age-related growth of larger LMTs was not confined to any particular period of life, but instead continued throughout life, including old age (Fig. 2B). This was not accompanied by a corresponding decrease in the average density of LMTs (average densities of LMTs per (92 x 92 x 7.5 μm) volumes of CA3a, normalized per mGFP-positive granule cell on the same section were: 1.14 ± 0.12 (3 months), 1.18 ± 0.20 (6 months), 1.37 ± 0.15 (16 months), 1.34 ± 0.18 (22 months); N=8 sections, 16 volumes, from 2 mice each; range of 21-42 LMTs per volume), arguing against the possibility that the higher contribution of the larger LMTs to the total volume of LMTs with increasing age was due to a corresponding loss of smaller LMTs.

A detailed comparison of larger LMTs at different ages revealed that the predominant contributions to their increase in size were longitudinal extensions, which were oriented transversal to the mossy fiber projection (Fig. 2C). This was reflected in a gradual increase in LMT long-to-short axis ratio values with increasing age (Fig. 2C). High-resolution analysis suggested that this reflected an expansion of the stretch of CA3 pyramidal neuron dendrite occupied by individual larger LMTs (Fig. 2C). Taken together, these results provide evidence that, in the mouse, there is a continuous net

growth of the largest subpopulations of LMTs throughout life, and that this growth mainly involves the expansion of LMT subsets along pyramidal neuron dendrites in CA3. This relationship between age and LMT size distributions was detected consistently among BalbC x C57/B16 mice grown under standard housing conditions, suggesting that it reflects the impact of a life-long developmental mechanism in the hippocampus.

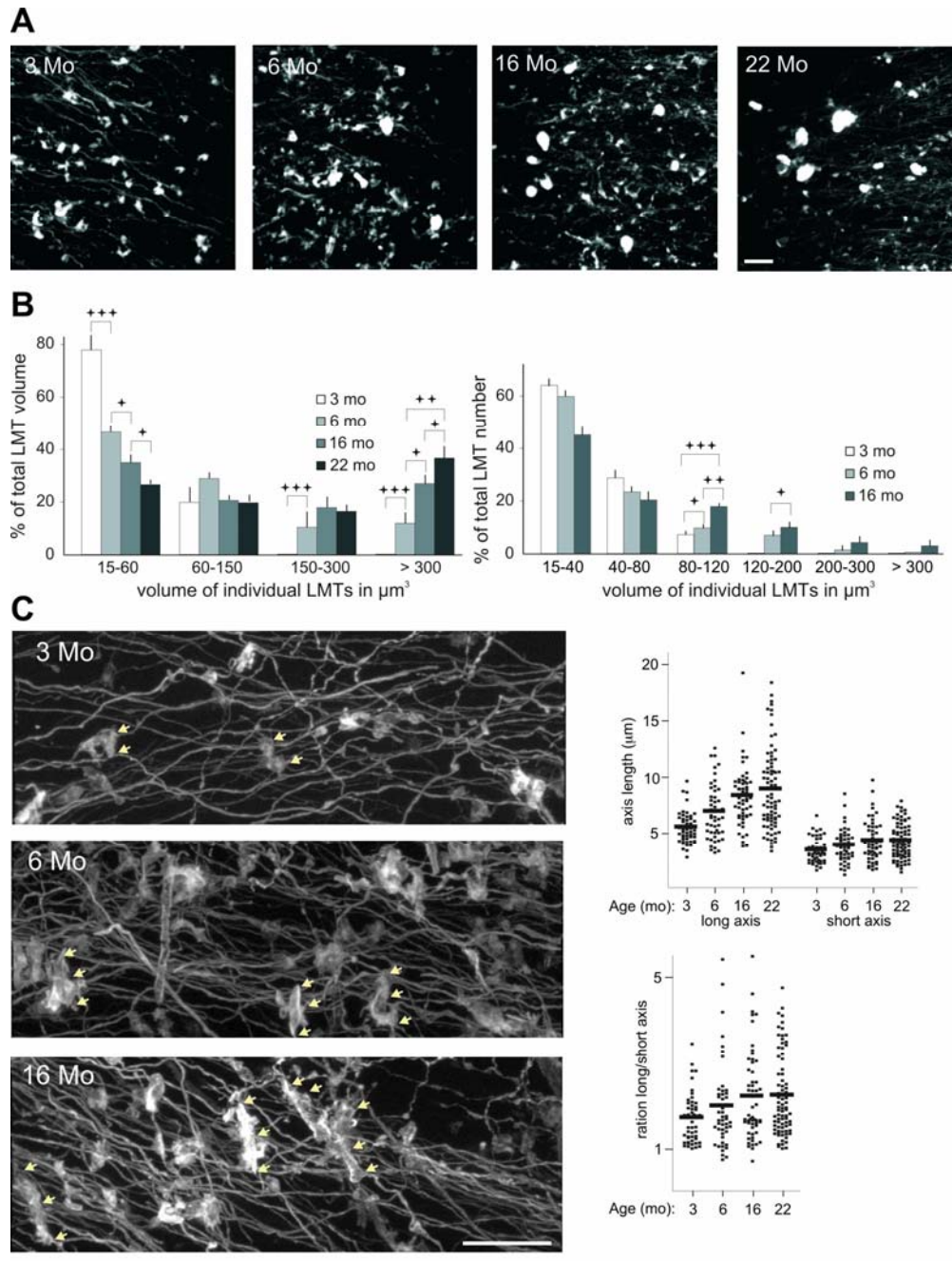
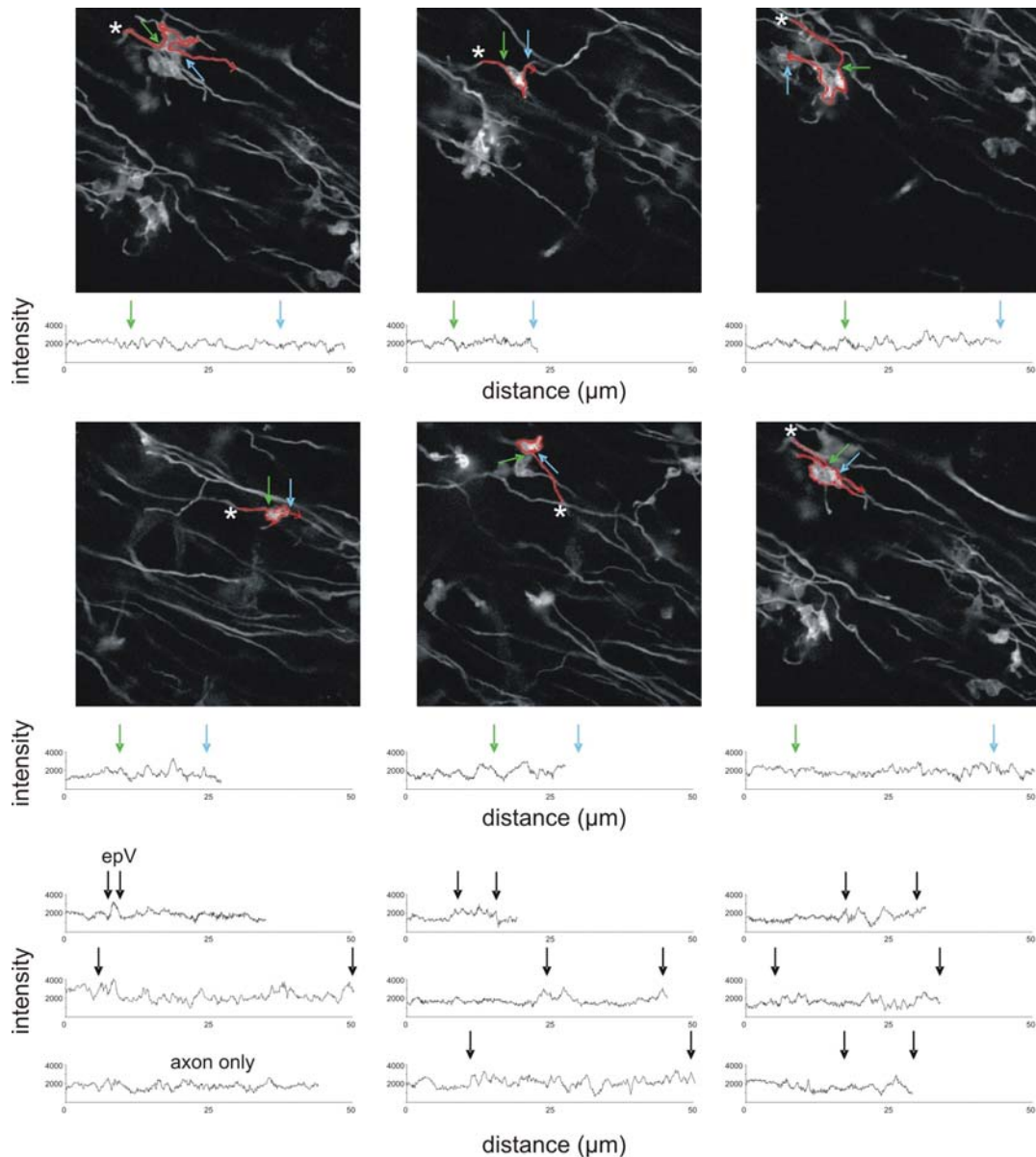


Figure 2. Life-long expansion of hippocampal LMT subsets along pyramidal dendrites.

A: Overview of LMT distributions in CA3a in male mice of different ages. Note higher incidence of large and very large LMTs in older mice. **B:** Quantitative analysis of LMT size distributions as a function of age (CA3a). Left: Overall contributions of LMTs grouped by volume to the total volume of LMTs in the sample. Note gradually increasing contribution of the larger LMTs (150-300, and > 300 μm^3) with increasing age. N= 9 cubes (from 3 male mice per age). One-way ANOVA: $p < 0.001$ (15-60 μm^3), $p = 0.45$ (60-150 μm^3), $p < 0.05$ (150-300 μm^3), $p < 0.001$ (>300 μm^3). Right: Relative prevalences of LMTs of different sizes as a function of age. N= 9 cubes (from 3 male mice per age). Post-hoc Student's t-test (left and right): $p < 0.05$ (*), $p < 0.01$ (**), $p < 0.001$ (***)). A Tukey HSD post-hoc test confirmed these significance relationships. **C:** LMT arrangements in CA3a as a function of age. Note longitudinal expansions of larger LMTs parallel to pyramidal neuron dendrites. Cream arrows delineate the longitudinal extension of some of the largest LMTs in each panel (3 Mo: 2 LMTs; 6 and 16 Mo: 3 LMTs each). Quantitative analysis: N= 80 LMTs, 3 mice per age; bars: median values; short axis perpendicular to longest axis; one-way ANOVA: $p < 0.01$ (ratio long/short). Scale bars: 25 μm .



Supplementary Figure 3. Homogeneity of axonal and LMT labeling by mGFP construct.

Upper six panels: examples of confocal images and corresponding signal intensity plots for the membrane stretches indicated by the red lines (6 months mouse). The following positions are indicated along the line, and again along the intensity plot: beginning of the trace (asterisk), beginning of LMT (green arrow), end of LMT (blue arrow). Lower nine histograms: more examples of membrane stretch intensities (mice: 6 months (first three), 16 months, and 22 months (last three)). Note that the signal intensity fluctuations do not change in amplitude or frequency along the membrane of axons or within LMTs. LMTs of different sizes, either from the same or distinct mice, and at different ages exhibited comparable intensity fluctuations, suggesting that mGFP did not accumulate selectively at LMT subsets. The variations in signal intensity appeared on a scale that was substantially smaller than the size of LMTs. Furthermore, changing thresholds in the volume rendering software, altered the sizes of individual objects to a comparable extent, without modifying the relative size differences of LMTs. Occasional areas of higher signal intensities within LMTs reflect highly convoluted membrane formations, which can be revealed by non-saturating imaging conditions (see Fig2A lower panels), and were also detected in the electron micrographs. Small areas of high membrane density and high signal intensity were detected at comparable frequencies at LMTs of different sizes, and from mice of different ages.

Experience-related increase of LMT-C complexities in adult mice

To investigate the possibility that experience might influence LMT-C size distributions and/or complexities, we analyzed LMTs of mice housed under enriched environment (EE) conditions known to promote brain and hippocampal plasticity (van Praag et al., 2000), and compared them to those of littermates kept under standard housing (Ctrl) conditions (see Experimental procedures). We carried out three types of EE experiments: 1) in the main set of experiments, mice were kept in EE from P40 to P80, and analyzed at P80 (EE-P40/P80); 2) in a second set of experiments aimed at comparing the effects of age and EE on LMT morphologies, mice were kept in EE from 4 months to 15 months, and analyzed at 15 months (EE-4Mo/15Mo); 3) the third set of experiments was aimed at determining whether changes due to EE (from 1 month to 4.5 months) might be maintained when mice were returned to standard conditions (from 4.5 months to 6 months; EE-1Mo/4.5Mo-Ctrl6Mo). As shown in Fig. 3A, all three experimental conditions produced a significant shift in the prevalence of larger LMT sizes compared to controls. At first approximation, EE thus appeared to accelerate the effects of age on LMT size distributions. However, a more detailed analysis revealed that the effects of EE and age on LMT-C morphologies were qualitatively different. Thus, EE conditions did not produce a corresponding net elongation of LMTs (Fig. 3B), and specifically induced a pronounced increase in the complexity of LMT-Cs, as revealed by the higher incidence of LMT-Cs with satellites, and the higher numbers of satellites per LMT-C (Fig. 3C). This specific increase in LMT size and satellite numbers was accompanied by a specific increase in the length and complexity of postsynaptic thorny excrescences upon EE (Fig. 3D). Significantly, increasing age did not lead to a comparable increase in postsynaptic thorn lengths (Fig. 3D), and LMTs of EE-4Mo/15Mo mice exhibited more satellites and complex outlines than those of corresponding Ctrl mice (not shown). Taken together, these results provide strong evidence for the existence of experience-related rearrangements of LMT-C connectivity *in vivo*, and suggest that EE conditions and age exert distinct influences on LMT-C rearrangement processes.

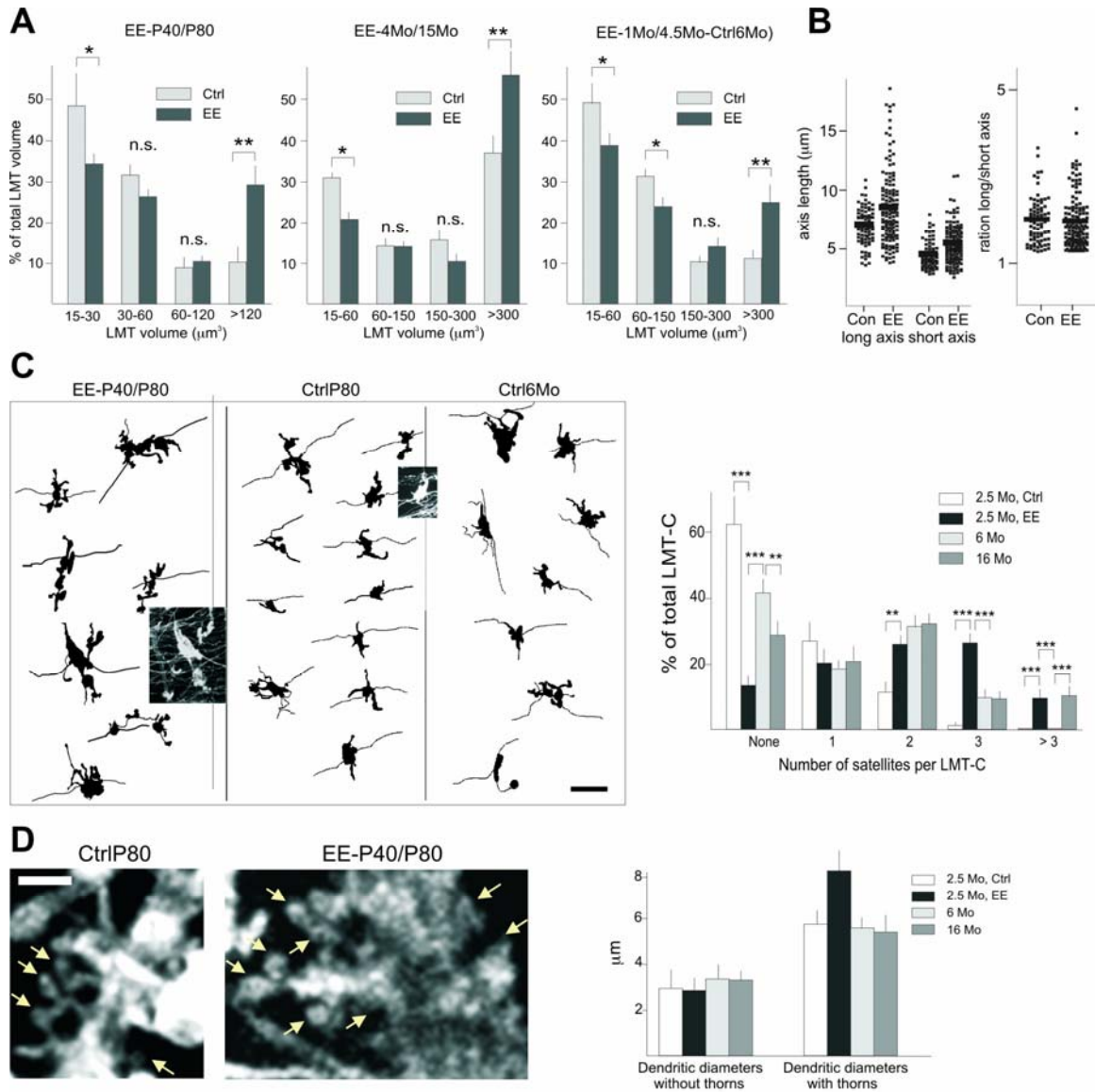


Figure 3. Experience-related increase in the complexity of LMT-Cs.

A: Quantitative analysis of LMT size distributions in the different EE protocols. Overall contributions of LMTs grouped by volume to the total volume of LMTs in the sample. Note how all EE experiments led to size distribution shifts resembling those induced by increasing age (compare to Fig. 2B, left). N=6 cubes (from 4 female mice each). Post hoc Student's t-test: $p < 0.05$ (*), $p < 0.01$ (**).

B: Quantitative analysis of long/short axis ratios in EE-P40/P80 versus control P80 mice. N=80 LMTs, 3 mice per condition; bars: median values; one-way ANOVA: non significant (ratio long/short).

C: Specific increase in the complexity of LMT-Cs induced by EE in vivo. Left: Camera lucida drawings of representative LMT-Cs (CA3a) from P80 mice, kept under EE (left) or Ctrl (center) conditions, and comparison to LMT-Cs from 6 months control mice. Note higher frequencies of satellites upon EE conditions. Right: Relative prevalences of LMT-Cs without and with satellites as a function of enriched environment and age. N=120 LMTs, from 3 female mice each.

D: Specific increase in thorny excrescence lengths and complexities upon EE conditions (CA3a). Left: High-magnification examples of thorny excrescences (mGFP signal; arrows point to some of the thorns). Right: Quantitative analysis of dendrite diameters excluding or including thorny excrescences (at clusters) as a function of EE and age. N=40 dendrites, from 2 female mice each. Bars: 15 (B), and 2 (C) μm .

Long-term rearrangements and growth of LMT-C subsets in slice cultures

To investigate LMT-C rearrangements and their regulation in a more experimentally accessible system, we analyzed organotypic slice cultures from *Thy1-mGFP^s* mice, where LMT-Cs can be imaged and treated in situ. The slices also allowed us to analyze entire sets of LMTs belonging to individual axons. In these cultures, LMT-Cs exhibited subcomponent arrangements, satellites and diversities comparable to those detected in vivo (Fig. 4A-C). Since we found that neurogenesis was extremely rare under our culture conditions (a total of 2 BrdU/calretinin double-positive cells out of 8 slices; BrdU labeling at day in vitro (DIV) 6, analysis at DIV9 or DIV16), age differences among individual granule cells could not account for the dramatic differences in LMT-C morphologies. Furthermore, comparable LMT-C diversities, including satellites were also detected when non-transgenic slice cultures were transfected with a cytosolic RFP construct (cRFP, see Fig. 6A), ruling out the possibility that the LMT-C morphologies were a property of transgene positive granule cells in *Thy1-mGFP^s* mice, or due to the activity of the Thy1 promoter in granule cells.

In order to capture any type of morphological plasticity by mossy fibers, we acquired high-resolution images of entire mossy fiber projections in CA3a-c (Fig. 4A) during periods ranging from a few days to several (up to 5) months. We found that when viewed at intervals of 3-5 days and more, many LMT-Cs exhibited dramatic alterations in their morphology (Fig. 4B, C). In contrast, even when mossy fibers were imaged for up to 3-4 months, we did not detect new process outgrowths from the mossy fiber axon itself. Instead, axonal dynamics was confined to remodeling and outgrowth events from LMT-Cs (the only exceptions were occasional short filopodial outgrowths from en-passant varicosities (De Paola et al., 2003), which are presynaptic terminals by mossy fibers onto inhibitory interneurons). In addition to changes in the shape and size of individual LMTs, we noticed that a fraction of LMT-Cs exhibited dramatic large-scale structural plasticity (Fig. 4B); this plasticity included process outgrowth or retraction events of up to more than 120 μm per day, and the rapid formation or loss of satellite LMTs (Fig. 4B). These satellite rearrangements frequently led to the establishment or dismantling of contacts

with distinct CA3 pyramidal neurons (Suppl. Fig. 4; in 5/5 investigated cases, the new contacts exhibited Bassoon-positive clusters (not shown, but see Fig. 5D)).

To determine whether LMT-C remodeling might lead to sustained changes in the arrangement and/or sizes of LMT-Cs in CA3 as a function of time, we repeatedly imaged the same mossy fibers and their identified individual LMT-Cs at 20 days intervals for periods of up to 4 months. We found that disappearance or appearance events, in which an entire LMT-C could either not be detected anymore at two subsequent imaging sessions, or appeared after DIV20, were not frequent (disappearances: 76/1500; appearances: 58/1500 LMT-Cs). Instead, many preexisting LMT-Cs grew in size during many months in slice cultures (Fig. 4C, D). To analyze the growth properties of LMT-Cs, we computed size differences for large sets of individual LMT-Cs as a function of time. Only LMT-Cs detectable throughout the entire experimental period were included in the analysis. Grouping of the results according to the absolute sizes of LMT-Cs at the first observation time revealed a net and sustained increase in the average sizes of persisting LMT-C over time in the slices, which was much more pronounced for larger LMT-Cs (Fig. 4D). A regression analysis revealed that the absolute magnitudes of LMT-C growth were strongly correlated to the initial sizes of individual LMT-Cs, but not to the actual sizes of LMT-Cs at successive imaging sessions (Fig. 4D). In a way strikingly reminiscent to the shifts of LMT sizes in vivo, LMT-C rearrangements in slices led to a gradual increase in the contribution by the largest LMT-Cs to total LMT-C volume (Fig. 4E). In further analogy to LMTs in vivo, LMT growth in slices mainly involved elongation, leading to a significant increase in the long-to-short axis ratio of LMTs with time in vitro (Fig. 4F). The fastest growing LMT-Cs also remodeled on a larger scale than the smaller LMT-Cs (not shown), suggesting that they exhibited stronger anatomical plasticity properties. LMT-C growth was not a consequence of the live imaging procedure, since slice cultures imaged for the first time at ages ranging from 20 days to 4 months in vitro exhibited average LMT-C sizes that were comparable to those that had been determined when following identified LMT-Cs longitudinally for a corresponding period of time in vitro (not shown). In addition to this presynaptic growth, and consistent with a net increase in active zone numbers (see Fig. 5D, E), we also detected remodeling,

growth and increased complexity of individual thorny excrescences (see Suppl. Fig. 5 for an example). We conclude that subsets of LMT-Cs rearrange extensively in organotypic slice cultures, altering the sets of pyramidal neurons with which they establish contacts through satellites, and consistently growing in size over many months. The arrangements and heterogeneities of LMT-Cs in slice cultures thus closely resemble those *in vivo*, and their remodeling and expansion properties exhibit features consistent with those inferred from comparing mice of different ages or housing conditions.

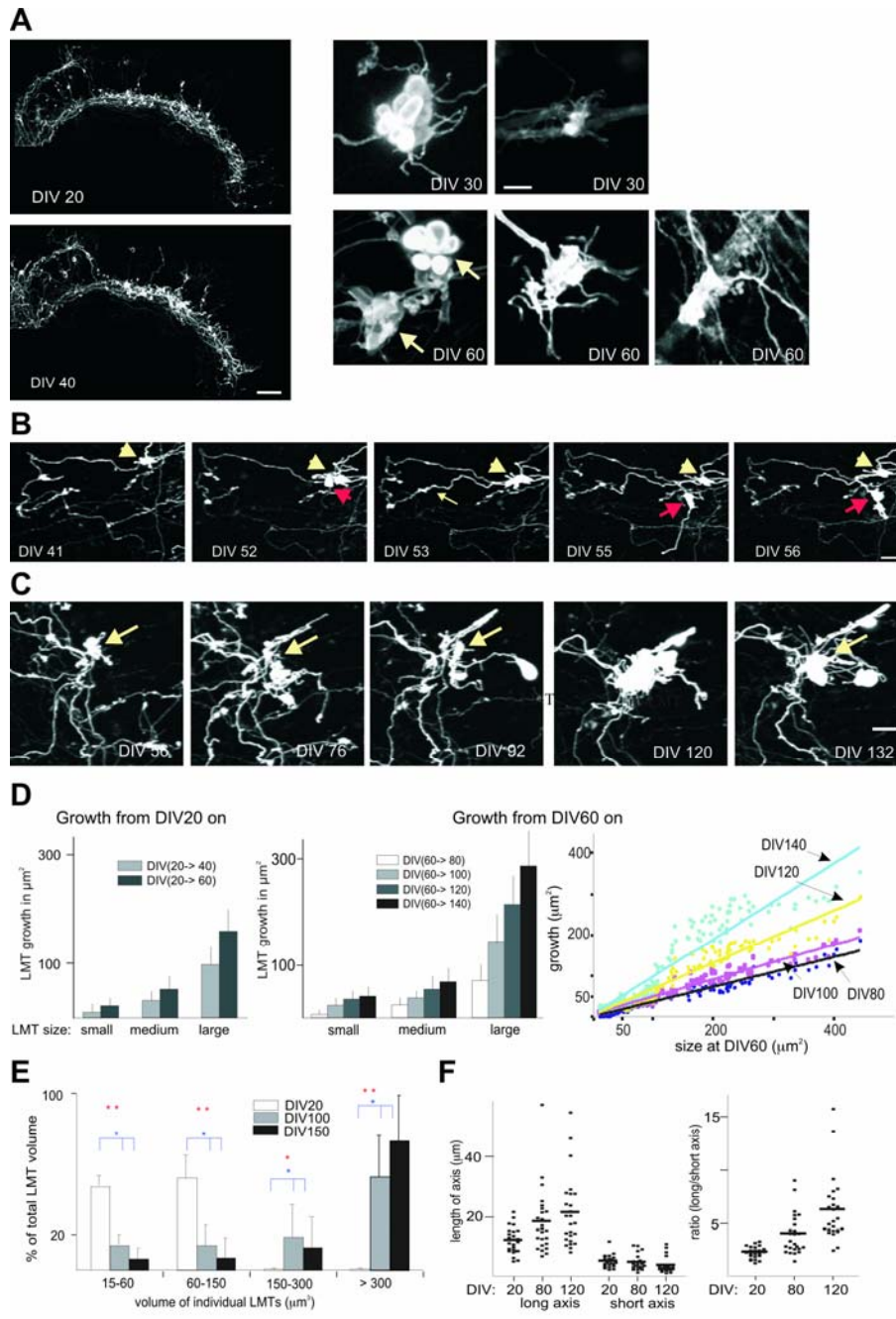
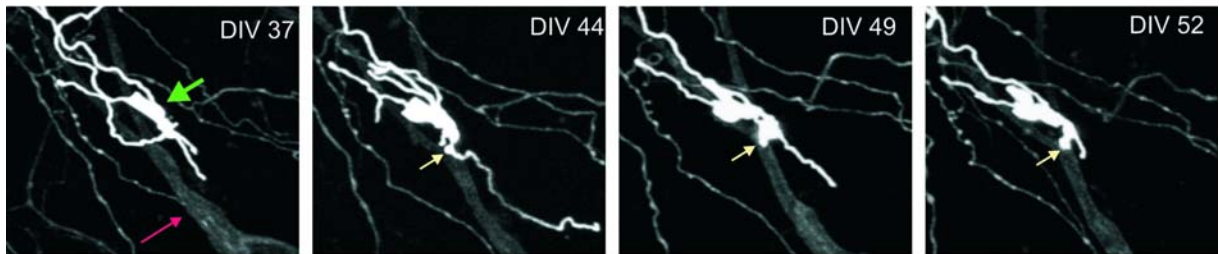
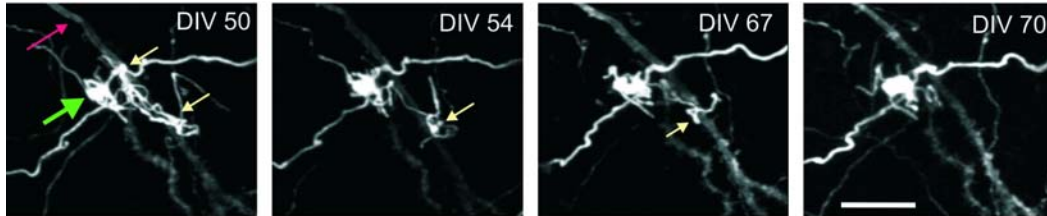


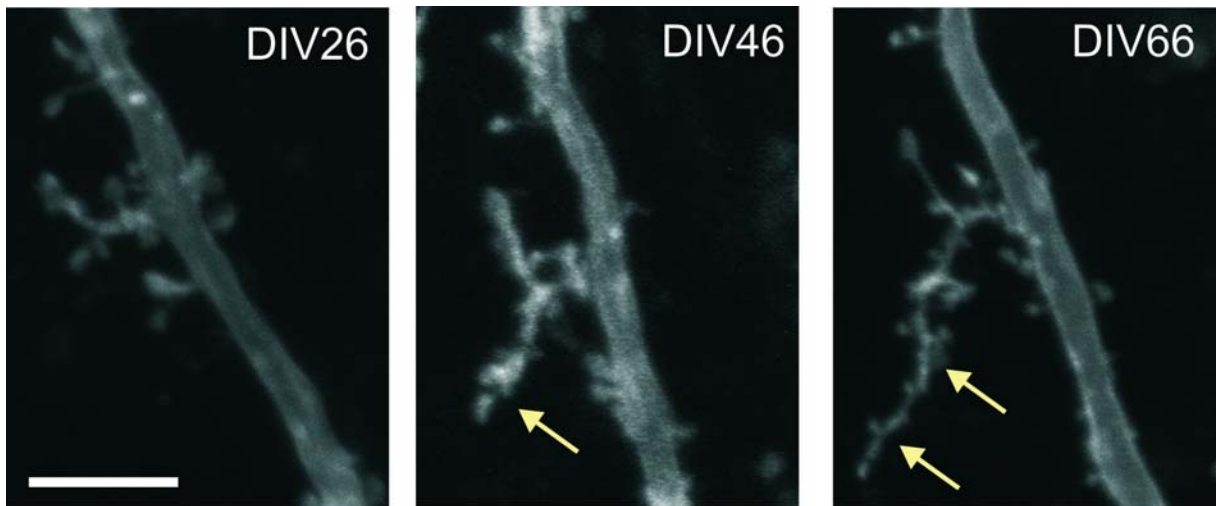
Figure 4. Rearrangements and growth of LMT-C subsets in organotypic slice cultures.

A: Left: Overview of an entire mossy fiber projection at DIV20 and DIV40. The dentate gyrus is to the left. Note growth of several LMTs. Right: Complexity and diversity of LMT-Cs in slice cultures. The images are maximum intensity projections (MIP), or raw data. The two LMTs in the lower left panel (DIV60, arrows) belong to the same complex. **B:** Large-scale anatomical plasticity at one LMT-C in CA3a (cream arrow). Note outgrowth of a long process within one day (DIV52 to DIV53; thin cream arrow), and formation of satellite LMTs (red arrows). **C:** Rearrangements and growth of a large LMT-C (cream arrow) from DIV56 to DIV132. **D:** Quantitative analysis of LMT-C growth in slice cultures. Left, and middle panel: Sizes of individual identified LMT-Cs that persisted throughout the analysis were compared at the indicated times, and LMT-Cs were then grouped into small ($< 30 \mu\text{m}^2$), medium ($< 60 \mu\text{m}^2$) and large ($\geq 60 \mu\text{m}^2$), according to their sizes at DIV20. $N=50$ identified LMT-Cs each, from 5 slice cultures. Right: Linear regression analysis of identified LMT-C sizes between DIV60 and DIV140. Linear correlation values (R^2): 0.95 (DIV80), 0.95 (DIV100), 0.92 (DIV120), 0.88 (DIV140). **E:** LMT-C volume distribution as a function of age. Contribution of LMT-C size groups to the total volume of LMT-Cs in slice cultures (comparable to the data of Fig. 2B). $N=5$ cubes, from 5 slices. One-way ANOVA (orange asterisk): $p < 0.05$ (*), $p < 0.01$ (**). Post-hoc t-test (blue): $p < 0.05$ (*). **F:** Quantitative analysis of long/short LMT axis as a function of age in vitro. $N=20$ LMTs, from 5 slices; bars: median values; one-way ANOVA: $p < 0.001$ (ratio long/short). Bars: 100 (A, left), 5 (A, right), and 10 μm (B, C).

A**B**

Supplementary Figure 4. Examples of LMT-C outgrowths establishing satellites on distinct pyramidal neurons in CA3a stratum lucidum.

Green arrows: main LMT; red arrows: mGFP-positive pyramidal dendrite. Physical contacts were analyzed using Imaris (3D) software. A: Example of new contact. This LMT-C did not contact the mGFP positive dendrite at DIV37. A contact was detectable at DIV44 (cream arrow), and a distinct LMT subunit (cream arrows) was maintained beyond DIV52. This LMT-C is linked to its mossy fiber (short segment just visible at upper left corner, DIV52 panel) through a ca. 35 μ m side-branch. B: Example of contact loss. The LMT-C contacts the mGFP positive dendrite at two positions (cream arrows) through satellites at DIV50. One of the contacts has been lost at DIV54, and the second one is lost between DIV67 and DIV70. Bar: 15 μ m.



Supplementary Figure 5. Elongation and increased complexity of a large thorny excrescence in slice culture (mGFP signal). Note how the thorny excrescence has elongated at DIV46 and DIV66 (arrows). Shorter thorny excrescences along this pyramidal neurons dendrite in CA3 exhibit smaller changes. Bar: 10 μ m.

Larger LMTs produce a stronger excitation of postsynaptic pyramidal neurons

Do LMT-C rearrangements and growth lead to changes in the functional connectivity of individual LMT-Cs? To determine whether larger LMTs might differ from smaller LMTs with respect to the strength of their output onto pyramidal neurons in CA3, we carried out intracellular pair recording experiments in slice cultures (DIV20-30). One mGFP-positive granule cell was recorded and stimulated under current-clamp mode and a second electrode filled with sulforhodamine or Lucifer-yellow was used to label CA3 pyramidal cell dendrites present in the close vicinity of one of its core LMTs (either its largest core LMT, or a smaller core LMT; see Experimental procedures). These CA3 neurons were then recorded under voltage clamp, and tested for monosynaptic connectivity to the mGFP-positive granule cell. In this way, we achieved intracellular pair-recordings among synaptically connected granule cells and pyramidal neurons in about 10% of the attempts (Fig. 5A; see Methods). We found that DCG-IV-sensitive (Ishida et al., 1993) excitatory postsynaptic responses evoked by granule cell stimulation were substantially stronger at larger LMTs than at the smaller LMTs (Fig. 5A). Significantly, the paired-pulse facilitation and frequency-dependent facilitation properties of large and small LMTs were not detectably different (Fig. 5B, C), suggesting that smaller (weaker) and larger (stronger) LMTs exhibit proportional short-term presynaptic plasticity, and that the greater synaptic strength might reflect a larger number of active zones in larger LMTs. To determine whether and how differences in the sizes of LMTs might reflect differences in numbers of synaptic release sites, we analyzed Bassoon-positive active zones (tom Dieck et al., 1998) in individual LMTs (Fig. 5D, E). We found that all elements of LMTs contained numerous active zones (Fig. 5D, see also Suppl. Fig. 2), and that LMT sizes and active zone numbers were closely correlated independent of time in culture (Fig. 5E). We found comparable correlations between LMT volumes and active zone numbers for LMTs and their satellites in vivo (N.G. and P.C., unpublished results). We conclude that the large variations among LMT sizes reflect corresponding variations in active zone numbers, that the expansion of LMT-Cs over time reflects an increase in the number of release sites at those LMT-Cs, and that the establishment of satellites reflects the addition of release sites by the LMT-C onto the same or new postsynaptic pyramidal neurons in CA3. Taken together, the results thus suggest that the profound anatomical

rearrangements of individual LMT-Cs in slice cultures reflect corresponding rearrangements of their local connectivities onto pyramidal neurons in CA3.

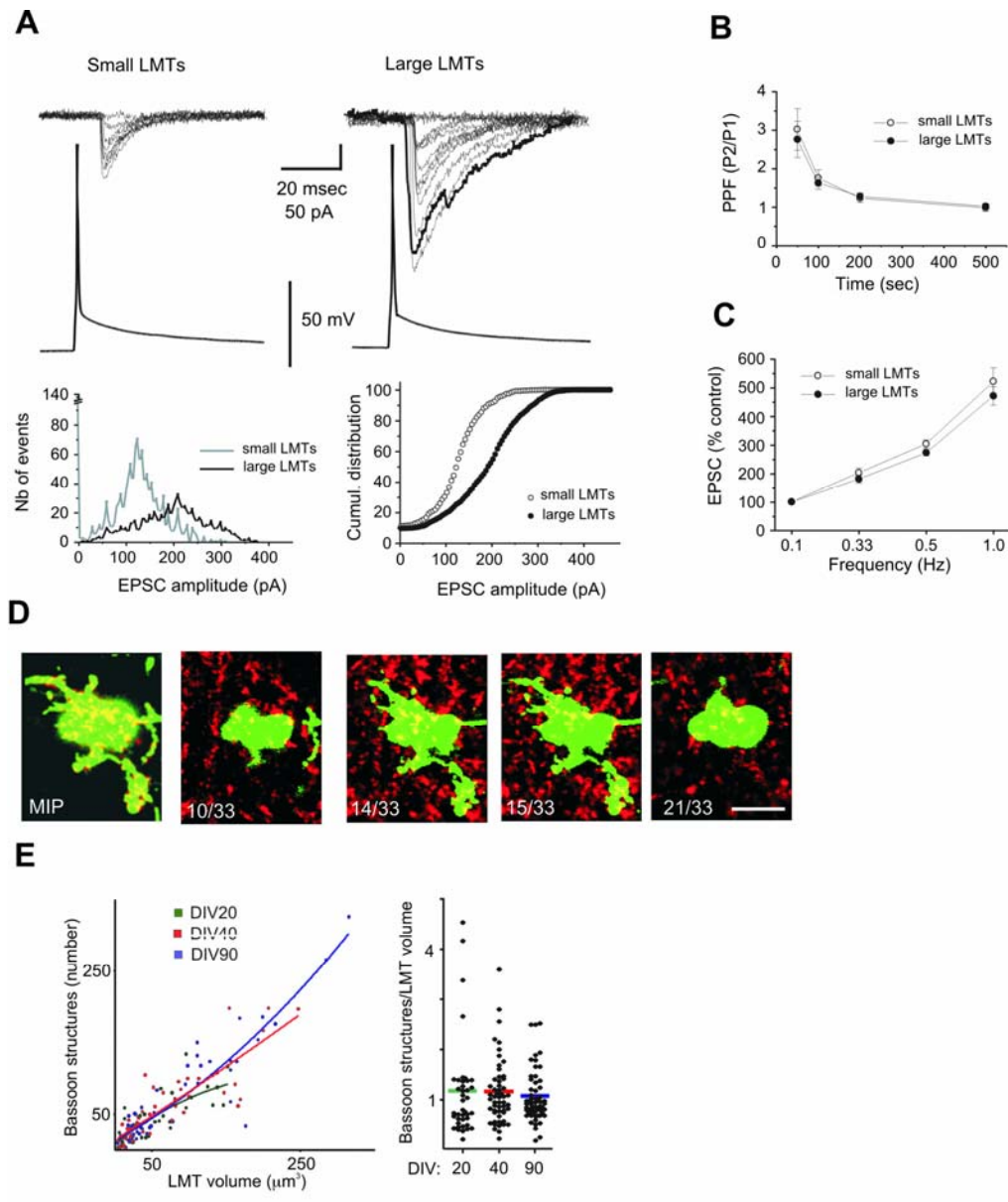


Figure 5. Larger LMTs elicit stronger postsynaptic responses in pyramidal neurons and have more active zones.

A: Monosynaptic CNQX-sensitive responses recorded in CA3 pyramidal neurons upon intracellular stimulation of mGFP-positive granule cells in DIV20-30 slice cultures. Top: ten superimposed recordings for small and large LMTs. Bottom: Amplitude distribution histogram (left) and cumulative plot of evoked amplitudes for the same set of data. Holding potential: -70mV; Bicuculine 10 μM , D-AP5 80 μM . Small LMTs: 8-25 μm^2 ; large LMTs: 80-150 μm^2 . Total of evoked currents: 1264 (small LMTs) and 923 (larger LMTs). **B:** Paired-pulse facilitation does not differ when recorded in large or small LMTs. N=5, $p>0.1$. **C:** Frequency-dependent facilitation does not differ in small and large LMTs. Data normalized to 0.1Hz values. Averages of 15 traces each; N=5, $p>0.1$. **D:** Distribution of active zones within an LMT-C with a satellite (DIV80); Bassoon immunocytochemistry red; mGFP green. Left: MIP; Bassoon labeling outside the LMT was cropped out. Right panels: single confocal planes (33 planes total; plane distance 0.3 μm). Note presence of active zones throughout the LMT and in its satellite. Bar: 5 μm . **E:** Contents of Bassoon-positive structures (active zones) as a function LMT volume and age in vitro. Left: regression analysis; the lines are polynomial fits. Note comparable, and near to linear relationships between LMT volume and active zone contents at DIV20, 40 and 90. Right: Active zone number/LMT volume ratios; bars: median values; N=80 LMTs per condition. One-way ANOVA: $p=0.76$ (i.e. no differences as a function of age).

Different LMT-Cs belonging to the same mossy fiber exhibit distinct plasticity properties

What underlies the dramatic differences in LMT-C arrangements, sizes and anatomical plasticity in slice cultures? One possibility was that differences in LMT sizes might reflect differences among granule cells and their mossy fibers. Alternatively, LMT-Cs belonging to the same mossy fiber might differ among each other. To address this issue, we first analyzed a large set of individual mossy fibers, focusing on the relative sizes of their LMT-Cs, and on whether or not they established satellites. To our surprise, we found that for the majority of mossy fibers (34/40) one LMT-C was at least three times as large as any of the remaining LMT-Cs along the same mossy fiber, which tended to exhibit more comparable sizes (Fig. 6A-C). These size relationships among the LMT-Cs of a given mossy fiber were detectable for slice cultures of any age beyond 5DIV (not shown), and were not restricted to granule cells exhibiting Thy1-driven mGFP expression (Fig. 6A).

We next reasoned that mossy fibers might exhibit some larger LMT-Cs at any given time, but that their position might change with time, in parallel with LMT-C remodeling and growth; alternatively, individual “plastic LMT-Cs” might maintain their growth properties and augment their relative sizes over time. We therefore carried out longitudinal studies, in which we followed all individual LMT-Cs of identified mossy fibers over months in slice cultures. We found that individual “plastic LMT-Cs” maintained this distinguishing property over months in culture, when they kept growing more than the smaller LMT-Cs (Fig. 6B, C). This led to a gradual shift of the total presynaptic volume of individual axons towards the largest LMT-C (Fig. 6E). Since “plastic LMT-Cs” also recovered more effectively from treatments that reversed LMT-C growth (see below; Fig. 6D), we concluded that the large differences in the plasticity and growth of LMT-Cs reflect local properties of individual LMT-Cs.

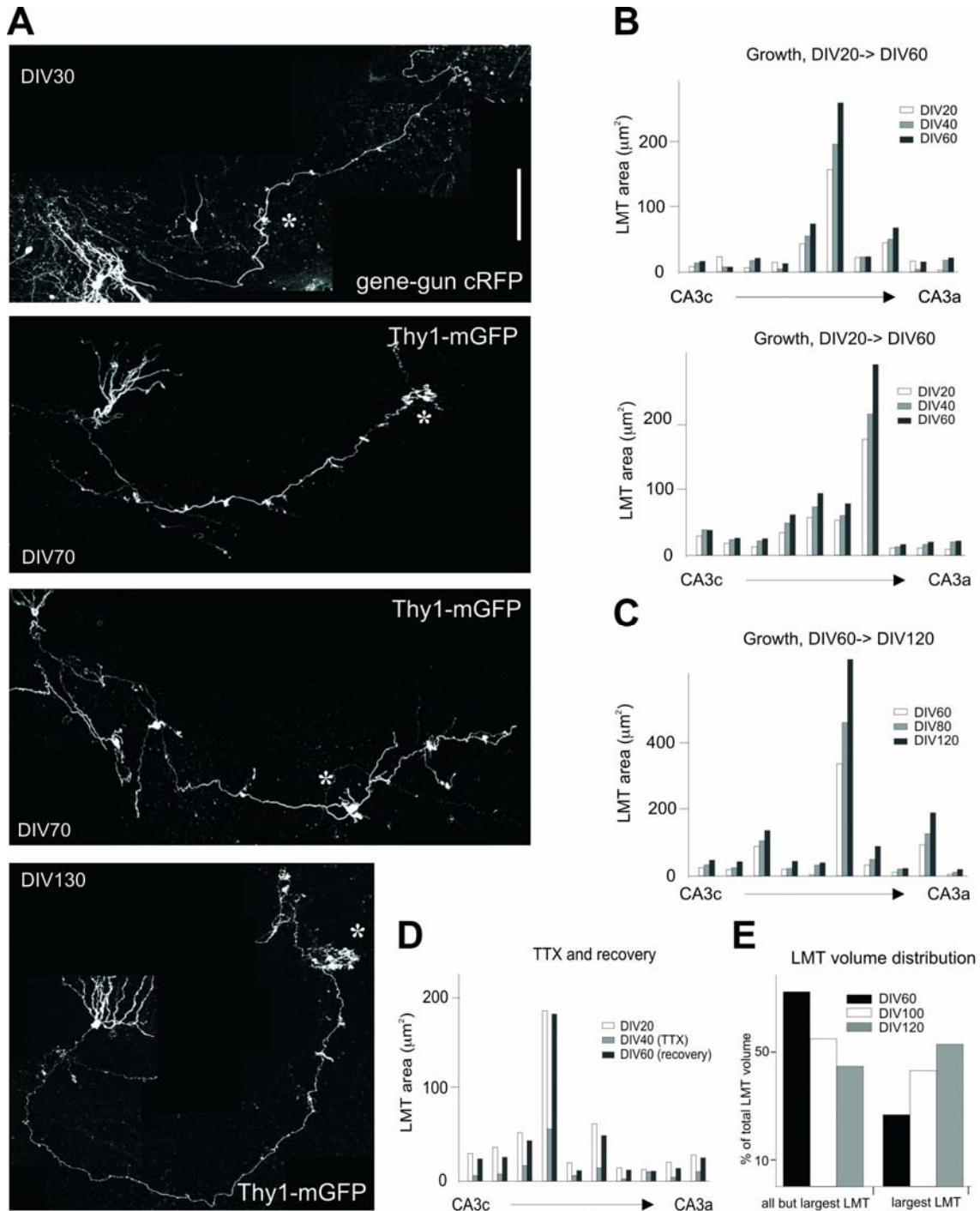


Figure 6. Plasticity and growth are specific properties of individual LMT-Cs, not mossy fibers.

A: Top: Example of mossy fiber from non-transgenic DIV30 slice expressing cRFP (gene-gun transfection); Middle and bottom: examples of DIV70 (two of them) and DIV130 (one) slice cultures, each with one well-labeled mGFP-positive granule cell. Cell bodies and dendrites are to the left; asterisk: position of the largest LMT-C. The cRFP expressing mossy fiber exhibits its largest LMT-C within the infrapyramidal projection; as expected, the largest LMT-C at DIV30 is smaller than those at DIV70, which are smaller than that at DIV130. **B-C:** Growth of individual LMTs between DIV20 and DIV60 (b), or DIV60 and DIV120 (c). Each graph represents one mossy fiber and its individual LMTs (CA3c to the left). **D:** Larger LMTs maintain this distinction when recovering from shrinkage induced by TTX, Experimental conditions as described for Fig. 7. **E:** Redistribution of total LMT volume as a function of age in vitro between largest LMT-C, and remaining LMT-Cs belonging to the same axon. Median values from 3 individual axons. Bar: 140 μm .

Local, activity-dependent regulation of LMT-C maintenance and growth

To investigate the mechanisms regulating LMT-C remodeling and growth, we carried out pharmacological experiments in slice cultures. Experimental conditions consisted of acquiring one set of images at DIV20 (control conditions), of including pharmacological agents to the culture medium during the next 20 days, of a second imaging session at 40DIV, followed by returning slices to control medium conditions. Further imaging at 60DIV and 80DIV was carried out to verify that any drug effect was reversible. In additional experiments aiming at excluding effects restricted to comparatively young slice cultures, we also carried out treatment experiments starting at 60DIV.

Under control conditions, current-clamp recordings of granule cells in slice cultures showed a level of background firing activity in the range of 3-3.5 Hz with occasional bursts of action potentials very much consistent with the firing properties reported *in vivo* (e.g. Penttonen et al., 1997). We found that the inclusion of a TTX dose sufficient to completely and reversibly block spiking activity in the slices (not shown) not only blocked LMT-C growth, but led to a substantial reduction in LMT-C average sizes in both, young (DIV20) and more mature (DIV60) slices (Fig. 7A, B). This reduction affected both the sizes of individual LMTs and the number of satellites by LMT-Cs (not shown). It was accompanied by a corresponding reduction in the number of active zones per LMT (i.e. average numbers of active zones per LMT volume were not affected by TTX; Fig. 7C), indicating that it reflected a net decrease in the number of release sites in the slices. The inhibitory neurotransmitter GABA also induced LMT-C shrinkage (Fig. 7B). The absolute extent of LMT-C shrinkage in the presence of TTX or GABA (or DCG-IV, see below) was closely correlated to LMT-C size (Fig. 7B), suggesting that both growth and maintenance of “plastic LMT-Cs” depend on spiking activity. Shrinkage of LMT-Cs in the presence of TTX was reversible (Fig. 7B). Significantly, larger LMT-Cs resumed growth at higher rates than smaller LMT-Cs when recovering from the TTX treatment, and this again applied to both populations of identified LMT-Cs (Fig. 7B), and the individual LMT-Cs of identified mossy fibers (Fig. 6D).

To determine whether transmitter release from LMTs is required to sustain LMT-C growth, we carried out experiments in the presence of the mGluR2 agonist DCG-IV (Ishida et al., 1993), which produces a specific and complete blockade of evoked transmitter release from LMTs in hippocampal slices (Kamiya et al., 1996). We found that DCG-IV was as effective as TTX in reversibly suppressing LMT-C growth and inducing LMT shrinkage (Fig. 7A, B). Interestingly, and unlike TTX, DCG-IV produced an over-proportional decrease in the number of active zones per LMT (Fig. 7C). We conclude that LMT-C growth and maintenance depend on spiking activity in the slices, and on the local release of transmitter from LMTs.

Long-term potentiation at mossy fiber to pyramidal neuron synapses in CA3 is NMDA receptor independent, PKC dependent, and predominantly controlled presynaptically. To determine whether signaling pathways related to the induction of LTP at these synapses might influence LMT growth and maintenance in slices, we carried out experiments in the presence of the specific inhibitor of PKC Chelerythrine. We found that the PKC inhibitor augmented growth at small LMTs, but caused shrinkage at large LMTs (Fig. 7D). At closer inspection, the growth of small LMTs was not distributed equally among many small LMTs, but instead led to the emergence of 1-2 larger LMTs, concomitant with shrinkage of the original large LMTs (not shown). In contrast, and in keeping with its lack of effect on synaptic plasticity at mossy fiber to pyramidal neuron synapses, the NMDA receptor antagonist APV did not significantly affect LMT growth (Fig. 7D). We conclude that differences among the growth properties of individual LMT-Cs are maintained across conditions allowing or preventing growth at all LMTs, suggesting that the relative extent of LMT growth is regulated locally at individual LMTs. However, this maintenance of LMT asymmetry depends on PKC activity, suggesting that whether a particular LMT grows over-proportionally might be affected by conditions influencing functional plasticity at these synapses.

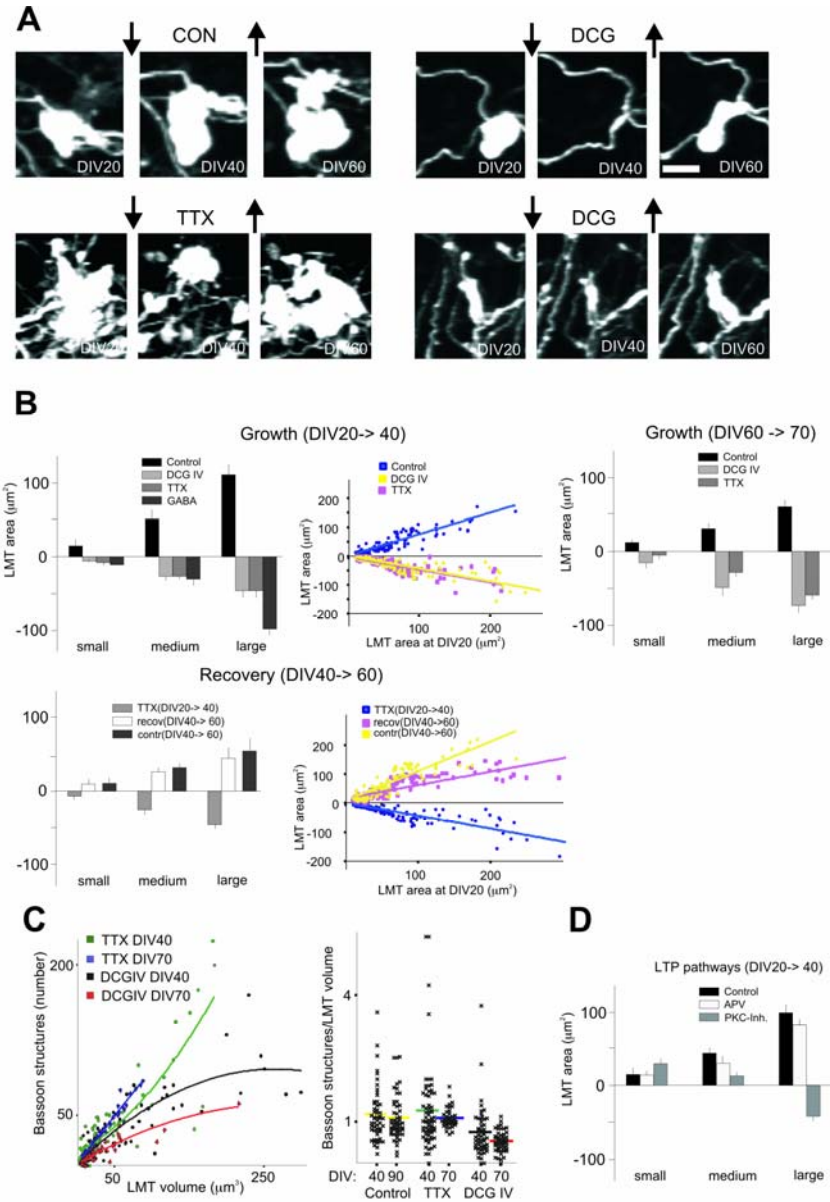


Figure 7. Regulation of LMT-Cs maintenance and growth by spiking activity, mGluR2 and PKC.

A: Reversible shrinkage of LMT-Cs in the presence of either TTX, or the mGluR2 agonist DCG-IV. Drugs were added to the slice medium just after the first imaging session at DIV20 (arrows pointing down), and washed out just after the second session at DIV40 (arrows pointing up). CON: medium change without added drugs. **B:** Quantitative analysis of LMT growth in the presence or absence of TTX, DCG-IV or GABA. Upper row: Shrinkage of LMT-Cs in the presence of drugs. Left and middle: Experimental conditions as in (A). Left: grouping of identified LMT-Cs according to sizes as described for Fig. 4. Middle: regression analysis of LMT-C growth versus LMT size at DIV20. Linear regression correlations (R^2): 0.85 (control), 0.81 (TTX), 0.86 (DCG-IV). Right: Drug-induced shrinkage of LMT-Cs in 2-months cultures. TTX or DCG-IV were added at DIV60, and their effects were analyzed at DIV70. Grouping of identified LMT-Cs as described for Fig. 4. Lower row: Recovery of LMT-C growth upon washout of TTX. Left and middle panel as described above. Linear regression correlations (R^2): 0.80 (DIV40, TTX), 0.78 (recovery TTX, DIV60), 0.78 (control DIV60). Growth values for control conditions are included for comparison (dark bars). N=50 LMT-Cs per size group, from 5 slice cultures. **C:** Active zone contents of LMTs in the presence of TTX or DCG-IV, as a function of LMT volume and age in vitro. Values are for 20 days (DIV40) or 10 days (DIV70) in the presence of drug. Left: regression analysis of LMT volume versus active zone numbers for different experimental conditions. The curves are polynomial fits. Right: distribution of active zone per LMT volume values. Note how DCG-IV induces an over-proportional reduction in the numbers of active zones per LMT volume. N=50 LMT-Cs per size group, from 5 slice cultures. One-way ANOVA for TTX versus DCG-IV: $p < 0.01$. **D:** Effect of PKC inhibitor Chelerythrine and NMDA receptor antagonist APV on LMT maintenance and growth. Experimental conditions and grouping of data as described in (B, upper row, left). N=50 LMT-Cs per size group, from 5 slice cultures. The effects of the PKC inhibitor (see text) were significant for all LMT size categories: $p < 0.01$ (small), $p < 0.05$ (medium), $p < 0.001$ (large); Student's t-test. Bar: 10 μm .

DISCUSSION

In this study we provide evidence that functionally important presynaptic complexes in the hippocampus rearrange their local connectivities throughout life, and that these rearrangements are influenced by experience and age. We first show how LMT-Cs are local presynaptic terminal arborizations of mossy fibers, exhibiting large differences in the magnitude and divergence of their local connectivities with pyramidal neurons in CA3. We then provide two independent lines of evidence that LMT-Cs rearrange their connectivities in the adult: we show that subsets of LMT-Cs expand along CA3 dendrites throughout life, and that the complexities of LMT-Cs are dramatically enhanced by housing mice in an enriched environment. We then analyze identified LMT-Cs longitudinally in organotypic slice cultures, and show that: 1) the arrangements and heterogeneities of LMT-Cs in slice cultures resemble closely those *in vivo*; 2) subsets of LMT-Cs rearrange their connectivities, and grow over weeks and months in slice cultures in patterns resembling those detected *in vivo*; 3) the anatomical rearrangements reflect corresponding rearrangements in functional connectivity; 4) the marked differences with respect to plasticity and growth reflect local properties of individual LMT-Cs, not their mossy fibers; 5) LMT-C growth and maintenance require spiking activity in the slices, and mGluR2-sensitive transmitter release from LMTs; 6) the stable maintenance of LMT-C size heterogeneities involves PKC activity. Below, we discuss the implications of these findings and their relationship to those from previous studies, focusing on the rearrangements of LMT-C connectivity, the regulation of these processes by synaptic activity and experience, and their possible impact on hippocampal network activity.

Rearrangements of LMT-C connectivity in the adult

Our results provide novel insights into the organization of mossy fiber terminals in CA3. While the complexity of LMTs had been documented by previous studies (Chicurel and Harris, 1992; Danzer and McNamara, 2004; Gonzales et al., 2001), imaging using *Thy1-mGFP^s* mice has revealed unsuspected further features, including the existence of satellite LMTs, a great diversity of sizes and morphologies, and the massive sizes of some of these terminals. It does not seem surprising that the satellites have been missed by previous studies, as they would have been very difficult to detect using electron

microscopy or traditional fill methods. Furthermore, most previous studies have focused on LMTs from young animals (ca. 3 weeks), when diversity and complexity are less pronounced. In a further departure from the results of previous studies, we provide evidence that individual LMT-Cs can contact several distinct pyramidal cells in CA3. Based on these results, we propose that instead of terminal boutons, LMTs should be considered as local terminal arborization complexes of mossy fibers (LMT-Cs), exhibiting great diversity in their sizes, and in their degrees of divergence onto pyramidal neurons in CA3. Although the satellites can clearly contact distinct pyramidal neurons, do exhibit numerous Bassoon-positive active zones, and are highly enriched in Synapsin I and synaptic vesicle markers (not shown), their functional status remains to be investigated. The recent demonstration that LMT membranes contain voltage-gated Na-channels and amplify action potentials (Engel and Jonas, 2005) is certainly consistent with the notion that the interconnected compartments of LMT-Cs can be efficiently triggered to release transmitter. Detailed functional investigations of these compartments should yield valuable novel insights into the function of these complex terminal structures.

We provide evidence that subsets of hippocampal LMT-Cs are sites of considerable anatomical plasticity in adult mice. This is consistent with results from recent studies, which have provided evidence for structural plasticity of presynaptic terminals in hippocampal slice cultures (De Paola et al., 2003), and in adult mouse barrel and visual cortex in vivo (De Paola et al., 2006; Stettler et al., 2006). A critical advance over previous studies is, however, that the structural plasticity of LMT-Cs leads to long-term rearrangements of local connectivity, suggesting that it might be an important aspect of hippocampal circuit plasticity in the adult. The rearrangements affected LMT-C connectivity in two distinct ways: 1) expansions along dendrites from the same pyramidal neuron added transmitter release sites, presumably altering the functional impact of mossy fiber spiking onto that particular postsynaptic pyramidal neuron in CA3; 2) the establishment of satellite LMTs onto distinct pyramidal neurons added and/or removed postsynaptic targets to individual LMT-Cs, altering the extent and quality of local divergence of pyramidal neuron innervation by individual LMT-Cs (Fig. 8).

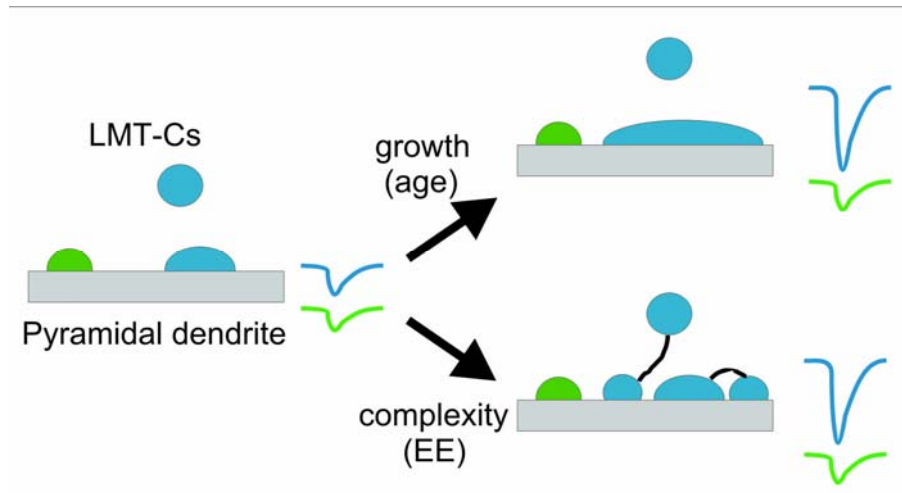


Figure 8. Schematic of how local anatomical rearrangements can lead to changes in the functional connectivity between mossy fiber LMT-Cs and CA3 pyramidal neurons in the adult.

Grey box: pyramidal neuron dendrite in stratum lucidum; blue and green ovals: individual LMT-Cs. The two blue LMT-Cs belong to distinct granule cells that are sometimes active at the same time (blue pattern of activation); green and blue are not recruited at the same time. The blue and green traces to the right indicate the postsynaptic excitatory responses of this dendrite at equal mossy fiber firing frequencies. Left: blue and green activation patterns elicit comparably weak postsynaptic responses. Right, upper part: lower blue LMT-C has expanded along the pyramidal dendrite (higher number of active zones), leading to potentiation of the blue postsynaptic response (e.g. age-related growth). Right, lower part: both blue LMT-Cs have established satellites onto the pyramidal dendrite (higher convergence of active zones), leading to potentiation of the blue postsynaptic response (e.g. enriched environment).

Regulation of LMT-C rearrangements

Having uncovered evidence for long-term rearrangements of hippocampal LMT-C connectivity influenced by experience in adult mice, we turned to organotypic slice cultures to investigate mechanisms controlling LMT-C remodeling. As outlined above, LMT-Cs in slices exhibited arrangements, heterogeneities, and remodeling properties consistent with the notion that regulation of their anatomical plasticity underlies principles comparable to those in vivo. Since the functional properties of hippocampal slice cultures and resemble those of acute slices (e.g. Gahwiler et al., 1997), it seems unlikely that principles underlying LMT-C rearrangements in vivo would be fundamentally different from those in slice cultures. On the other hand, slices cultures do lack inputs from entorhinal cortex and neuromodulatory systems, suggesting that important aspects of connectivity and network activity in slices might be significantly different from in vivo. Investigations in slice cultures thus provide valuable insights into mechanisms controlling LMT-C rearrangements, but the actual impact of these principles for hippocampal plasticity and their age-related properties will eventually need to be verified in vivo.

This study provides evidence that anatomical plasticity and rearrangements of connectivity by LMT-Cs in slice cultures are controlled by local factors. The results suggest that “plastic LMT-Cs” differ stably from less plastic ones with respect to some property affecting anatomical growth, either intrinsically, or in response to graded signals from their local environment. Interestingly, maintenance of the original set of “plastic LMT-Cs” depended on PKC activity, suggesting that synaptic plasticity might have a significant impact on the outcome of LMT-C rearrangements. That in the presence of the PKC inhibitor new growth and shrinkage of LMT-Cs appeared to be balanced suggest that in addition to local factors, LMT-C rearrangements might also be influenced by the allocation of synaptic resources within individual axons. The finding that conditions affecting synaptic plasticity influenced synaptic turnover is reminiscent of several recent studies relating LTP and LTD to spine density and growth (e.g. Muller et al., 2000; Nagerl et al., 2004; Zhou et al., 2004). We find that larger LMT-Cs can be detected at all positions along individual mossy fibers in slices, and along the mossy fiber projection in CA3 *in vivo*. It is well established, that there is topography with respect to connectivity in the hippocampus, and that pyramidal neurons at distinct positions along CA3 project to different regions along CA1 (Johnston and Amaral, 1998). Our results thus raise the possibility that individual mossy fibers might exhibit topographical preferences with respect to the anatomical plasticity and strength of their outputs along CA3 in the adult; such preferences might contribute to topography in the flow of information from the dentate gyrus to CA1.

In addition to uncovering a requirement for synaptic activity in LMT-C maintenance and growth, the pharmacological experiments in slice cultures have provided insights into how LMT-C plasticity might be regulated locally. The finding that LMT-C growth was reversed by an mGluR2 agonist known to specifically block transmitter release from LMTs suggests that local release is important to promote growth. Released transmitter might act on presynaptic receptors (Nicoll and Schmitz, 2005), to promote growth. In addition, several studies have provided evidence that the thorny excrescences of pyramidal cell dendrites in CA3 are particularly sensitive to experience, and can expand

or shrink in response to learning, stress and hormones (e.g. McEwen 1999; Kavalali et al., 1999; Sandi et al., 2003). A second, non-exclusive possibility is thus that synaptic activity might influence LMT growth indirectly, by regulating thorny excrescence growth. This might involve activation of AMPA receptors, since their blockade counteracts growth by individual LMTs in slices (I.G. and P.C., unpublished results). The high affinity of mGluR2 for glutamate, and the peripheral presynaptic distribution of mGluR2 at LMT synapses (Nicoll and Schmitz, 2005) suggest a further mechanism through which stronger LMTs could destabilize neighboring weaker LMTs via ambient glutamate. Such a mechanism might mediate competitive interactions between LMTs converging within thorny excrescence clusters in a way reminiscent of the role of activity in synapse elimination processes (Lichtman and Colman, 2000). It had long been appreciated that in addition to stretches of pyramidal cell dendrite in stratum lucidum exhibiting thorny excrescences distributed in a scattered manner, thorny excrescences can be clustered locally, and many of these clusters can extend for very long distances (>20-30 μm) along pyramidal neuron dendrites in CA3 (Gonzales et al., 2001; Qin et al., 2001; Kavalali et al., 1999). We find that LMTs from several distinct mossy fibers can converge at such clusters (Fig. 1B), and that postsynaptic territories at the clusters expand upon enriched environment through elongation and increased complexity of thorny excrescences. We further find a great degree of heterogeneity in the density and distribution of thorny excrescences among pyramidal neuron dendrites in stratum lucidum. The clusters might thus reflect specialized postsynaptic territory sites for competitive interactions among convergent LMTs regulated by experience.

Functional significance of LMT-C rearrangements in the adult

What could be the functional significance of the long-term rearrangements of LMT-C connectivity in the adult? Both, the rearrangements related to age and those induced by EE conditions led to a net growth in size by the fraction of larger LMTs, and thus to a net local increase in the numbers of active zones onto pyramidal neurons in CA3 by “plastic LMT-Cs”. Since larger LMTs with higher numbers of active zones elicit stronger excitatory responses in postsynaptic pyramidal neurons (Fig. 5), the growth of individual LMTs would lead to a greater frequency-dependent impact of their activation onto their

postsynaptic pyramidal neurons in CA3. This might, for example, lead to supra-threshold activation of pyramidal neurons by individual LMT-Cs at lower spiking frequencies, and/or to more effective synergisms by small numbers of synchronously active converging LMTs (Fig. 8). Accordingly, the expansion and activity-regulated divergence of LMT-C subsets along pyramidal cell dendrites in CA3 throughout life might result in an increasing focusing of information flow from individual spiking mossy fibers, selectively to a local segment of the associative network in CA3. This focusing might mediate the emergence of microcircuits of preferentially interconnected neurons (Chklovskii et al., 2004; Ikegawa et al., 2004; Yoshimura et al., 2005; Song et al., 2005). In addition to its effects on LMT size distributions, EE specifically increased the frequency of satellites by LMT-Cs, and the lengths and complexities of thorny excrescences. Since LMTs from several distinct mossy fibers intermingle at thorny excrescence clusters (Fig. 1B), the larger and more complex thorns at individual pyramidal neuron dendrites likely accommodate terminals and satellites from a larger number of distinct mossy fibers under EE conditions, reflecting an increase in local divergence and convergence driven by experience. The outcome of LMT rearrangements at thorny excrescence clusters might then involve activity-dependent growth, mGluR2-dependent inhibition of growth, and PKC-mediated competition among LMT-Cs. In this way, the increased complexity of LMT-Cs and thorns under enriched environment conditions might support hippocampal learning by providing more opportunities for local convergence of co-active terminals onto pyramidal neurons in CA3.

Acknowledgments

We are particularly grateful to Patrick Schwarb and Thierry Laroche for competent and extensive help with the imaging experiments. We thank Lan Xu (FMI, Basel) for excellent assistance with the electron microscopy data, and Yan-Ping Zhang (FMI, Basel) for help with the gene-gun experiments; we thank Andreas Luthi (FMI, Basel) and Silvia Arber (FMI and Biozentrum, Basel) for valuable comments on the manuscript. The Friedrich Miescher Institut is part of the Novartis Research Foundation.

2.2 SPATIALLY PREDETERMINED STRUCTURAL PLASTICITY OF GRANULE CELL SUBTYPES IN THE HIPPOCAMPAL MOSSY FIBER PROJECTION

Ivan Galimberti & Pico Caroni
unpublished results

SUMMARY

We investigated morphological properties of hippocampal granule cells in two transgenic mouse lines that label subsets of neurons (*Thy1-mGFP^s* (Lsi1) and (Lsi2)). We found that Lsi1 and Lsi2-granule cells differed in plastic terminal numbers along CA3, and in collateral patterns in the dentate hilus. Their plastic terminals remodeled selectively as a function of age and experience. Furthermore, Lsi1 and-Lsi2 granule cells exhibited different maturation rates in early postnatal life, and were not produced in the adult. Interestingly, Lsi1 and-Lsi2 granule cells produced synaptic contacts preferentially on Lsi1 and Lsi2-CA3 pyramidal neurons, respectively. Our results suggest that Lsi1 and Lsi2 label two subtypes of granule cells that differ in connectivity properties, and seem to belong to distinct microcircuits.

INTRODUCTION

Neuronal subtypes differ from each other by a combination of morphological and electrophysiological properties, and by patterns of gene expression. For example, in the mammalian neocortex distinct populations of projection neurons are located in different cortical layers and areas, have unique morphological features, express different genes and serve different functions (Wonders & Anderson 2006 and Migliore & Shepherd 2005). In recent years, tremendous progress has been made in understanding the mechanisms underlying the specification of projection neurons within the mammalian brain. Neuronal progenitors were identified and revealed to underly the specification of individual neuronal subtypes (Wonders & Anderson 2006). To what extent neurons of the same type might differ is still poorly understood. One possible scenario is that a large fraction of progenitor cells produce different subtypes of the same type of neuron. In fact, it is known that some type of neurons, e.g. hippocampal CA1 pyramidal cells or granule cells, derive from large progenitor pools (~ 7000 progenitor cells for each side of the hippocampus in the case of CA1 pyramidal cells, and ~ 400 in the case of granule cells (Loren et al. 2002). Furthermore, it is clear from a recent study in *Drosophila* that similar types of neurons can have quite different axonal patterns and might derive from different progenitor cells (Jefferis et al. 2007). But why should the same type of neuron have different subtypes? One possibility could be that similar neuronal circuits encode slightly

different types of information using distinct microcircuits. In fact, in *Drosophila* it was shown that uniglomerular projection neurons (PNs) relay olfactory information to the mushroom body (MB) and lateral horn (LH) in a highly stereotyped manner. In particular, PNs from different sensillar groups were clustered in the LH according to biological values of olfactory input, indicating that different odors are processed through specific microcircuits (Jefferis et al. 2007). This data indicates a new concept of the organization of neuronal circuits. The existence of microcircuit elements in higher order areas such as neocortex and hippocampus is well established, but the relationship between microcircuits based on functional connectivity and the existence of neuronal subtypes remains to be determined.

In recent years, the appearance of *Thy1-mGFP^s* transgenic mouse lines that express membrane-targeted GFP in only few neurons has provided an enormous progress in detecting subset of neurons in the nervous system (De Paola et al. 2003). The study of axonal structural plasticity in different *Thy1-mGFP^s* transgenic mouse lines could help to understand whether similar type of neurons have internal subtypes that differ in morphological properties. Ideally, one should monitor the entire axonal length of a neuronal subtype in time-lapse imaging experiments and observe the structural plasticity of all its boutons using different *Thy1-mGFP^s* lines. It is difficult to monitor entire axonal length, because the majority of axons cover very long distances between different brain regions. Nevertheless, hippocampal mossy fibers are organized in a lamellar manner and cover relatively short distances that can be monitored entirely in organotypic slice cultures over many time points. Moreover it has been shown to exhibit structural plasticity at the level of the large mossy fiber terminals (LMTs) (Galimberti et al. 2006) and therefore represent a nice system to investigate.

Here, we used two transgenic mouse lines that label subsets of neurons (*Thy1-mGFP^s* (Lsi1) and (Lsi2)) to image hippocampal mossy fiber projections in time-lapse imaging experiments in slice cultures and in sections of mice at different ages. We analyzed our data through a detailed 3D reconstruction of the individual mossy fibers with all their LMTs. We found that Lsi1 and Lsi2-granule cells differed in plastic-LMT numbers along

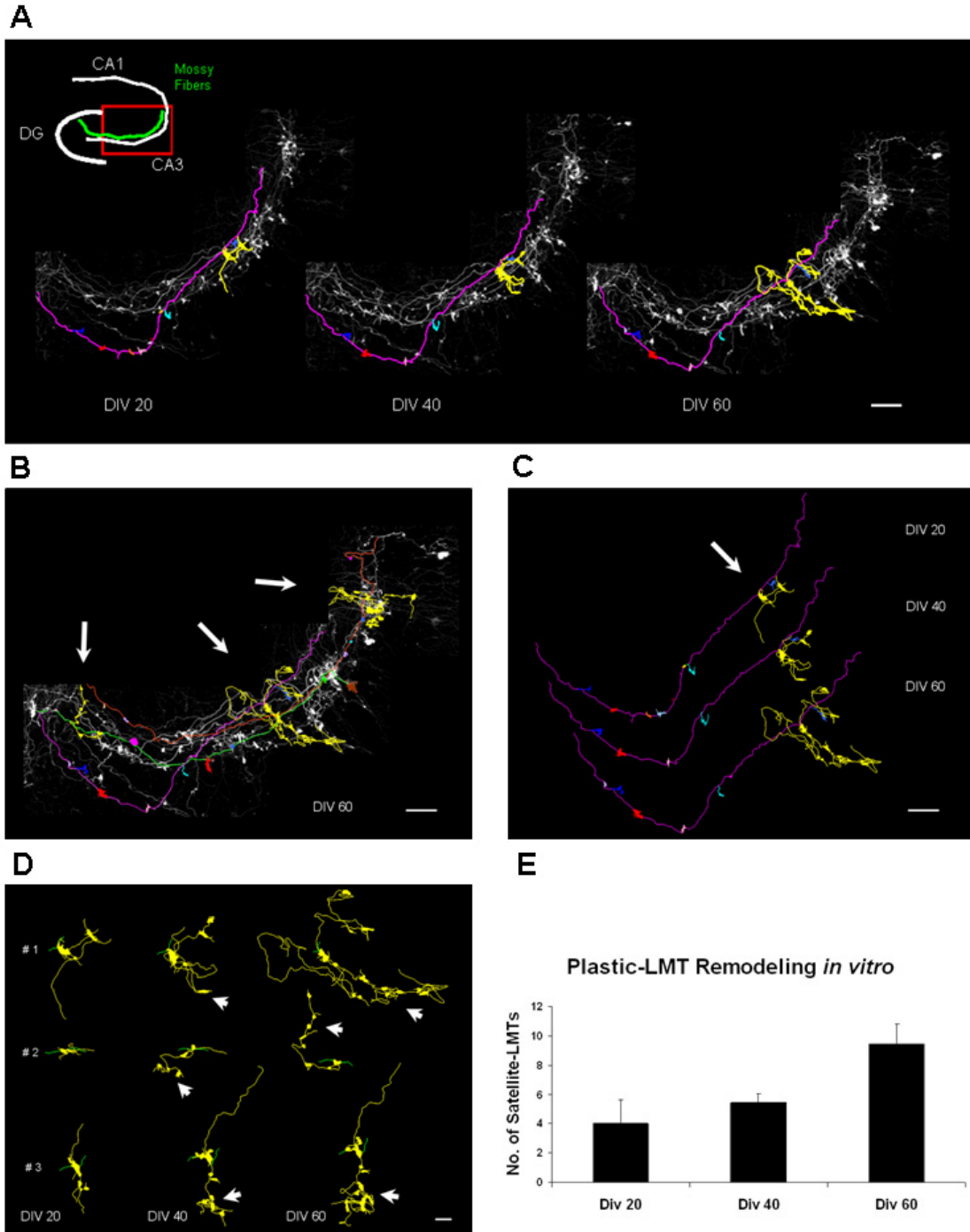
CA3 and collateral patterns in the dentate hilus. Their plastic-LMTs responded selectively to age and experience. Double staining with Doublecortin and NeuN revealed that Lsi1 and Lsi2-granule cells had different maturation rates in early postnatal life, and were not produced in the adult. Interestingly, Lsi1 and Lsi2 granule cells produced synaptic contacts preferentially on Lsi1 and Lsi2-CA3 pyramidal cells. Taken together, these results indicate that Lsi1 and Lsi2 label two subtypes of granule cells that exhibit different numbers of plastic and non-plastic terminals and seem to belong to distinct microcircuits.

RESULTS

Remodeling of individual Lsi1 hippocampal mossy fiber projections

We started our investigation using the transgenic mouse line Lsi1 (*Thy1-mGFP^s*) and analyzed whether all LMTs of individual Lsi1 mossy fibers exhibited a similar structural plasticity. We reconstructed in 3D individual Lsi1 mossy fibers with all their LMTs along CA3 in time-lapse imaging experiments and found that they had one plastic-LMT that remodeled extensively and continuously throughout all our time points, whereas the other LMTs from the same axon remodeled much less (Figure 1A and 1C). Plastic-LMTs from different Lsi1 mossy fibers were found at different locations along CA3 (Figure 1B). We quantified plastic-LMT remodeling by counting the number of satellite-LMTs from DIV 20 to DIV 40 and DIV 60 (N=10 plastic-LMTs, from 5 different slices) and found a significant increase (from ~ 4 satellite-LMTs at DIV 20 to ~ 9 satellite-LMTs at DIV 60). We then wondered whether individual Lsi1 mossy fibers might also have one plastic-LMT *in vivo*. In addition, since LMT-sizes were shown to shift gradually throughout age, we also wondered whether existing plastic-LMTs might increase their complexity in aging hippocampus (Galimberti et al. 2006). To get maximal 3D resolution *in vivo*, we sliced perfused hippocampi similarly to organotypic slice culture preparations, and in this way could trace almost 80 % of individual Lsi1 mossy fiber projections along CA3 (N=25). We found that one LMT per individual Lsi1 mossy fiber had satellite-LMTs and that the number of satellites increased in response to age (from ~2 satellite-LMTs at P30 to ~6 satellite-LMTs at P720, Figure 2A, 2B and 2D). Satellite-LMTs contained

functional pre-and postsynaptic markers e.g. Bassoon and phospho-GluR1 (Figure 2C), indicating that they increased locally functional connectivity with CA3 pyramidal neurons. Plastic-LMTs *in vivo* had less satellite-LMTs than *in vitro*. This could be due to differences in connectivity density between the two systems. In fact, it is known that connectivity in slice cultures is much higher than *in vivo*, and this seems to affect plastic-LMTs by increasing satellite numbers. Nevertheless, our results suggest that a similar remodeling is happening *in vitro* and *in vivo*, and that this remodeling might represent an important property of the mossy fibers projection.



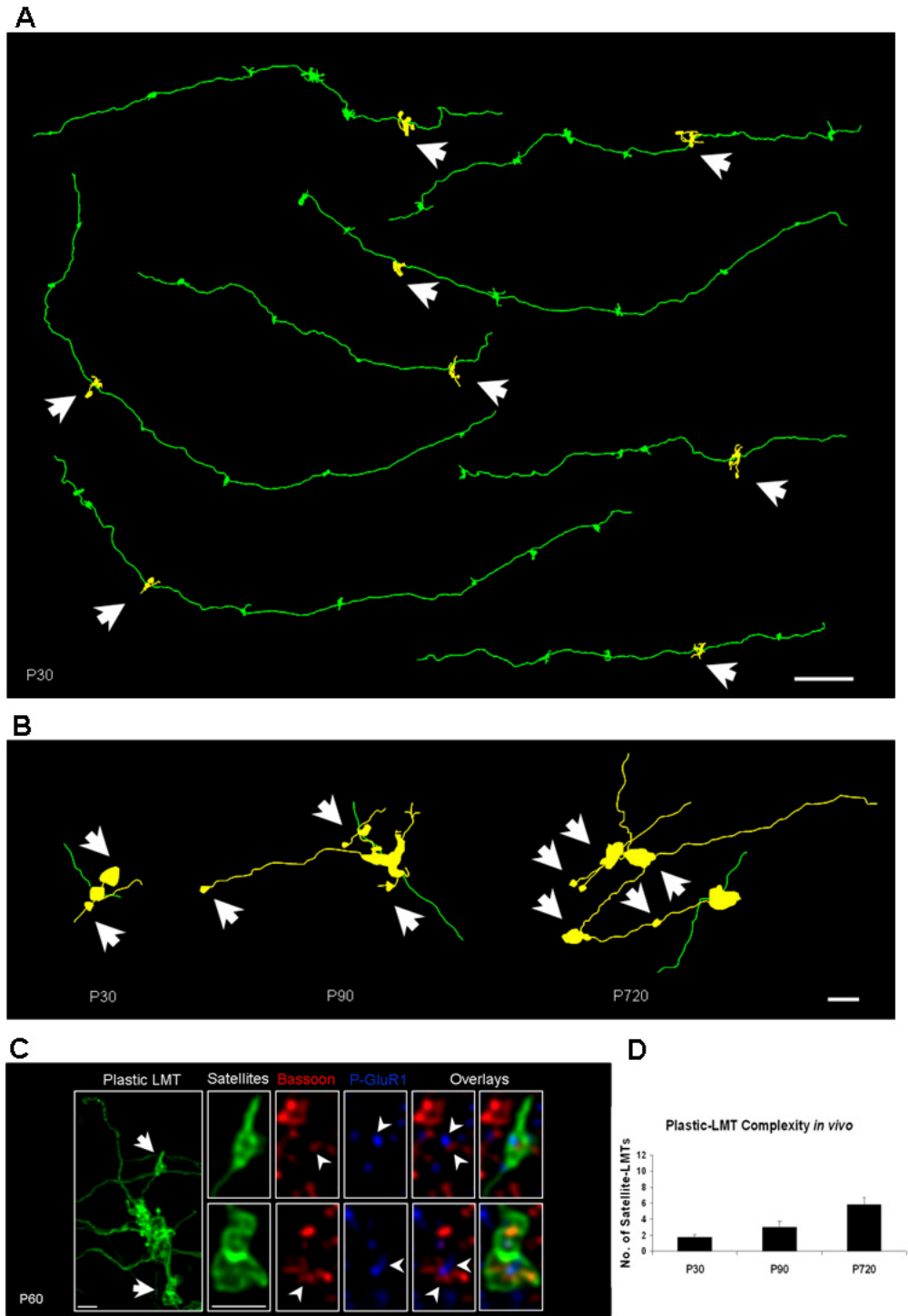


Figure 2. Individual Lsi1 Mossy Fibers *in Vivo*

(A) Overview of traced Lsi1 mossy fibers in CA3 at P30 (N=25). Note that each mossy fiber has only one LMT (arrows on yellow LMTs) with satellite-LMTs. (B) Three different complex-LMTs at P30, P90 and P720. Note how the complexity of these terminals appears to increase with age (arrows). (C) Double staining with synaptic markers (Bassoon and phospho-GluR1) of one plastic/complex-LMT at P60. Note the presence of two satellite-LMTs (left picture large white arrows). Both satellite-LMTs contain synaptic markers (see zooms of the two satellite-LMTs). (D) Quantification of plastic-LMT remodeling. Note the increase of the number of satellite-LMTs from P30 to P720 (average values of N=10 plastic-LMTs from 3 animals/age). Scale bars, 100 μ m (A), 10 μ m (B), and 2 μ m (C).

Remodeling of individual Lsi2 hippocampal mossy fiber projections

To determine whether Lsi1 remodeling was representative of how all mossy fibers remodeled, we performed a similar analysis using the transgenic mouse line Lsi2 (*Thy1-mGFP^s*), which also labels subsets of neurons in the adult. To our surprise, we found that in most cases Lsi2 mossy fibers had two plastic-LMTs along CA3 (Figure 3A, 3B and 3C). We quantified the plastic-LMT remodeling for Lsi2 *in vivo* and *in vitro* by pooling the two plastic-LMTs together. In both cases there was a clear increase of satellite-LMTs (from ~ 3 satellite-LMTs at DIV 20 to ~ 8 satellite-LMTs at DIV 60 and from ~ 2 satellite-LMTs at P30 to ~ 6 satellite-LMTs at P720). The most striking result was when we compared Lsi2 remodeling with Lsi1. We should keep in mind that we are comparing one plastic-LMT (Lsi1) versus two plastic-LMTs that are pooled as one (Lsi2). The results indicated that there was a similar net increase of satellite-LMTs between Lsi1 and Lsi2-mossy fibers (Figure 3D and 3E). The difference was the strength and location of this remodeling. Lsi1 mossy fibers concentrate one plastic-LMT in a specific region along CA3, whereas Lsi2 mossy fibers split this remodeling with two weaker plastic LMTs.

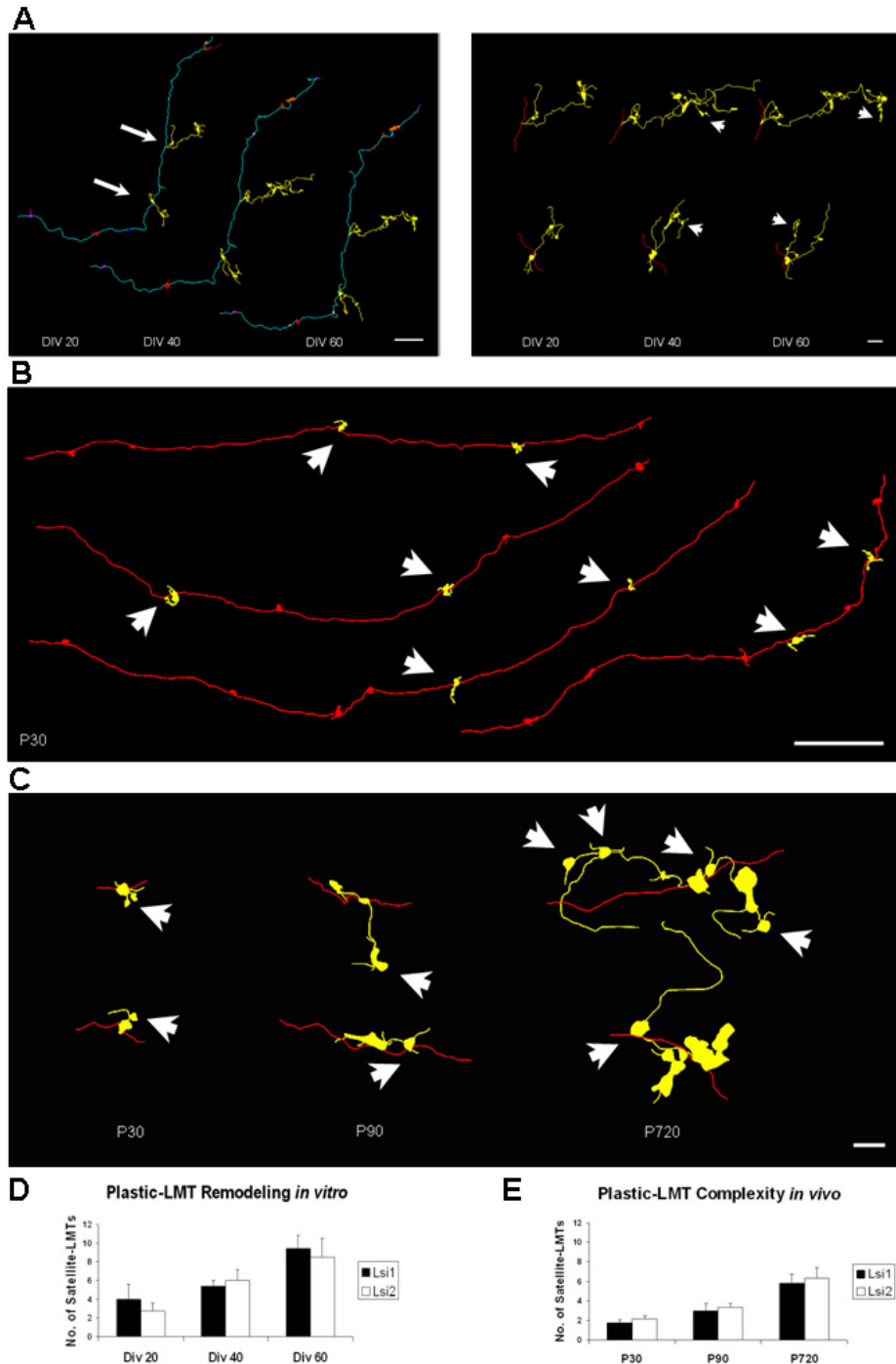


Figure 3. Individual Lsi2 Mossy Fibers in Slice Culture and *in Vivo*

(A) Left panel, camera lucida of a traced individual Lsi2 mossy fiber in CA3 at DIV20, 40 and 60. Note the presence of two plastic-LMTs (arrows). Right panel, remodeling of these two plastic-LMTs (arrows indicate new satellite-LMTs). (B) Overview of traced Lsi2 mossy fibers in CA3 at P30 (N=20). Note that each mossy fiber has two LMTs (arrows) with satellite-LMTs. (C) Three different couples of complex-LMTs of the same Lsi2 mossy fiber at P30, P90 and P720. Note that the number of satellite-LMTs increases throughout age (arrows). (D) Quantification of Lsi2 and Lsi1 plastic-LMT remodeling *in vitro*. The two Lsi2 plastic-LMTs were pooled as one and compared with the single Lsi1 plastic-LMT. Note that in both cases there is a similar increase of the number of satellite-LMTs from DIV20 to 60 (average values of N=10 plastic-LMTs from 5 slice cultures). (E) Quantification of Lsi2 and Lsi1 plastic-LMT remodeling *in vivo*. Again there is a similar increase of the number of satellite-LMTs from P30 to P720 (average values of N=10 plastic-LMTs from 3 animals/age). Scale bars, 100 μ m (A, left) and 30 μ m (A right), 100 μ m (B) and 10 μ m (C).

Collateral patterns of Lsi1 and Lsi2-granule cells in the dentate hilus

Hippocampal granule cells synapse with different neurons along the mossy fiber projection. In the dentate hilus, they produce collaterals with LMTs that synapse on mossy cells and in the CA3 region LMTs that synapse on CA3 pyramidal cells. Mossy cells are excitatory interneurons that synapse with granule cells through the so called *ipsilateral associational-commissural projections* and provide a feed forward excitation to the dentate gyrus granule cells. This means that mossy cells can modulate significantly the excitability of the granule cells. Since we knew that Lsi1 and Lsi2-granule cells differed in connectivity properties in CA3 (Figure 1, 2 and 3) we wondered whether they might also differ in their collateral patterns in the dentate hilus. We traced entire individual Lsi1 and Lsi2-mossy fibers in organotypic slice cultures (N=7 in both lines) and analyzed their collateral patterns in the dentate hilus. Lsi1 granule cells extended collaterals throughout the entire hilus, whereas Lsi2 tended to maintain their collaterals closer to the main axon (Figure 4). This suggests that Lsi1 and Lsi2-granule cells might excite different fractions of mossy cells, thus triggering distinct feed forward excitation patterns. These data together with the previous observations suggest that Lsi1 and Lsi2 label two subtypes of granule cells that differ in connectivity properties.

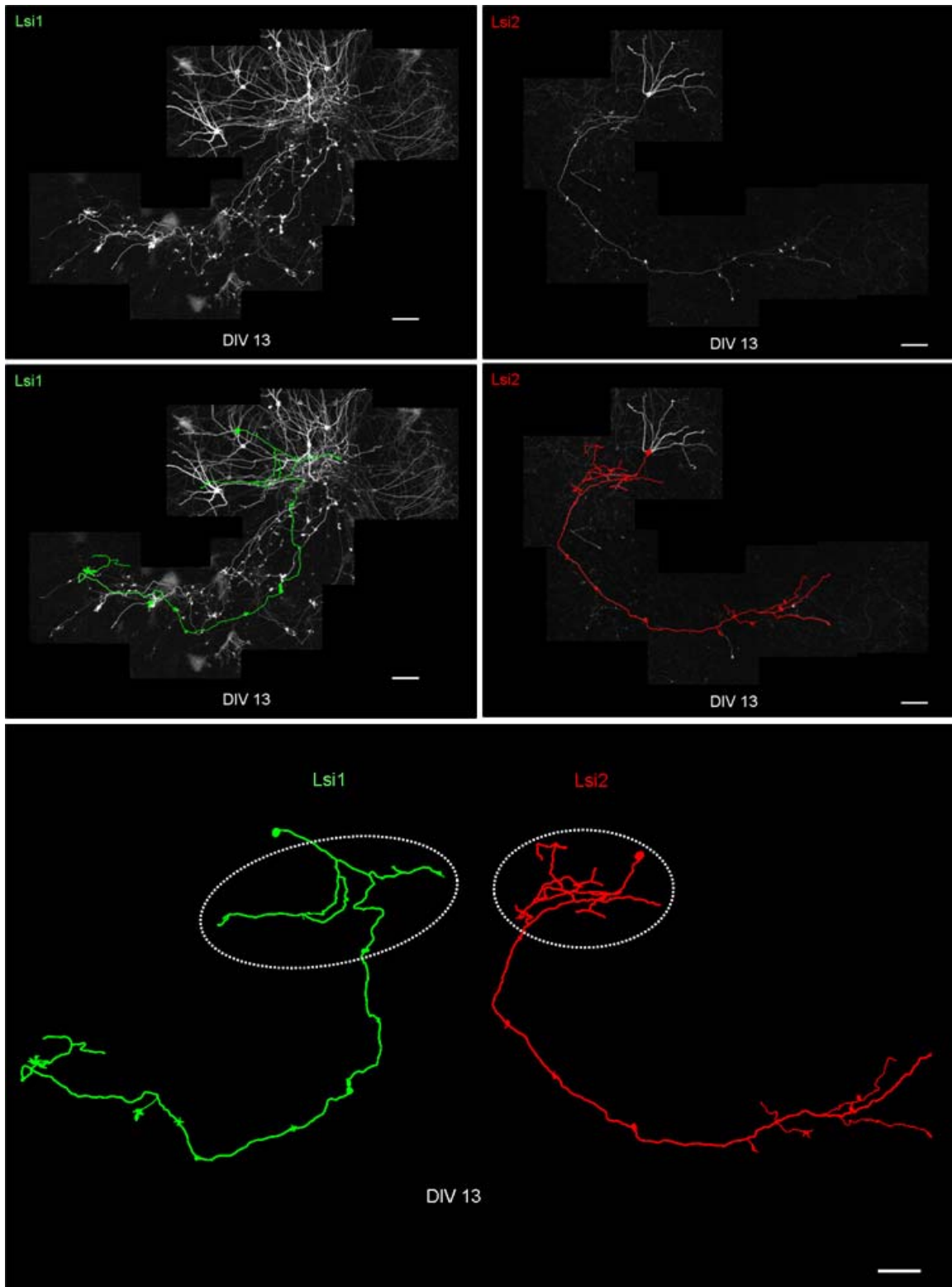


Figure 4. Collateral patterns of Lsi1 and Lsi2-granule cells in the dentate hilus

Left top panels, example of one traced Lsi1 mossy fiber in its entire length at DIV 13. Right top panels, example of one traced Lsi2 mossy fiber in its entire length at DIV13. Lower panel, camera lucida drawings of the two examples. Note the difference of the collateral pattern in the dentate hilus between Lsi1 and Lsi2 granule cells (white circles). (N= 7 different examples for each lines). Scale bar, 100 μ m

Maturation of Lsi1 and Lsi2 granule cells

Hippocampal granule cells are generated over a protracted period of time, and have been shown to also undergo adult neurogenesis (Danglot et al. 2006). Accordingly, we wondered whether Lsi1 and Lsi2-granule cells might differ in the kinetics at which they are generated postnatally. We included in this analysis an additional transgenic mouse line (*Thy1-mGFP^m* Lmu) with more widespread expression in the dentate and in CA3, in order to determine the extent to which granule cells in the Lsi1 and Lsi2 lines might differ from average granule cells. To monitor postnatal neurogenesis, we used markers that are expressed at different stages of granule cell maturation. For example, doublecortin (DCX is a protein that promotes microtubule polymerization) is present in migrating neuroblasts and young neurons and its expression is thought to be specific for newly generated postmitotic neurons. In contrast, NeuN (a soluble nuclear protein) is expressed in late postmitotic neurons, and is a marker for mature neurons. We therefore used double-labeling with DCX and NeuN to discriminate between immature and mature hippocampal granule cells. We focused our analysis on the suprapyramidal blade of the dentate gyrus between bregma -1.955 mm and -2.255 mm, in order to compare similar groups of granule cells from mice of different ages. We found that Lsi1, Lsi2 and Lmu-granule cells were positive for NeuN, but not for DCX at P90, indicating that these three transgenic mouse lines seemed not to label granule cells that undergo adult neurogenesis (not shown). We then analyzed granule cells between P3 and P30 (Figure 5A, left part). When found that Lsi1, Lsi2 and Lmu-granule cells matured faster than the bulk of the granule cells. When comparing the proportion of DCX and DCX/NeuN positive granule cells between Lsi1, Lsi2 and Lmu at P5 and P7, it became clear that Lsi1-granule cells exhibited the fastest maturation, followed by Lsi2 and Lmu (Figure 5B). At P30, Lsi1, Lsi2 and Lmu-granule cells were all NeuN positive, indicating that these transgenic mouse lines label hippocampal granule cells that are born during early postnatal neurogenesis (Figure 5A, right panel; Fig 5B). These results thus demonstrate that the transgenic lines highlight subpopulations of granule cells that mature at different rates during the first 2-3 postnatal weeks. The distinct maturation rates are consistent with the notion that the granule cells belong to distinct subtypes.

Preferred connectivity of Lsi1 and Lsi2 granule cells

Lsi1 and Lsi2 *Thy1-mGFP^s* transgenic mouse lines label subsets of neurons in the nervous system. In the hippocampus, subsets of granule cells and CA3 pyramidal neurons are in both lines m-GFP positive. In many samples of both lines we could image labeled CA3 pyramidal neurons and mossy fibers. We realized that in about 90 % of the cases m-GFP positive LMTs were physically in contact with m-GFP CA3 thorny excrescence clusters. In some cases, we found that up to 4 LMTs from 4 distinct mossy fibers were in contact with one CA3 pyramidal neuron (Figure 6A). We first wondered whether these contacts were functional and decided to stain for pre-and postsynaptic markers, e.g. Bassoon and phospho-GluR1. In all cases we found that these contacts were indeed functional and contained pre-and postsynaptic markers (Figure 6B). At this point we started to wonder whether these mGFP-mGFP contacts might indicate a preferential connectivity. The connectivity between granule cells and CA3 pyramidal neurons is extremely low. Each CA3 pyramidal cell is supposed to receive inputs from 30-50 different granule cells, and each granule cell contacts 10-15 different CA3 pyramidal cells. The fraction of labeled granule cells and CA3 pyramidal cells is very low in both lines. Lsi1 labels ~ 0.006% of granule cells (6000 over 1.10^6 cells) and ~ 0.003% of CA3 pyramidal cells (900 over 3.10^5 cells), whereas Lsi2 labels ~ 0.002% of granule cells (2000 over 1.10^6 cells) and ~ 0.002% of CA3 pyramidal cells (600 over 3.10^5 cells). These low numbers clearly suggest that connectivity between Lsi1 or Lsi2 granule cells and CA3 pyramidal neurons is not random.

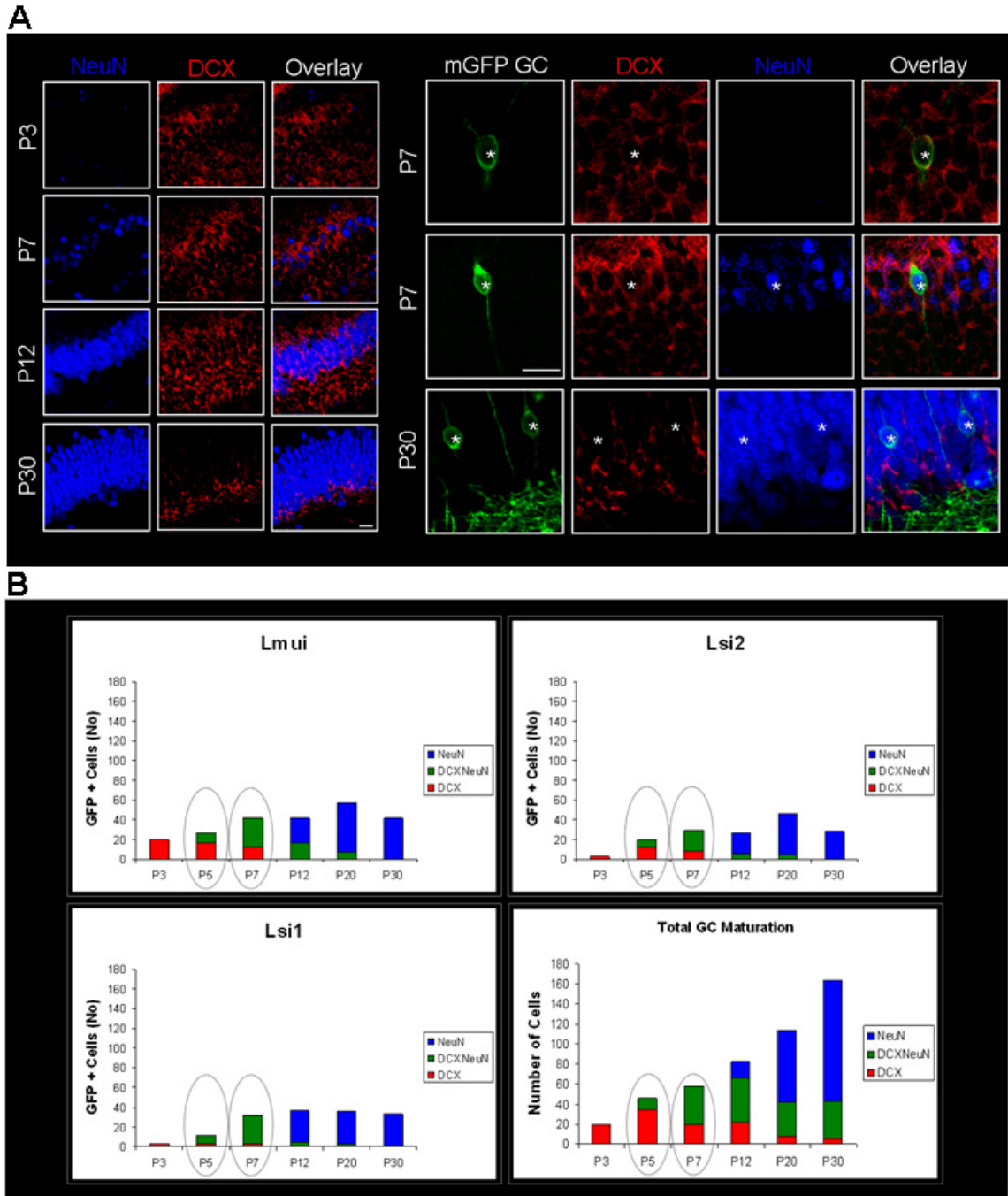


Figure 5. Maturation of Lsi1 and Lsi2 granule cells

(A) Left part, maturation of all granule cells in the upper blade between bregma -1.955 mm and -2.255 mm throughout P3, P7, P12 and P30. Note how double labeling with doublecortin DCX and NeuN reveal that at P3 all granule cells are only doublecortin positive and at P30 almost only NeuN positive. Right panel, examples of double labeling for DCX and NeuN in Lsi1 (examples at P7) and Lsi2 (example at P30) lines at P7 and P30. Note that at P7 there are mGFP granule cells positive for DCX (very immature) only and for DCX/NeuN (intermediate stage). However at P30 all mGFP granule cells are positive for NeuN only (mature), (see asterisk). (B) Absolute numbers of DCX, DCX/NeuN and NeuN positive granule cells in Lsi1, Lsi2, Lmu at P3, P5, P7, P12, P20 and P30. Note that the portion of DCX/NeuN granule cells at P5 and P7 is much higher in Lsi1 than Lsi2 and Lmu (N= 3 mice for each line and age). Scale bar, 20 μ m (A)

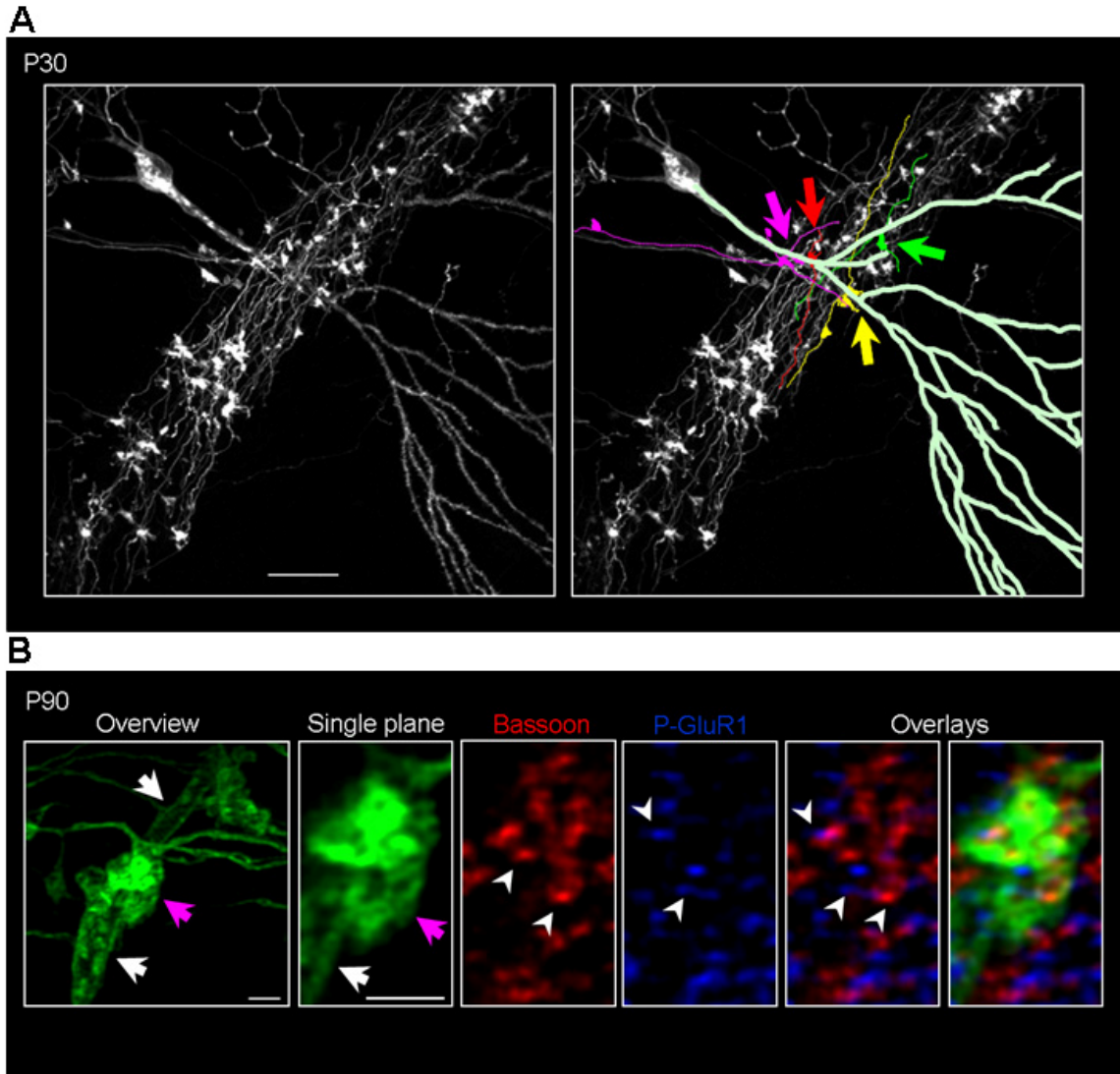


Figure 6. Preferred connectivity of Lsi1 and Lsi2 granule cells

(A) Left part, Lsi1 mossy fibers and one CA3 pyramidal cell in CA3 at P30. Right panel, 4 individual mossy fibers establishing LMTs in contact with the Lsi1 CA3 pyramidal cell (colored arrows). (B) Left part, Lsi2 LMT (purple arrow) in contact with Lsi2 CA3 dendritic branch (white arrows). Right part, single plane zoom of the contact site between LMT and thorny excrescences. Note that double labeling with synaptic markers (Bassoon and phospho-GluR1) reveal functional synapses on these mGFP-mGFP contacts. Scale bars, 20 μm (A), 2 μm (B)

Selective remodeling of Lsi1 and Lsi2 plastic-LMTs in response to experience

Several studies have shown that experience is involved in structural plasticity of dendritic spines and presynaptic terminals in different regions of the mature brain (Knott et al. 2002 and Galimberti et al. 2006). LMTs were shown to respond to experience by increasing the number of satellite-LMTs when mice were exposed to an enriched environment (Galimberti et al. 2006). We exposed Lsi1 and Lsi2 mice to an enriched environment to monitor whether all LMTs or just plastic-LMTs would be affected. We designed two protocols, in the first one we exposed mice to an enriched environment for 20 days starting at P30 (young) in the second for 30 days starting at P60 (old). Lsi1 and Lsi2 individual mossy fibers were solved and quantified as previously described. We found that Lsi1 and Lsi2-plastic-LMTs were affected in both protocols (Figure 7A and 7B) compared with control animals that were not exposed to an enriched environment (for example for the second protocol: ~ 3 satellite-LMTs at P90 and ~ 6 satellite-LMTs at P90EE for Lsi1 and ~ 3 satellite-LMTs at P90 and ~ 5 satellite-LMTs at P90EE for Lsi2, Figure 7C). Single Lsi1 plastic –LMTs responded similarly to pooled Lsi2 plastic-LMTs, indicating that similarly to age they kept their differences along CA3. In addition, all other LMTs of Lsi1 and Lsi2-individual mossy fibers did not remodel, suggesting that plastic LMTs remodeling of both Lsi1 and Lsi2 mossy fibers is selective in response to experience.

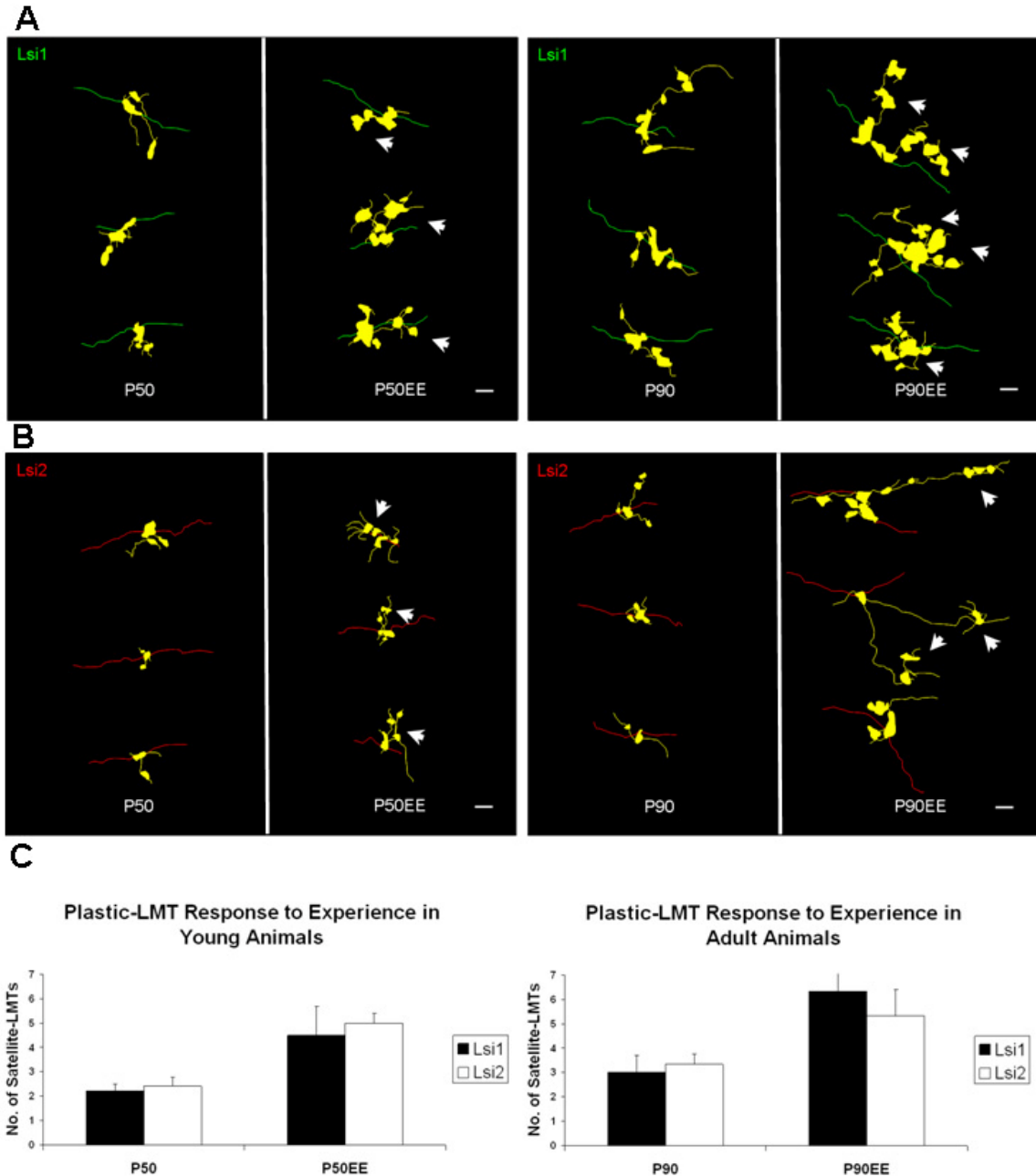


Figure 7. Selective remodeling of Lsi1 and Lsi2 plastic-LMTs in response to experience

(A) Camera lucida drawings of representative Lsi1 plastic-LMTs from P50 and P90 mice, kept under EE or Ctrl conditions. Note higher number of satellite-LMTs upon EE conditions (arrows). (B) Similar analysis in (A) for Lsi2 plastic-LMTs. (C) Quantification of Lsi1 and Lsi2 plastic-LMT remodeling upon EE conditions. As in Figure 3 (panel E) Lsi2 plastic-LMTs were poled as one and compared with the single plastic-LMT of Lsi1. Note that in both protocols the number of satellite-LMTs increases similarly in Lsi1 and Lsi2.

Scale bar, 10 μ m (A and B)

DISCUSSION

In this study we provide evidence that hippocampal granule cells consist of at least two subtypes with distinct connectivity properties and maturation rates, and that these subtypes seem to prefer distinct postsynaptic CA3 pyramidal cells. We first show that Lsi1 and Lsi2-granule cells differ in plastic-LMT numbers along CA3 and collateral patterns in the dentate hilus. We then show that they differ in their maturation rates in early postnatal life and are not produced during adult neurogenesis. Furthermore, in both lines plastic-LMTs respond selectively to age and experience by increasing local synaptic connectivity, suggesting that plastic-LMTs are important elements in the elaboration of sensory information. Finally, we realized that Lsi1 and Lsi2-granule cells make synaptic contacts preferentially with Lsi1 and Lsi2 CA3 pyramidal neurons and might represent distinct microcircuits. These results provide new insights about the organization of mossy fibers and their connectivity, and provide evidence for the existence of principal neuron subtypes in the hippocampus.

Individual Lsi1-mossy fibers place one plastic-LMT along CA3 and have collaterals throughout the dentate hilus, whereas individual Lsi2-mossy fibers place two plastic-LMTs and have collaterals that tend to extend in the vicinity and in parallel to the main axon. These results suggest that Lsi1 and Lsi2-granule cells produce synaptic contacts with different fractions of mossy cells and CA3 pyramidal cells. In the hilus, Lsi1 granule cells appear to recruit mossy cells throughout the dentate hilus, whereas Lsi2 outputs might be more spatially restricted to. In the CA3 region, Lsi1 granule cells can recruit locally several CA3 pyramidal cells with one plastic-LMT, whereas Lsi2 appear to recruit pyramidal cells within a broader spatial extension of CA3. This suggests that Lsi1 and Lsi2-granule cells can have different impacts on the feed forward excitation of the dentate gyrus, and can activate different patterns of pyramidal cells within CA3. Clearly, Lsi1 and Lsi2-granule cells might just be two out of many more subtypes of granule cells. The investigation of further subtypes should be possible using additional Thy1 transgenic lines, in combination with virus transduction experiments. Our preliminary analysis suggests that some subtypes might not have plastic-LMTs. In parallel, gene

profiling analysis of the different *Thy1-mGFP^s* granule cells will clarify whether these subtypes might also differ in gene expression and have specific markers.

The fact that individual Lsi1-granule cells have one plastic-LMT at different locations in CA3 indicates two aspects. First, it defines the Lsi1 granule cell subtype and second it suggests that Lsi1-mossy fiber projections could be organized topographically in CA3. One could speculate that some granule cells (Lsi1) can recruit preferentially few CA3 pyramidal neurons by focusing their outputs at preferred locations. Why this? It is known that the hippocampus have place cells that exhibit spatially localized firing patterns when rodents explore the environment (Smith et al. 2006). One possibility could be that granule cells are topographically organized in respect to CA3 pyramidal cells in order to discriminate spatial firing patterns (place fields) by recruiting distinct neurons within the circuitry. In fact, a topographic organization between GC and CA3 pyramidal cells could represent an anatomical representation of a hierarchical coding scheme that might provide a mean of differentiating spatial learning. Which molecules could be involved in this topographic maps? Presumably, semaphorins, netrins and ephrins, but how and in which proportion need investigations. It could be that Lsi1 mossy fibers follow gradients of one or more of these molecules in CA3 and place their plastic-LMTs at preferred locations according to intrinsic properties.

Neurogenesis of hippocampal granule cells occurs throughout the entire life and its efficiency declines in aging animals. In mice, the first hippocampal granule cells are born by E18 and the peak of their production is between P5-P7. Afterwards, their neurogenesis decreases and only few new granule cells mature and integrate functionally in the adult hippocampus. We found that Lsi1, Lsi2 and Lmu-granule cells are not produced in the adult, and differ in their maturation rates in early postnatal life. The proportion of DCX/NeuN positive granule was much higher in Lsi1 than Lsi2 and Lmu between P5 and P7. This indicates that Lsi1 granule cells mature faster than Lsi2 and Lmu, and Lsi2 mature faster than Lmu. Moreover, all are born during the first peak of neurogenesis (between E14 and P10). This result is remarkable, because it suggests that subtypes of granule cells are integrated at different rates, and may contribute differently to the

development of dentate gyrus-CA3 circuitry. These results further suggest that there might be granule cell subtypes that only mature during adult neurogenesis. This could be investigated using further *Thy1-mGFP^s* lines.

It is very interesting that Lsi1/Lsi2-granule cells seem to contact preferentially Lsi1/Lsi2 CA3 pyramidal cells. This might underly the existence of subtype specific microcircuits that might, for example, have specialized roles in pattern separation. In order to elucidate mechanisms that underly these synaptic preferences, one should perform gene profiling analysis of both Lsi1/Lsi2 granule and CA3 pyramidal cells, looking for example for Cell Adhesion Molecules CAMs (e.g. cadherins or protocadherins) that are exclusively expressed in Lsi1 and Lsi2.

3. GENERAL DISCUSSION

Overview

Recent neurobiological studies have begun to reveal the cognitive and neuronal coding mechanisms that underly *episodic* learning and memory (Vazdarjanova et al. 2004, Guzowski et al. 2001, Gabrieli et al. 1997 and Henke et al. 1997). The hippocampus has been shown to encode the sequences of places and events that compose episodic memories, and plays a critical role between the initial formation and their final repository elsewhere in the brain (Gabrieli et al. 1997 and Henke et al. 1997). However, we have only begun to conceptualize how information is encoded and preserved for long periods within the hippocampus. In fact, the exact contribution of each hippocampal cell type, which molecules are predominant and which kind of plasticity is crucial, is still poorly understood. Here I discuss new insights of the hippocampal granule cell organization that might be crucial to encode information that compose episodic learning and memory. In summary, we found: (1) that hippocampal mossy fibers exhibit structural plasticity at the level of the large mossy fiber terminals (LMTs); (2) that this remodeling respond to experience and age, (3) is regulated by spiking activity and mGluR2-sensitive transmitter release from LMTs (4) and can define subtypes of hippocampal granule cells that seem to belong to distinct microcircuits.

Remodeling of LMTs

We took advantages from recent technological advances and brought the first evidence that hippocampal mossy fiber terminals had “satellite-LMTs” that could contact additional CA3 pyramidal cells in adult mice. Furthermore, we showed that these “satellite-LMTs” are established and dismantled in organotypic slice cultures and can alter the strength of preexisting connectivity with CA3 pyramidal cells. Our results demonstrate that hippocampal mossy fibers are capable to modify locally their connectivity with CA3 pyramidal cells throughout life. Does this remodeling represent how mossy fibers encode information in general or just in special cases? We changed mice life styles by exposing them to an enriched environment and analyzed the number of satellite-LMTs. We found that they increased significantly and concluded that mossy

fibers utilize this remodeling in response to experience. Nevertheless, this does not mean that mossy fibers utilize this remodeling to encode any information. In fact, it could be that mossy fibers exhibit different structural changes for distinct life styles or learning tasks. Indeed, we know that age is affecting LMT sizes with the appearance of very long LMTs suggesting that age has preferred remodeling. Additional studies will elucidate whether mossy fibers react to different conditions by exhibiting distinct LMT-remodelings and for example whether stress is different than spatial learning and enriched environment.

Regulation of LMT remodeling

We utilized hippocampal slice cultures to understand molecular mechanisms that are involved in the regulation of LMT-remodeling. We found that by blocking spiking activity with TTX all LMTs, including satellite-LMTs, shrank and recovered when TTX was washed out. Furthermore, we obtained similar results when we agonized mGluR2 with DCGIV, or blocked PKC activity. Our results suggest that LMT-remodeling depends on spiking activity, vesicle release from LMTs, and PKC activity. We then wondered whether ionotropic glutamate receptors might be involved and blocked NMDA, Kainate and AMPA receptors. By blocking NMDA and Kainate receptors the number of satellite-LMTs were not changing, whereas when we blocked AMPA receptors there was a significant increase of satellite-LMTs (data not shown). This suggests that AMPA receptors might play an important role in the regulation of LMT-remodeling. Nevertheless, many issues are not clear yet. We still do not know how AMPA receptors affect the number of satellite-LMTs. For example, we have preliminary evidence suggesting that PKA activity might have a role comparable to that of PKC activity, and is mainly involved in maintaining satellite-LMTs but not in producing new ones (data not shown). One possibility could be that AMPA receptors trigger the modulation of second messengers e.g. NO, which is known to act on presynaptic plasticity. Additional experiments are needed to elucidate whether NO or other second messengers or even other molecules e.g. CAMs are downstream of AMPA receptors in the formation of satellite-LMTs.

Hippocampal microcircuits

Each hippocampus in the mouse contains about 2 millions of different neurons that are interconnected with each other in highly complex ways, and allow to perceive and elaborate polymodal sensory information. The granule cells are one type of these neurons that produce an elaborated and highly precise hippocampal neuronal circuitry. However, how these circuits discriminate and encode sensory information has remained unclear, in part because the functional connectivity of the circuits has been difficult to determine. One possibility is that information might be channeled through specialized microcircuits, but there is no evidence in support of this possibility yet. We now found that hippocampal granule cells can be subdivided into subtypes that differ in their connectivity properties, and seem to connect preferentially to defined subsets of CA3 pyramidal cells. In addition, we have provided evidence that structural plasticity of axon terminals can differ among neuronal subtypes, and represents a morphological parameter that can define those subtypes. Taken together, our results thus suggest the existence of distinct neuronal microcircuits between the dentate gyrus and the CA3 area of the hippocampus. However, much remains to be done in order to characterize these microcircuits at the structural and functional level. For example, it will be important to determine whether neurons of one microcircuit can be defined with specific markers, and whether these markers might reveal specific properties. This could lead to genetic approaches to manipulate these microcircuits *in situ* and test their relevance in distinct hippocampal paradigms. It will also be important to determine how many of these circuits might exist, and whether CA1 pyramidal cells might also participate, thus forming “trisynaptic loop microcircuits”.

While the anatomical and molecular characterization of hippocampal microcircuits will likely be challenging, one can safely predict that elucidating their functional significance will be even more challenging. On the other hand, the rewards might be significant. Thus, structure-function relationships in the hippocampus are currently being elucidated at the level of entire projections (e.g. the role of the enthorinal shortcut to CA3 or CA1). That information will be important to define “what” is being computed by a projection, but it will provide little information as to “how” the circuit carries out the computation. Information at the level of microcircuits might help to bridge the gap between circuit organization and the representation of information in the hippocampus.

4. MATERIALS AND METHODS

Mice and reagents

Transgenic mice expressing membrane-targeted GFP in only few (*Thy1-mGFP^s*, Lsi1 and Lsi2) or most neurons (*Thy1-mGFP^{mu}*, Lmui) were as described (De Paola et al., 2003). Transgenic males were crossed over more than 10 generations with non-transgenic F1 offspring from C57Bl6 x BalbC crosses, so that the genetic background of the mice was 50% each of C57Bl6 and BalbC. For enriched environment experiments, sets of female littermates (3-4 mice each) were either kept in normal-sized cages without additional objects (1 mouse per cage; Ctrl conditions), or in large (rat) cages with running wheels and several objects for exploration (3-4 mice per cage; EE conditions). Transgenic mice expressing cytosolic YFP in few neurons (*Thy1-cYFP*) (Feng et al., 2000) were obtained from Jackson Laboratories. Drugs and their final concentrations in the culture medium were as follows: TTX (Latoxan, 1 μ M, stock in acetate buffer), DCG-IV (Tocris, Bristol, 1 μ M), GABA (Fluka Biochemica, 100 μ M), Chelerythrine (Sigma, 1 μ M), APV (Sigma, 100 μ M). Antibodies: Bassoon (monoclonal mouse IgG2a, Stressgen, 2 μ g/ml), phospho-GluR1 (polyclonal rabbit, Upstate, 2 μ g/ml), DCX (polyclonal goat, Santa Cruz, 2 μ g/ml), NeuN (monoclonal mouse, Chemicon, 2 μ g/ml) anti-mouse/goat Alexa-Fluor-568 (Molecular Probes) and anti-rabbit Alexa-Fluor-647 (Molecular Probes)

Slice cultures

The slice cultures were established according to the procedure described by Stoppini and colleagues (Stoppini et al. 1991). Brains of P6-P9 transgenic mice were dissected in MEM (GIBCO)-based ice-chilled medium, and hippocampal coronal sections of about 400 μ m were produced with a tissue chopper (McIlwain). Slices were selected, placed on Millicell (Millipore, PICM03050) and cultured in 6-well dishes at 35°C and 5% CO₂ in the presence of 1ml of medium. The entire slice isolation procedure took about 30 min. The culture medium was exchanged every third day, and drugs were added in fresh culture medium. For drug wash-out, individual slices were placed in 35 mm Petri dishes, washed twice with 1 ml of Tyroid's buffer, returned to 6-well dishes, and washed again

twice with 1 ml culture medium during the next 10 min. For all drug treatments, control slices were treated in the same way, except for the absence of the drug.

For some experiments, DIV10-15 slice cultures from non-transgenic mice were transfected with cRFP cDNA under the control of the hSynapsin1 promoter (pMH4-pSYN-t-dimer RFP, generous gift from Thomas Oertner (FMI, Basel)). Gene gun transfection was performed according to the instructions of the manufacturer (Bio-Rad, Hercules, CA), except for a 100 μm nylon mesh which was inserted as a pressure-deflecting screen. Slices were imaged 10-15 days after transfection.

Imaging

For time-lapse imaging, slices were placed in 2 ml of physiological Tyrode solution at 37°C, and imaged under controlled temperature conditions (either incubation chamber (in most cases), or heating plate). For routine imaging of the entire mossy fiber projection and its LMTs, we used an Olympus set-up consisting of a Bx61 LSM Fluoview confocal microscope, a 40X/0.75W water immersion objective, and the following settings: PMT 653, Gain 2.4, pinhole 105 μm , 0.62 μm /stack in the z-dimension, 512x512 pixels, and fast scan rate at 9% laser intensity. High-resolution imaging was carried out using a Zeiss set-up consisting of an Axioplan2 LSM 510 Meta Zeiss confocal microscope. In either case, all focal planes within the slice were acquired and analyzed. All slices and structures included in the analysis were examined 5, 10 and 20 days after the last imaging session to verify that no signs of phototoxicity could be detected (e.g. swelling and beading of axons, blurring of the fluorescence signal due to membrane damage). We found that in most cases (more than 98% of the slices), if cell bodies were only imaged at the first session, slices could be imaged repeatedly for at least 8 times without any sign of phototoxicity. For imaging of LMTs from mice of different ages, male transgenic mice were perfused transcardially with 100 ml ice-chilled 4% paraformaldehyde in PBS, and brains were kept in fixation solution over-night at 4°C. Vibratome coronal sections (60 μm) were then cut using a LEICAVT 100S vibratome (Leica), and mounted in Airvol for fluorescence imaging. High-resolution images were acquired on an upright Zeiss Axioplan2 LSM510 Meta confocal microscope, using a Plan-Neofluar 40x/1.3 oil immersion objective (pinhole size of 65 μm), or a 100x/1.4 oil immersion objective

(pinhole sizes between 100-150 μm). Images were opened and processed using Imaris 4.2 (Bitplane AG) and Image Access (IMAGIC) softwares. Deconvolution was performed with Huygens Deconvolution Software from Scientific Volume Imaging SVI (Hilversum, Netherlands). The iterative Maximum Likelihood Estimation (MLE) algorithm was used with the computed Point Spread Function (PSF). For 3D analysis of LMT-Cs, images were opened in Imaris 4.2, smoothed by the Gaussian filter and Background subtraction tools of the software, cropped in 3D to reveal the regions of interest; 300 frames movies were then produced in the animation mode.

Immunocytochemistry and histology

Slice cultures were fixed for 10 min in ice-chilled 20% methanol in PBS, rinsed 3 times with PBS, and post-fixed for 10 min at 4°C in 4% paraformaldehyde, PBS. Tissues were then washed in PBS, solubilized in 0.4% triton X-100, PBS (over-night at 4°C), blocked in the presence of PBS and 20% BSA (4h, RT), and incubated with primary, and then secondary antibody (over-night at 4°C, each).

For electron microscopy, mice were perfused with buffered 2.5% glutaraldehyde, followed by fixation in buffered 2.5% glutaraldehyde (2h), post-fixation in buffered 2% Osmium tetroxide (2h), and dehydration through alcohol, followed by propylene oxide. Fixed brain material (hippocampal CA3a) was embedded in Docupon, stained with uranyl acetate and lead hydroxide, and sectioned with a diamond knife. Complete serial sections (75-85 nm each; total of 8-10 μm) were deposited on slot grids with formvar. Sections were recorded on Kodak electron image plates using a Zizze EM900 at 100 kV.

Analysis of imaging data

We defined LMTs as mossy fiber terminal regions of $> 2.5 \mu\text{m}$ diameter in CA3a-c, which were arranged either en-passant, or as side structures connected to the mossy fiber projection by short (in most cases less than 10 μm) side-branches. As expected, individual LMTs exhibited highly complex morphologies (Chicurel and Harris, 1992; Danzer and McNamara, 2004). We found that they could be further subdivided into three subcomponents: 1) core terminal regions consisting of flattened domains of greatly varying sizes, and of beaded subunits of 2.5-3.5 μm diameter, arranged in grape-like

arrays (range of 0-25 bead subunits per LMT), 2) filopodia tipped by swellings of 1-2 μm diameter (range of 2-10 filopodia per LMT; lengths of 5-15 μm), 3) processes of 10-200 μm length, emanating from LMTs and terminating in “satellite LMTs” (range of 0-5 satellites per LMT) (Fig. 1a; Suppl. Fig. 1).

For the quantification of LMT sizes in slice cultures, images were all acquired using the same settings, and processed using Imaris 4.2 and Image Access software. Acquisition settings (see above) were selected to minimize phototoxicity, but at the same time allow visualization of the thin axonal processes connecting LMTs to their satellites. The latter were defined as terminal structures of more than 2.5 μm in diameter, which were unambiguously connected to the main LMT as confirmed by a 3D analysis using Imaris software. Mossy fibers running deep in the slices exhibited thinner axons, and some of them were lost when cultures were kept for more than 4-5 weeks, possibly due to suboptimal access to oxygen. These deeper fibers could also be recognized by their weaker GFP signals, and were excluded from the analysis. LMT areas were derived from z-projections using ImageJ software. When LMT complexes unambiguously included satellites (about 10-20% of all LMTs), their terminal areas were included in the total size of the LMT complex. Sizes of individual identified LMTs were compared at the indicated times, and LMTs were subsequently grouped and analyzed according to their sizes at DIV20 (small < 30 μm^2 ; medium < 60 μm^2 ; large > 60 μm^2). For the quantification of LMT volumes at different ages, at least three confocal 3D stacks (total volume of 230 μm x 230 μm x 40 μm) were acquired in CA3a for each preparation (three mice per age), and analyzed using Imaris 4.2 software. Individual LMT volumes contained in these cubes were measured using the Surpass/ Isosurface function of the software. Non-saturating imaging conditions were chosen for all size analyses. An intensity threshold of 300 was chosen to selectively analyze LMTs (excluding axons and other smaller objects). All identified objects were verified by eye inspection. Generally, the settings for the analysis were identical for all samples of all ages, but in some cases we verified the settings through internal calibration using the diameters and signal intensities of axons. After these measurements, LMTs were grouped according to their volumes. The volumes of all LMTs in one group were added up, and expressed as percentage of the total volume of all LMTs measured per cube. For the quantification of LMT subunit compositions as a

function of age, samples were processed as described above (230 μm x 230 μm x 40 μm). Image settings were then chosen to emphasize the beaded subunit compositions of individual LMTs. To analyze labeling homogeneities by the mGFP construct, 3D images (voxel sizes of 0.09 x 0.09 x 0.49 μm) were acquired using LSM510 Meta (100x/1.4 oil objective, 150 μm pinhole size), and opened in Zeiss LSM 510 Image examiner software. Membrane outlines of axons and LMTs included in one confocal plane were followed manually, and light intensities were plotted against distance. To determine numbers of Bassoon-positive structures per individual LMTs, 3D images of Bassoon stained slice cultures were acquired (LSM 510 Meta, 100x/1.4 oil, voxel sizes: 0.09 x 0.09 x 0.28 μm , 150 μm pinhole size for both channels), and LMT volumes were derived as described above. Bassoon-positive structures were defined as single spots of 0.2 - 0.3 μm in diameter. Double counting of active zones was avoided by comparing adjacent confocal planes.

Electrophysiology

Slice cultures (DIV20-30) were transferred to a submerged recording chamber mounted on an upright microscope (BX50WI, Olympus, Germany), and continuously perfused (2-2.5 ml/min) using a solution containing (in mM): NaCl 142, KCl 1.6, CaCl₂ 2.5, MgCl₂ 1.5, NaHCO₃ 24, KH₂PO₄ 1.2, bicuculline methochloride 0.02, D-AP5 0.08, NBQX 0.0003, glucose 10, ascorbic acid 2; saturated with 95% O₂ and 5% CO₂ (pH 7.4; temperature 34°C). To establish pair recordings, a pipette supplemented with sulforhodamine (1%) or Lucifer Yellow (1%) was closely approached to a small (8-25 μm^2) or large LMT (80-150 μm^2) and gentle, positive pressure applied in order to stain juxtaposed CA3 pyramidal neuron dendrites. As soon as dendrites adjacent to the LMT were visible, the pipette was moved along the dendrites to the soma, and the cell was recorded under whole cell patch conditions. Granular cells were recorded under current-clamp mode with pipettes (3-5 M Ω) filled with a solution containing (in mM): K-gluconate 135, HEPES 10, EGTA 0.4, MgCl₂ 10, phosphocreatine 14, Mg-ATP 2, Na₂-GTP 0.2 (pH 7.2-7.3; osmolarity 295-310 mosm). CA3 pyramidal cells were recorded under voltage-clamp mode with pipettes filled with a solution containing (in mM):

Cs-methanesulfonate 130, HEPES 10, EGTA 10, MgCl₂ 5, phosphocreatine 14, QX-314 5, picrotoxin 1, Na₂-ATP 2 and Na₂-GTP 0.2 (pH 7.2-7.3 adjusted with CsOH; osmolarity: 295- 310 mosm). Current and voltage recordings were obtained using an Axoclamp-2A and an Axopatch 200B amplifier respectively (Axon Instruments, Union City, CA., USA). Membrane potentials were corrected for liquid junction potentials. Series resistance was compensated up to 50-80 % in order to avoid unstable recordings. Series and input resistances of voltage-clamp recordings were monitored throughout experiments, and data were discarded if they varied by more than 20%. Presynaptic action potentials were evoked by injecting depolarizing current pulses (1-1.5 nA for 2 ms) at 0.5 Hz unless otherwise stated. Signals were filtered at 2 kHz, digitized at 5-10 kHz and stored on hard disk. Data acquisition and analysis were performed using homemade A/D converter and software. The standard deviation of the latencies was used to calculate the jitter. Average values are expressed as mean \pm S.E.M. Statistical differences were assessed by Student's *t*-test.

Protocols

**Preparation of organotypic hippocampal slice cultures
for long-term live imaging**

Nadine Gogolla^{1,3}, Ivan Galimberti^{1,3}, Vincenzo DePaola² and Pico Caroni¹

¹Friedrich Miescher Institute, Maulbeerstrasse 66, CH-4058 Basel, Switzerland.

²Cold Spring Harbor Laboratories, Cold Spring Harbor, New York, USA.

³These authors contributed equally to this work.

Nature Protocols

2006 (1(3):1165-71)

ABSTRACT

This protocol details a method to establish organotypic slice cultures from mouse hippocampus, which can be maintained for several months. The cultures are based on the interface method, which does not require special equipment, is easy to execute and yields slice cultures that can be imaged repeatedly – from when they are isolated at postnatal day 6–9, and up to 6 months *in vitro*. The preserved tissue architecture facilitates the analysis of defined hippocampal synapses, cells and entire projections. Monitoring of defined cellular and molecular components in the slices can be achieved by preparing slices from transgenic mice or by introducing transgenes through transfection or viral vectors. This protocol can be completed in 3 h.

INTRODUCTION

Recent advances in gene delivery and live imaging technology have had a marked impact on the range of experimental tools that are available to life scientists (Conchello et al. 2005 and Yuste 2005). For research in neuroscience, these developments have meant that studying the structure and function of biologically relevant neuronal circuits can now be approached in a non-invasive way and with unprecedented analytical power. To fully exploit these technological developments, adequate biological preparations to investigate neuronal circuits have to be established in parallel. Fortunately, preparations that were developed by physiologists more than a decade ago (Gahwiler 1981, Stoppini et al. 1991 and Gahwiler et al. 1997) could be readily adapted for live imaging studies of defined neuronal circuits (DePaola et al. 2003 and Galimberti et al. 2006).

Advantages of the method

Key features of the hippocampal organotypic slice cultures (Stoppini et al. 1991) include: well-defined cellular architecture of the hippocampal circuit, which preserves the organization *in vivo*, and allows the identification and manipulation of defined neurons and synapses (Gahwiler 1981, Stoppini et al. 1991, Gahwiler et al. 1997, DePaola et al. 2003 and Galimberti et al. 2006); presence of axonal projections (mossy fiber axons extending from dentate gyrus granule cells to the distal end of CA3), which can largely be recovered in the slices in their original state (that is, without lesioning) and which establish stereotypic numbers of readily identifiable presynaptic terminals onto excitatory

and inhibitory neurons in the hilus and in CA3 (DePaola et al. 2003 and Henze et al. 2000); a long-term thickness of 100–150 μm , preserving three-dimensional organizations of connectivity (Stoppini et al. 1991 and Gahwiler et al. 1997); maturation of the slice cultures, closely reflecting the corresponding schedule *in vivo* (De Simoni et al. 2003 and Henze et al. 2000); option to prepare the slices from mice of any genetic background, including those of poor postnatal viability.

Critical aspects

The main critical issues relate to the extent to which organotypic slice cultures reproduce the properties of hippocampal circuits *in vivo* (Gahwiler et al. 1997). This information is important for deciding whether the approach is appropriate for addressing the particular experimental issues that might be in mind. These issues have been investigated in much detail by physiologists, who have demonstrated extensive similarities, but also a few discrepancies, to properties of the corresponding circuits in the adult brain (Gahwiler et al. 1997). With respect to development, the slice cultures exhibit a temporal profile of excitatory and inhibitory miniature synaptic events, which closely match, qualitatively and quantitatively, the corresponding times *in vivo* (De Simoni et al. 2003). This indicates that features that are critical to hippocampal circuit development and maturation are well established at 1 week postnatally, and are stable under organotypic culture conditions. A further critical issue involves the unavoidable separation of the hippocampal slices from their natural inputs, outputs and neuromodulatory systems. It turns out that most neuronal excitability and network properties are well preserved, in spite of the fact that the actual activity in the slices must be significantly different from the *in vivo* situation (Gahwiler et al. 1997). Predictably, synaptic connectivity in the slice cultures is initially greatly reduced due to the isolation procedure but, during the first 2–3 weeks *in vitro*, synapse numbers recover to a level comparable to that *in vivo* (Gahwiler et al. 1997), and the cultures are stable with respect to total synapse numbers from about 3 weeks *in vitro* (DePaola et al. 2003). As a result, the degree of connectivity between some of the individual neurons that are present in the slices (e.g., pyramidal neurons in CA3) is higher than *in vivo*, a fact that facilitates the analysis of synaptically connected neurons (Gahwiler et al. 1997). With the exception of the molecular layer of the dentate gyrus, in

which the occasional recurrent mossy fiber collaterals can produce an excitation level that is higher than that of normal granule cells, this higher connectivity does not seem to produce aberrant patterns of activity (Gahwiler et al. 1997). The slices can, however, be electrically labile, and gentle handling is important to avoid epileptic-like discharges. One way to avoid higher excitability in granule cells is to prepare slices from P20-30 mice when the circuits are more stable (Xiang et al. 2000). Finally, attempts to investigate adult neurogenesis in hippocampal slice cultures have suggested that the phenomenon is much less frequent than *in vivo*. This might be influenced by the culture medium, but the issue requires further investigation.

Possible results and outlook

Organotypic slice cultures from ~1-week-old mouse hippocampus appear to reproduce most anatomical and functional properties of the corresponding hippocampal circuits *in vivo* for at least 6 months *in vitro* due to the intrinsic properties of their neurons. Accordingly, limitations to their applications might be confined to studies of hippocampal input–output relationships. This leaves an exciting range of possibilities for the exploration of mechanisms that control the assembly and function of neuronal circuits. Some of these include: time-lapse imaging from the sub-second to the months range, and from individual molecules to entire neuronal projections and circuits; imaging of neuronal (DePaola et al. 2003, Galimberti et al. 2006, Caroni 1997 and Feng et al. 2000) and glial (Dailey et al. 1999) subtypes; molecular manipulation using transfection (Lo et al. 1994 and Benediktsson et al. 2005) or viral approaches (Ehrengruber et al. 1999 and Miyaguchi et al. 1999) to knock down or overexpress genes, silence or activate neurons, render neurons responsive to light or selective drugs and to highlight sub-circuits; combined physiology-imaging methods; manipulations to investigate lesion-induced plasticity and pathways of neurodegeneration and repair (e.g., amyloid- or epilepsy-related); following the insertion of new neurons, the development of axons and their connections, or the insertion of exogenously added stem cells; *post-hoc* analysis using, for example, tracers, electron microscopy and single-cell genomic methods.

MATERIALS

Reagents

- Animals: 6–9-day-old mouse pups. You can prepare slices from six pups within one session, but for the beginner it may be preferable to start with two or three pups

! CAUTION All animal experiments must comply with national regulations.

- Hand sterilizing solution, e.g., [Sterilium \(Bode\)](#) or equivalent
- [Penicillin/streptomycin](#) (Invitrogen, cat. no. 16050-122)
- HEPES
- Hank's balanced salt solution ([HBSS](#); Invitrogen, cat. no. 24020-083)
- Horse serum
- 2 \times MEM (liquid Eagle's with Hank's Salts and 25 mM HEPES; Gibco, cat. no. 04195120M)
- Tris-(hydroxymethyl)aminomethane

Equipment

- Dissection microscope (e.g., ZEISS Stemi 2000-C binocular with 10 \times 23 objectives, but any 5–10 \times magnifying dissection microscope is suitable)
- [McIlwain tissue chopper \(The Mickle Laboratory Engineering Co. Ltd.\)](#)
- Sterile dissection hood
- Razor blades that can be fixed in the McIlwain tissue chopper
- [Filter paper](#) (e.g., Schleicher & Schuell, cat. no. 300009, or Whatman paper)
- Small (35 mm \times 10 mm) and large (100 mm \times 20 mm) [cell culture dishes](#) (Corning, cat. no. 430165 and 430293, respectively)
- [6-well culture plates](#) (Corning, cat. no. 3516)
- [Culture plate inserts](#): 0.4 μ m Millicell membrane, 30 mm diameter (Millipore, cat. no. PICM03050)

- [Vacuum filter sterilizer](#) for medium (e.g., Vacuum-driven disposable filtration system, 0.22 μm pore width; Millipore, cat. no. SCGPU02RE)
- Cell culture incubator at 35 °C, 95% air, 5% CO₂

Equipment Setup

- **Dissection tools** Scalpel, two round-ended spatulas, small scissors, large scissors, one pair of fine straight forceps, two pairs of curved fine forceps and two glass Pasteur pipettes that have to be custom designed as follows: one pipette is fire-polished at the tip so that it adapts a round shape, has no sharp edges, but still has a small opening; the second pipette is cut at the intersection of the fine and thick tube using a canula opener (glass cutter), and the resulting large opening of this pipette is fire-polished to smooth the edges.

Reagent Setup

- **Penicillin/streptomycin solution** Dissolve 1.6 g penicillin G (100 U ml⁻¹) and 2.5 g streptomycin (0.1 mg ml⁻¹) in 200 ml H₂O, filter-sterilize and store at -20 °C in 2-ml aliquots. Note that penicillin can reduce GABAergic neurotransmission in slices (Andersen et al. 1983). Signs of epileptic activity have, however, not been detected under these culture conditions.
- **Horse serum** Heat-inactivate the complement system of the horse serum at 56 °C for 30 min; aliquots can be stored at -20 °C for at least 1 year.

?Troubleshooting

- **Dissecting medium** 50 ml MEM 2x, 1 ml penicillin/streptomycin solution, 120 mg Tris (hydroxymethyl)aminomethane (final concentration: 10 mM); add up to 100 ml with ddH₂O.
▲ CRITICAL Prepare within 24 h of the experiment, filter-sterilize through a 0.22 μm membrane and keep it at 4 °C until dissection.
- **Culture medium** 50 ml MEM 2x, 1 ml penicillin/streptomycin solution, 120 mg Tris (hydroxymethyl)aminomethane (final concentration: 10 mM), 910 μl of a 7.5% NaHCO₃ aqueous solution, 50 ml heat-inactivated horse serum, 50 ml 1x

HBSS; add up to 200 ml with ddH₂O.

▲ **CRITICAL** Filter-sterilize through a 0.22 μm membrane and keep at 4 °C.
Pre-heat only the medium that is needed for a medium change on the same day.
Culture medium can be stored at 4 °C for at least 1 month.

Overview

- [Step 1 - 4 Preparation of membrane inserts and culture medium](#)
- [Step 5 - 9 Preparation of dissection medium and chambers](#)
- [Step 10 - 13 Preparation of dissection material](#)
- [Step 14 - 17 Hippocampus dissection and cutting of coronal sections](#)
- [Step 18 - 47 Dissection](#)
- [Step 48 Cold incubation](#)
- [Step 49 - 59 Selection and incubation of hippocampal slices](#)

PROCEDURE

Preparation of membrane inserts and culture medium • TIMING 10-30 min

1. Prepare the culture medium and filter-sterilize it.
2. Add 1 ml culture medium per well of a 6-well plate; prepare 3–4 wells for each pup to be dissected (one pup should yield 6–8 usable hippocampal slices and about two slices are cultured on one membrane).
3. Add one culture plate insert into each prepared well, so that the insert membranes touch the medium, but are not covered by it.
4. To warm up the medium, put the prepared 6-well plates into the cell culture incubator.

**Preparation of dissection medium and chambers • TIMING 10-20 min preparation
+ 15 min sterilization**

5. Prepare the dissection medium, filter-sterilize and keep it at 4 °C.
6. Cut a small triangle (about 4 x4 x4 cm) out of the filter paper, take the cover of a 100-mm cell culture dish and place the filter paper triangle into it. Prepare 1 cover + filter paper for each pup to be dissected.
7. Sterilize the covers containing the filter papers under ultraviolet light in the culture hood for 15 min.
8. Add 1 ml of cold dissection medium on top of each filter paper and cover with the bottom of the cell culture dish under sterile conditions.
9. Keep these 'dissection chambers' at 4 °C until dissection.

Preparation of dissection material • TIMING 5-15 min

10. Clean all dissection tools with 70% ethanol, fire-sterilize them inside the dissection hood and keep them there. Clean a fresh razor blade with a chloroform:isoamylalcohol (49:1) solution, followed by 100% ethanol and 70% ethanol and fix it in the McIlwain tissue chopper placed inside the dissection hood.

! CAUTION Chloroform is toxic; avoid inhalation, ingestion or contact with skin, eyes or mucous membranes.

11. Fix the plastic platform on the McIlwain tissue chopper and clean it with 70% ethanol; switch the chopper on and adjust the cutting thickness to 400 µm.
12. Keep the dissection medium on ice inside the dissection hood.
13. Put one 35-mm cell culture dish per pup to be dissected under the dissection hood.

Hippocampus dissection and cutting of coronal sections • TIMING 15-30 min/pup

14. Place one of the prepared, cold 'dissection chambers' under the dissection microscope and remove the top plate so that the filter paper covered with cold dissection medium is exposed.

▲ **CRITICAL STEP** Steps 14–38 are carried out under sterile conditions inside a dissection hood unless otherwise mentioned.

15. Decapitate one pup outside the dissection hood using large scissors. Note that anesthesia of pups is notoriously difficult (dry ice is one possibility), and that decapitation as described above is usually advised. Nevertheless, make sure that the procedure complies with local regulations.

16. Flush the head with 70% ethanol and transfer it into the hood.

▲ **CRITICAL STEP** The fur of the pup is a potential contamination source.

?[Troubleshooting](#)

17. Sterilize your gloves with Sterilium or 70% ethanol before you proceed.

▲ **CRITICAL STEP** Proceed carefully for Steps 18–24. The delicate nervous tissue of the brain is easily damaged by the sharp dissection tools or the edges of the cut skull. ?[Troubleshooting](#)

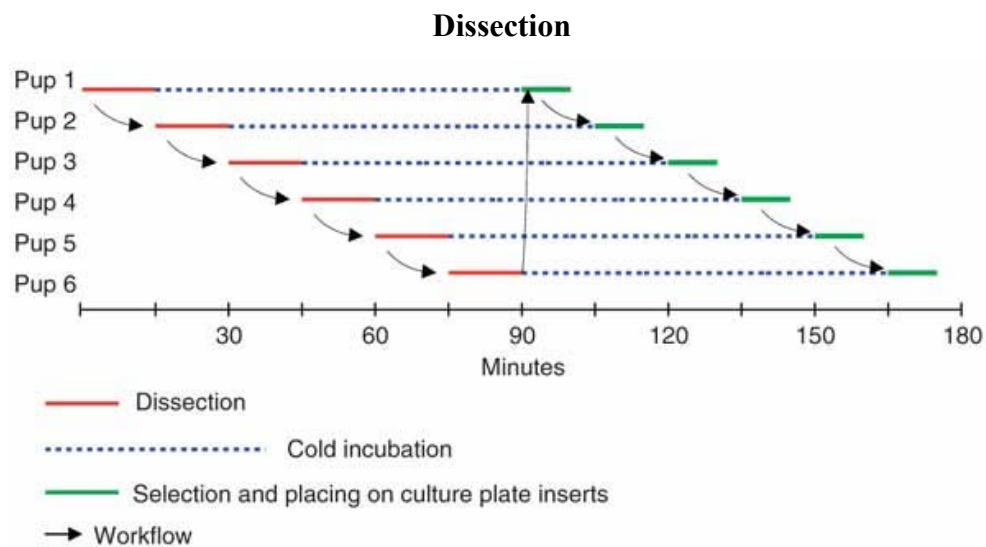


Figure 1. Workflow diagram. Slices from pups 1 to 6 are prepared sequentially: dissection, cold incubation and slice selection are performed in a staggered way.

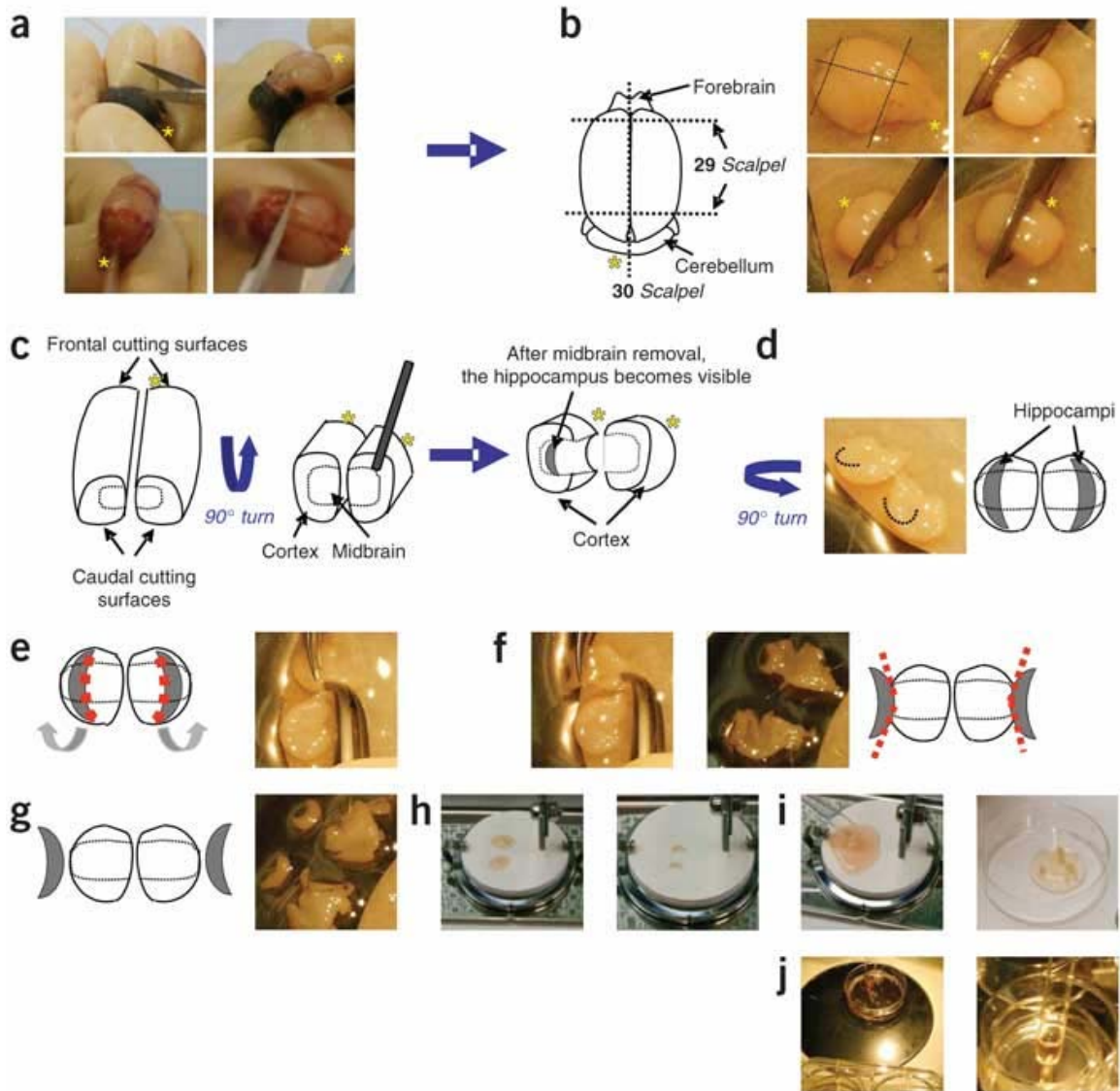


Figure 2. Illustration of hippocampal slice preparation protocol (Steps 18-53). (a) Steps 18-22; (b) Steps 28-30; (c) Steps 31-32; (d) Step 33; (e) Step 34; (f) Steps 35-36; (g) Step 38; (h) Steps 39-43; (i) Steps 44-46; (j) Steps 50-53. * Back of the head (neck).

Dissection

18. Make an incision into the skin along the midline of the head, starting at the neck up to between the eyes using the small scissors (see [Figs. 1-3](#)).
19. To hold the head more easily and to expose the skull, flip the skin around the head and pull it to the lower side, where you pinch it between your fingers.
20. Use the small scissors and the fine straight forceps to remove neck muscles and the first vertebrae.
21. Insert the lower part of the small scissors carefully into the foramen magnum and cut the skull along the midline from the foramen magnum to the front until you reach between the eyes.
22. Make two lateral cuts starting from the midline towards the sides.
23. Peel away the skull using the fine straight forceps.
24. Hold the head upside down above the prepared filter paper, which should be covered with cold dissection medium.
25. Introduce the spatula carefully between the brain and the skull and remove the brain from the skull, cut the cranial nerves and, if necessary, the olfactory bulbs with the spatulas.
26. Let the brain drop gently onto the filter paper covered with dissection medium.
27. Immediately put a few drops of cold dissection medium onto the exposed brain.
28. Put the brain upside up with the ventral side lying on the filter paper.
29. Use the scalpel to cut off the forebrain and the cerebellum by coronal cuts.
30. Using the scalpel, separate the two hemispheres cutting along the inter-hemispheric fissure.
31. Place one brain hemisphere on the frontal or caudal cutting surfaces; the intersection between cortex, midbrain and brainstem becomes visible.
32. Separate the cortex with the underlying hippocampus from the brainstem, midbrain and striatum using the two spatulas.

▲ CRITICAL STEP Do not touch the hippocampus with the spatulas.

?Troubleshooting

33. Place the cortex upside down, so that the hippocampus is exposed.
34. Use the curved forceps to cut the connections of the hippocampus to the ventral side (fimbria); leave it connected to the cortex by the subiculum.
35. Flip the hippocampus over and out.
36. Using the scalpel, cut the connection of the hippocampus to the enthorinal cortex (subiculum).
37. Flush the dissected hippocampus with ice-cold dissection medium.
38. Prepare the second hippocampus of the opposite hemisphere in the same way (see [Fig. 2](#)).
39. Use the wide-bore, custom-made Pasteur pipette to suck one hippocampus into the pipette along with some dissection medium and transfer it to the plastic platform on the McIlwain tissue chopper.
40. Repeat the same for the second hippocampus.
41. Using the narrow-bore pipette, align the two hippocampi perpendicularly to the chopper blade.

▲ CRITICAL STEP Avoid touching the slices; instead, use medium to push and pull them into the right position. **?Troubleshooting**

42. Remove all dissection medium around the hippocampi.
43. Chop rapidly into 400 μ m thick transverse sections.
44. Float the freshly cut sections immediately with cold dissection medium.
45. Use the wide-bore pipette to transfer the sections into a 35-mm cell culture dish.
46. Separate the sections by shaking the dish gently. If the sections stick together, remove all dissection medium and shake harshly but not for too long; alternatively, use the narrow-bore pipette and try to separate the sections by the flow of some dissection medium.

▲ CRITICAL STEP Use great care as the sections are very easily damaged!

47. After separation, fill the 35-mm dish with cold dissection medium so that all sections are covered; push floating sections down to the bottom of the dish by dropping medium onto their tops.

Cold incubation • TIMING 30 min-1.5 h/pup

48. Cover the 35-mm cell culture dish with its cover and label it with the number of the pup and the exact time. Incubate the separated slices for a minimum of 30 min at 4 °C (up to 1.5 h). Repeat Steps 14–48 for all pups (see [Fig. 1](#)).
▲ CRITICAL STEP After incubation of each pup, clean and fire-sterilize all dissection tools and the chopper platform; take a fresh and cold 'dissection chamber'; change and sterilize your gloves! [?Troubleshooting](#)

Selection and incubation of hippocampal slices • TIMING 10-20 min /pup

49. After completing the dissection of the last pup, start the selection of slices from the first dissected pup (see label) and proceed with the selection in the same sequence as in the dissection (see [Fig. 1](#)).
▲ CRITICAL STEP Make sure that slices from each pup were cold incubated for at least 30 min (check the time on the label). Place the first 35-mm dish (slices of the first pup) under the dissection microscope in the dissection hood.
50. Remove the lid of the 35-mm dish and select the best slices for culturing according to the following criteria (see [Fig. 3](#)) Slices should have smooth margins and be clearly visible, have uniform and well-defined cell layers in the dentate gyrus and in CA1-3; the dentate gyrus should be tightly connected to the rest of the slice, and the fimbria should be intact. [?Troubleshooting](#)
51. Collect one pre-heated 6-well plate containing culture medium and a cell culture insert from the 35 °C incubator.
52. Using the wide-bore pipette, transfer the selected slices individually onto the membranes along with some dissection medium. Alternatively, some labs use

thin spatulas for the transfer, but we have no direct experience with this alternative method.

53. Using the narrow-bore pipette, orientate the slices to the middle of the membrane by pushing and pulling them with the stream of dissection medium.

54. You can place up to four slices on one membrane but the number of slices on one membrane has to be adapted to the planned experiments.

▲ CRITICAL STEP For live imaging, you should only place one or two slices on each membrane. Place the slices as close to the center as possible, so that the plastic edge of the membrane insert will not hinder the microscope's access to the top of the slices. Adapt the slice number that you put on one membrane to the estimated time required for later imaging of all slices on one culture plate insert. The time you can keep one culture plate insert outside the incubator during imaging is restricted to a maximum of 30 min (see also Imaging Protocol (Gogolla et al. 2006)). Keep a minimal distance of 2 mm between the slices to avoid fusion when flattening out during the culture period.

55. Using the narrow-bore pipette, remove all dissection medium around the slices.

▲ CRITICAL STEP This is critical because any remaining dissection medium covering the slices hinders oxygen exchange.

56. To avoid cooling, put the 6-well culture plate back into the incubator immediately after having placed the slices.

57. After 3–4 d, remove all culture medium below the insert and replace it with 1 ml of fresh, 35 °C-warmed culture medium.

58. Replace the culture medium every 3–4 d.

59. The slice cultures can be maintained for several months. Criteria to verify viability: the slices must be transparent, firmly attached to the membrane and the dentate gyrus must be visible to the naked eye. In addition, if neurons are labeled with fluorescent markers, microscopic examination should reveal an absence of axonal and dendritic beading. If necessary, cell death in the slices can be assayed with propidium iodide (DePaola et al. 2003).

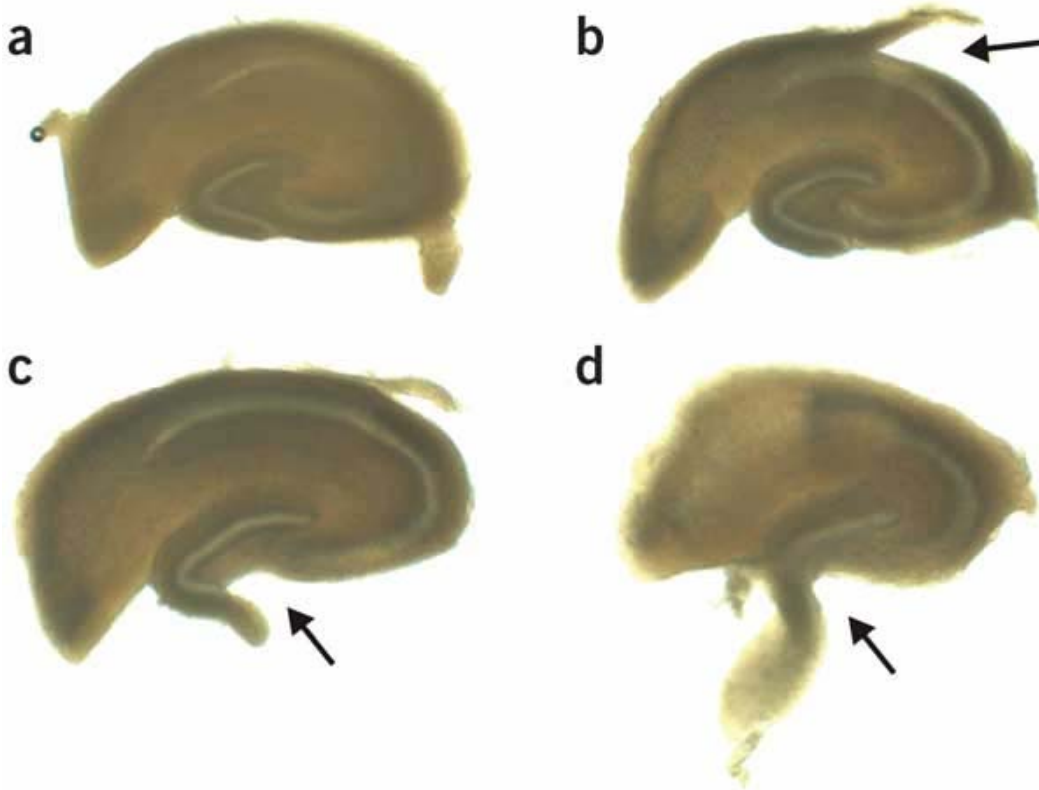


Figure 3. Selection of slices for culturing. (a) Optimal slice with nice cell layers in the dentate gyrus and CA1-3 and smooth margins (b) slice in which the CA1 region was lesioned during preparation (arrow); (c) slice in which the dentate gyrus was lesioned (arrow); (d) slice in which the dentate gyrus detached from the rest of the section (arrow). Only the slice in a should be selected for culturing.

? Troubleshooting

Problem	Possible Reason	Solution
Slices become contaminated soon after preparation	Contamination by the fur or blood of the pups	Use 70% ethanol to repeatedly flush the head after decapitation
		Change and sterilize the gloves after having touched the pups' fur and blood
Slices detach from the membrane of the cell culture plate insert soon after preparation	Check for the correct composition and pH of the culture medium	Always adjust the pH of the culture medium to 7.2
	Change the horse serum	Inactivate the horse serum carefully and note the batch number, if possible; keep using a batch that has worked as long as possible (make many aliquots)
Slices die prematurely during the culturing period	Slices can become epileptic if treated too harshly	Always move slices slowly and smoothly
		Avoid strong vibrations
Axons and/or dendrites assume a beaded appearance	Wrong medium composition	Strictly follow the indications in the protocol concerning media and times during preparations and handling
	Wrong pH of culture medium	
	Treatment during preparation too harsh	
	Slice preparation took too long	
	Media were not at the right temperature	
	Incubator at wrong temperature or atmosphere	
Aberrant axonal projections	The slices that were selected for culturing did not show the right morphology or were injured	Select only slices in which the cell layers can be clearly seen and have the expected shape
		Make sure that you do not touch the slices with any sharp tools
	The cutting angle was not perpendicular to the long axis of the hippocampus	Make sure that you cut and then select slices that were cut perpendicularly to the long axis of the hippocampus

• TIMING

Steps 1–4:	10–15 min (For trained experts);	20–30 min (For beginners).
Steps 5–9:	10 + 15 min (For trained experts);	20 min (For beginners).
Steps 10–13:	5–10 min (For trained experts);	15 min (For beginners).
Steps 14–47:	15 min per pup (For trained experts);	30 min per pup (For beginners).
Step 48:	30–90 min (For trained experts);	30–90 min (For beginners).
Steps 49–56:	10 min per pup (For trained experts);	20 min per pup (For beginners).

Anticipated results

Critical factors to reproducibly achieve good yields and quality of slice cultures are speed, avoiding physical damage of the hippocampus and avoiding contaminations during the preparation (see [Figs. 1- 3](#)). These requirements mainly depend on training and concentration. We therefore recommend that beginners practice repeatedly during the first 2–4 weeks, in order to become confident and to acquire good experimental skills. A trained user should produce 6–8 good quality slices per pup, which can be maintained and imaged for at least 6–10 weeks.

Acknowledgments

We are very grateful to Dominique Muller (University of Geneva, Switzerland) for introducing us to his hippocampal slice culture method. We thank M. Abanto, E. Bednarek and S. Saxena (Friedrich Miescher Institut (FMI)) for comments on the manuscript. The FMI is part of the Novartis Research Foundation.

Long-term live imaging of neuronal circuits in organotypic hippocampal slice cultures

Nadine Gogolla^{1,3}, Ivan Galimberti^{1,3}, Vincenzo DePaola² and Pico Caroni¹

¹Friedrich Miescher Institute, Maulbeerstrasse 66, CH-4058 Basel, Switzerland.

²Cold Spring Harbor Laboratories, Cold Spring Harbor, New York, USA.

³These authors contributed equally to this work.

Nature Protocols

2006 (1, - 1223 – 1226)

ABSTRACT

This protocol details a method for imaging organotypic slice cultures from the mouse hippocampus. The cultures are based on the interface method, which does not require special equipment, is easy to execute, and yields slice cultures that can be imaged repeatedly after they are isolated on postnatal day 6–9 and for up to 6 months *in vitro*. The preserved tissue architecture facilitates the analysis of defined hippocampal synapses, cells and entire projections. Time-lapse imaging is based on transgenes expressed in the mice, or on constructs introduced through transfection or viral vectors; it can reveal processes that develop over time periods ranging from seconds to months. Imaging can be repeated at least eight times without detectable morphological damage to neurons. Subsequent to imaging, the slices can be processed for immunocytochemistry or electron microscopy, to collect further information about the structures that have been imaged. This protocol can be completed in 35 min.

INTRODUCTION

Recent advances in live-imaging technology have had a dramatic impact on the range of experimental tools available to life scientists (Conchello et al. 2005 and Yuste 2005). These include the following: microscopes with greatly improved sensitivity, temporal/spatial resolution and spectral versatility; powerful image-acquisition and image-processing software; and an ever growing repertoire of fluorescent reagents to monitor second messengers, and to identify macromolecules and their physiological modifications as well as subcellular structures *in situ*. For research in neuroscience, these developments have meant that studying the structure and function of biologically relevant neuronal circuits can now be approached in a noninvasive way, and with unprecedented analytical power. In order to fully exploit these technological developments, adequate biological preparations have to be established in parallel to investigate neuronal circuits. Fortunately, preparations developed by physiologists more than a decade ago (Gahwiler et al. 1981, Stoppini et al. 1991 and Gahwiler et al. 1997) can be readily adapted for live-imaging studies of defined neuronal circuits (DePaola et al. 2003 and Galimberti et al. 2006). Labeling subsets of neurons and their subcellular structures can be achieved using transgenic mice and a mouse Thy1-promoter cassette (Caroni 1997, Feng et al. 2000).

While cytosolic fluorescent proteins work well (Feng et al. 2000), expression of membrane-targeted GFP constructs provides optimal visualization of neuronal outlines (DePaola et al. 2003 and Galimberti et al. 2006). Further constructs available for Thy1-transgenic mice include, for example, synaptopHluorin (Araki et al. 2005). Alternatively, transgenes can be introduced directly into slice cultures using transfection methods (Lo et al. 1994 and Benediktsson et al. 2005) or viruses (Ehrengruber et al. 1999 and Miyaguchi et al. 1999).

Advantages of the method

Key features of the organotypic hippocampal slice cultures (Stoppini et al. 1991) include the following: (i) well-defined cellular architecture of the hippocampal circuit, which preserves the organization *in vivo*, and allows the identification and manipulation of defined neurons and synapses (Gahwiler 1981, Stoppini et al. 1991, Gahwiler et al. 1997, DePaola et al. 2003 and Galimberti et al. 2006); (ii) the presence of axonal projections (mossy fiber axons extending from dentate gyrus granule cells to the distal end of CA3), which can largely be recovered in the slices in their original state (i.e., without lesioning), and establish stereotypical numbers of readily identifiable presynaptic terminals onto excitatory and inhibitory neurons in the hilus and CA3 (DePaola et al. 2003, Galimberti et al. 2006 and Henze et al. 2000); (iii) a long-term thickness of 100–150 μm , preserving the 3D organizations of connectivity (Stoppini et al. 1991 and Gahwiler et al. 1997); (iv) maturation of the slice cultures closely reflecting the corresponding schedule *in vivo* (De Simoni et al. 2003); and (v) the option to prepare the slices from mice of any genetic background, including those with poor postnatal viability.

Critical aspects

One set of critical issues relates to the extent to which organotypic slice cultures reproduce the properties of hippocampal circuits *in vivo* (Gahwiler et al. 1997). This information is important for deciding whether the approach is appropriate to address the particular experimental issues of interest. These issues have been investigated in detail by physiologists, who have demonstrated extensive similarities, but also a few discrepancies, with respect to the properties of the corresponding circuits in the adult brain (Gahwiler et

al. 1997 and De Simoni et al. 2003). Further critical issues relate to the manipulations involved in the imaging procedures. The slices can be electrically labile, and gentle handling is important in order to avoid epileptic-like discharges (Gahwiler et al. 1997). In addition, it is essential to minimize the times during which the slices are kept outside of the tissue-culture incubator, and to allow sufficient recovery times between single imaging sessions (see PROCEDURE). These factors must be balanced against the requirements of the experimental questions. We recommend always optimizing and standardizing the particular experimental protocols, taking into account reproducibility and negative side-effects. By contrast, contaminations and phototoxicity can largely be avoided through appropriate precautions.

Possible results and outlook

Organotypic hippocampal slice cultures from mice aged \approx 1 wk appear to reproduce most anatomical and functional properties of the corresponding hippocampal circuits *in vivo* for at least 6 months *in vitro*, due to the intrinsic properties of their neurons. Accordingly, the slices provide an exciting range of possibilities for the exploration of mechanisms controlling the assembly and function of neuronal circuits. These include the following: (i) time-lapse imaging over periods ranging from sub-seconds to months, and of objects in the slices ranging from individual molecules to entire neuronal projections and circuits; (ii) imaging of neuronal (DePaola et al. 2003, Galimberti et al. 2006 and Feng et al. 2000) and glial (Benediktsson et al. 2005) subtypes; (iii) molecular manipulation using transfection or viral approaches to knock down or overexpress genes, silence or activate neurons, render neurons responsive to light or selective drugs, and highlight sub-circuits; (iv) combined physiology and imaging methods; (v) manipulations to investigate lesion-induced plasticity, and pathways of neurodegeneration and repair (e.g., amyloid-related or epilepsy-related pathways); (vi) following the insertion of new neurons, the development of axons and their connections, or the insertion of exogenously added stem cells; and (vii) *post-hoc* analysis using, for example, tracers, electron microscopy and single-cell genomic methods.

MATERIALS

Reagents

- Mouse organotypic hippocampal slice cultures (see [Reagent setup](#))
- [Fungizone](#) antimycotic, liquid (Gibco, cat. no. 15290-018)
- Tyrode salt solution (see [Reagent setup](#))

Equipment

- [Single-point scanner upright confocal microscope with spectral detection](#) (e.g., Olympus Bx61 LSM Fluoview or Zeiss LSM 510) equipped with a 40 \times /0.75W water-immersion objective
- [35-mm Petri dishes](#) (Corning, cat. no. 430165)

Reagent Setup

- **Mouse organotypic hippocampal slice cultures** Prepared from mice aged 6–9 d (see PROCEDURE). We have imaged slices at times ranging from 5 d to 6 months *in vitro*. **! CAUTION** All procedures must adhere to local laws regulating handling of experimental animals.
- **Tyrode salt solution** 2.7 mM KCl, 0.5 mM MgCl₂, 136.9 mM NaCl, 0.36 mM NaH₂PO₄, 1.4 mM Na₂HPO₄, 5.5 mM glucose, 1.8 mM CaCl₂ (pH 7.26)
▲ CRITICAL Filter-sterilize through a 0.22- μ m membrane.

PROCEDURE

Overview

- [Step 1](#) [Set up of the confocal microscope](#)
- [Step 2 - 6](#) [Imaging session](#)

Set up of the confocal microscope • TIMING 10 min

1. Optimal acquisition settings are adapted to the intensity of the labeled cells based on the following criteria: use the smallest laser intensity possible, and enhance the intensity by increasing the gain and photo-multiplier (PMT) strength and/or opening the pinhole; also, use the largest step size possible (adapted to the size of the imaged objects). We obtained the best results for mossy fiber terminals using a step size of 0.62 μ m. In order to allow fast acquisition (and, thus, cause minimal damage to the slice cultures), use a low-resolution mode, avoid using averaging functions (e.g., Kalman) and apply the fastest scanning rate available to the microscope. We imaged mossy fiber terminals at 512 \times 512 pixels.

!Troubleshooting

Imaging session • TIMING 30 min maximum

2. Working in the cell-culture hood, place the cell-culture insert into a 35-mm Petri dish and add 2 ml pre-warmed Tyrode salt solution at 37 °C (1 ml above and 1 ml below the membrane).
3. Move to the confocal microscope. Use the 40 \times /0.75W water-immersion objective and the mercury lamp to look for labeled cells.
4. **▲ CRITICAL STEP** To avoid contaminations originating during the imaging sessions, we clean the objective with 70% (vol/vol) ethanol in water before imaging individual slices. By taking this simple precaution, and using Fungizone and antibiotics in the culture media (see slice-preparation protocol, Gogolla et al.

(2006) Nat. Prot. 1, 1165-1171) we rarely experience contaminations upon imaging sessions.

5. In order to include all labeled structures in the 3D region of interest (ROI), set the start point of the z-stack slightly below the first labeled structure, and the stop point slightly above the last labeled structure. For example, acquisition of the entire mossy fiber projection required four or five 3D stacks of 40–60 confocal planes in 10–15 min.

▲ CRITICAL STEP The slices should not stay in the Tyrode salt solution and outside the incubator for more than 30 min.

6. After imaging, remove the Tyrode salt solution, return the culture-plate insert into the six-well plate and place it back in the incubator.

▲ CRITICAL STEP From now on, to avoid contaminations, the slices should be kept in culture medium supplemented with Fungizone ($0.25 \mu\text{g ml}^{-1}$).

7. Repeat Steps 2–5 for the next imaging session, keeping the same settings. In most cases, slices can be imaged repeatedly at least eight times, although some precautions should be taken (see below).

▲ CRITICAL STEP Generally, we have observed that when the experiments require more than two or three imaging sessions, good results depend on allowing long recovery time intervals between individual imaging sessions (e.g., 10–20 d), and keeping slices outside of the incubator for no longer than 20 min during imaging sessions. Our observations suggest that, provided one adheres to the principles outlined above (also see TROUBLESHOOTING), phototoxicity is not the major limiting factor. Instead, most damage to the slices associated with the imaging sessions is due to the changes of medium, and the times when the slices are kept outside of the incubator. It is important to note that our protocol was optimized for imaging granule cells and their mossy fibers. We have noticed that pyramidal neurons in CA3 appear to be more vulnerable to repeated handling, and recommend that repeated imaging protocols should be initially tested and optimized. Characteristic

signs of selective damage include major reductions in the intensity of the GFP signal (Thy1-driven expression of membrane-targeted GFP), thinning of neuronal processes and losses of spines. [!Troubleshooting](#)

[!Troubleshooting](#) for imaging organotypic slice cultures.

Problem	Possible reason	Solution
Phototoxicity Possible signs include the following: abrupt weakening of fluorescence intensity; swellings and breakdowns of axons and dendrites into beaded chains; blurred GFP signal around membranes; formation of large blebs on cell bodies, dendrites or presynaptic terminals; loss of dendritic spines.	Too high and/or long exposure to UV light.	Use appropriate filters to reduce the intensity of the UV light when inspecting the fluorescent signal; reduce the exposure time to UV light to a minimum; search the ROI wherever possible using the live-scanning mode of the microscope avoiding using UV light; use fast and precise shutters.
	Too high laser intensity.	Adapt imaging settings to use the lowest laser intensity possible; optimize the imaging settings outside the ROI; acquire the images using the 16-bit mode, in order to be able to use low laser intensities; select the appropriate emission filter, in order to maximize signal intensity without increasing laser strength.
	Too long exposure to laser energy.	Use the fastest scan mode and the smallest amount of confocal images that still allow proper analysis; avoid time consuming averaging options during acquisition; instead, optimize image quality after acquisition (e.g., by applying deconvolution).
	Too high light energy (UV and/or laser).	Use the smallest magnification objective possible to resolve the structures of interest; choose a high numerical aperture objective; choose an objective lens that is optimized for your emission wavelength.

Anticipated results

Critical factors for a successful imaging experiment are careful handling of the slices and rapid image acquisition. We strongly recommend always using the same confocal settings for comparable imaging sessions, and practicing the rapid identification of the orientation of labeled slices when first looking at a new type. It is also important to be able to rapidly re-identify the ROI within a given slice. This can be helped by making a schematic drawing, with landmarks of the particular slice, and using it for rapid orientation during the next imaging session ([Fig.1](#)).

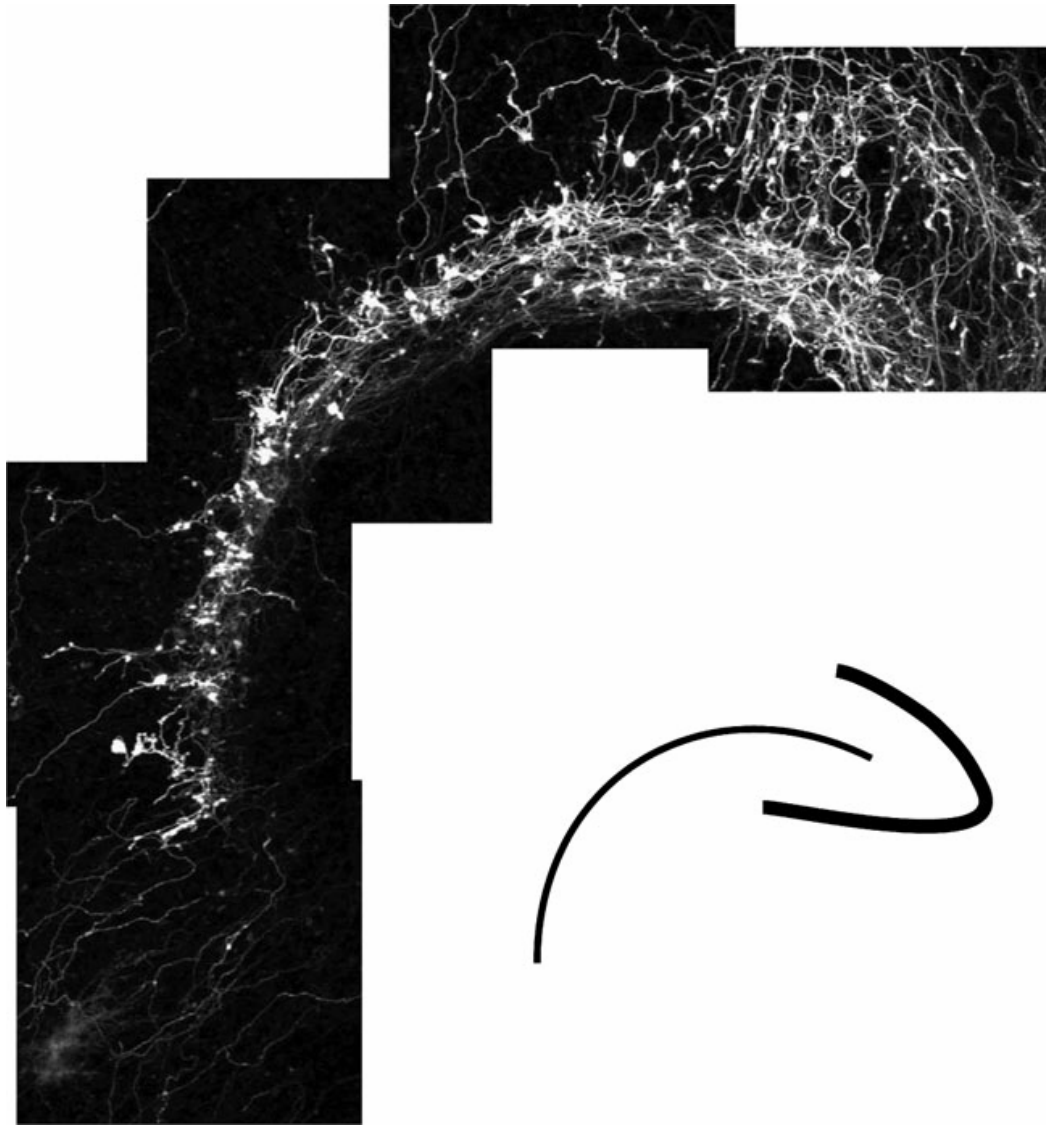


Figure 1. The five images were acquired with a 40x objective and then tiled. The schematic on the right indicates the orientation of the hippocampus (dentate gyrus on the right). The axons are labeled by a membrane-targeted GFP construct, as described in the text.

Staining protocol for organotypic hippocampal slice cultures

Nadine Gogolla^{1,3}, Ivan Galimberti^{1,3}, Vincenzo DePaola² and Pico Caroni¹

¹Friedrich Miescher Institute, Maulbeerstrasse 66, CH-4058 Basel, Switzerland.

²Cold Spring Harbor Laboratories, Cold Spring Harbor, New York, USA.

³These authors contributed equally to this work.

Nature Protocols

2006 (1, 2452 – 2456)

ABSTRACT

This protocol details a method to immunostain organotypic slice cultures from mouse hippocampus. The cultures are based on the interface method, which does not require special equipment, is easy to execute and yields slice cultures that can be imaged repeatedly, from the time of isolation at postnatal day 6–9 up to 6 months *in vitro*. The preserved tissue architecture facilitates the analysis of defined hippocampal synapses, cells and entire projections. Time-lapse imaging is based on transgenes expressed in the mice or on constructs introduced through transfection or viral vectors; it can reveal processes that develop over periods ranging from seconds to months. Subsequent to imaging, the slices can be processed for immunocytochemistry to collect further information about the imaged structures. This protocol can be completed in 3 d.

INTRODUCTION

Recent advances in live imaging and transgenic technology have had a substantial impact on the range of experimental tools available to life scientists (Conchello et al. 2005 and Yuste 2005). These include microscopes with greatly improved sensitivity, temporal and spatial resolution and spectral versatility; powerful image acquisition and processing software; and an ever-growing repertoire of fluorescent reagents to monitor second messengers, identify macromolecules and their physiological modifications, and examine subcellular structures *in situ*. In the field of neuroscience, these developments have allowed studies of the structure and function of biologically relevant neuronal circuits to be approached in a noninvasive way and with unprecedented analytical power. To fully exploit these technological developments, adequate biological preparations must be adapted for live-imaging studies of defined neuronal circuits (Gahwiler 1981, Stoppini et al. 1991, Gahwiler et al. 1997, DePaola et al. 2003 and Galimberti et al. 2006). Subsequent immunostaining of the preparations allows retrospective definition of the cellular and molecular identity of the imaged structures and their local surroundings, as well as molecular correlation of the dynamic processes.

Advantages of the method

Key features of the hippocampal organotypic slice cultures (Stoppini et al. 1991) from mice include (i) well-defined cellular architecture of the hippocampal circuit, which preserves the organization *in vivo* and allows for the identification and manipulation of defined neurons and synapses (Gahwiler 1981, Stoppini et al. 1991, Gahwiler et al. 1997, DePaola et al. 2003 and Galimberti et al. 2006); (ii) presence of axonal projections (mossy fiber axons extending from dentate gyrus granule cells to the distal end of CA3) that can largely be recovered in the slices in their original state (that is, without lesioning) and that establish stereotypic numbers of readily identifiable presynaptic terminals onto excitatory and inhibitory neurons in the hilus and CA3 (DePaola et al. 2003, Galimberti et al. 2006 and Henze et al. 2000); (iii) a long-term thickness of 100–150µm, preserving three-dimensional organizations of connectivity (Stoppini et al. 1991 and Gahwiler et al. 1997); (iv) maturation of the slice cultures closely reflecting the corresponding schedule *in vivo* (De Simoni et al. 2003); (v) the option to prepare the slices from mice of any genetic background, including those expressing fluorescent transgenes in selected neurons (DePaola et al. 2003, Galimberti et al. 2006, Caroni 1997 and Feng et al. 2000) and those of poor postnatal viability. Imaging coupled to retrospective immunocytochemistry allows the acquisition of information about unlabeled structures in the areas surrounding the imaged (fluorescent) structures, and the investigation of molecular mechanisms at the level of local identified structures within neuronal circuits.

Critical aspects

The main critical issues relate to the extent to which organotypic slice cultures reproduce the properties of hippocampal circuits *in vivo* (Gahwiler et al. 1997). This information is important in deciding whether the approach is appropriate to address the particular experimental issues one has in mind. These issues have been investigated in much detail by physiologists, who have demonstrated extensive similarities, but also a few discrepancies, between properties of the corresponding circuits in the neonatal and adult mouse brains (Gahwiler et al. 1997, DePaola et al. 2003, Galimberti et al. 2006, Henze et al. 2000 and De Simoni et al. 2003). Critical limitations of the immunocytochemistry protocol mainly involve issues of antibody penetration and antigen accessibility. Some of

these problems can be solved by varying the fixation and permeabilization protocols or by cutting sections of the slices.

Possible results and outlook

Organotypic slice cultures from approximately 1-week-old mouse hippocampus seem to reproduce most anatomical and functional properties of the corresponding hippocampal circuits *in vivo* for at least 6 months *in vitro* as a result of the intrinsic properties of their neurons. Imaging of the slices coupled to *post hoc* immunocytochemistry thus provides an exciting range of possibilities for the exploration of mechanisms controlling the assembly and function of neuronal circuits. Some of these possibilities include (i) time-lapse imaging and molecular analysis over periods ranging from sub-seconds to months, and from individual molecules to entire neuronal projections and circuits; (ii) imaging and analysis of neuronal (DePaola et al. 2003, Galimberti et al. 2006, Caroni 1997 and Feng et al. 2000) and glial (Benediktsson et al. 2005) subtypes; (iii) molecular manipulation using transfection (Benediktsson et al. 2005 and Lo et al. 1994) or viral approaches (Ehrengruber et al. 1999 and Miyaguchi et al. 1999) to knock down or overexpress genes, silence or activate neurons, render neurons responsive to light or selective drugs, and highlight subcircuits; (iv) protocols that combine physiology, imaging and immunocytochemistry; (v) manipulations to investigate lesion-induced plasticity and pathways of neurodegeneration and repair (such as amyloid- or epilepsy-related pathways); (vi) the potential to follow and characterize the insertion of new neurons, the development of axons and their connections, or the insertion of exogenously added stem cells; and (vii) additional *post hoc* analysis using methods involving tracers, electron microscopy and single-cell genomics.

MATERIALS

Reagents

- Organotypic hippocampal slices
- [Paraformaldehyde](#) (PFA; Merck, cat. no. 1.04005.1000)
- [Methanol](#) (MeOH; Merck, cat. no. 1.06009.1000)
- [Triton X-100](#) (Fluka Chemika, cat. no. 93420)
- [BSA](#) (Sigma, cat. no. A3912-100G)
- PBS (with or without magnesium and/or calcium)
- Primary and secondary antibodies suitable for immunohistochemistry
- 4% PFA in PBS (cooled to 4 °C)
! CAUTION PFA is toxic. Avoid inhalation, ingestion or contact with skin, eyes or mucous membranes.
- 20% MeOH in PBS (cooled to 4 °C)
- Permeabilization solution: 0.5% Triton X-100 in PBS

? TROUBLESHOOTING

- Blocking solution: 20% BSA in PBS
- Antibody solutions: 5% BSA in PBS + antibodies at specific dilution
- First washing solution: 5% BSA in PBS
- Second washing solution: PBS

Equipment

- Scalpel or razor blade
- Fine straight forceps
- [Microscope slides](#) (e.g., 76 x 26 mm; Menzel-Gläser)
- [Thin cover glasses](#) (e.g., 40 x 24 mm, 170 nm thick; Assistant)
- Mounting medium (e.g., [ProLong Gold antifade reagent](#), Invitrogen, cat. no. P36934)
- [12- or 24-well plates](#) (Corning, cat. no. 3513)

PROCEDURE

Overview

- [Step 1 - 8 Fixation of slice cultures \(day 1\)](#)
- [Step 9 - 10 Permeabilization of slice tissue \(day 1\)](#)
- [Step 11 - 12 Blocking \(day 2\)](#)
- [Step 13 - 15 Cutting slices off membrane of culture plate inserts \(day 2\)](#)
- [Step 16 - 19 Incubation with primary antibody \(day 2\)](#)
- [Step 20 - 23 Washing off primary antibody \(day 3\)](#)
- [Step 24 - 26 Incubation with secondary antibody \(day 3\)](#)
- [Step 27 Washing off secondary antibody](#)
- [Step 28 - 32 Mounting of stained slice cultures \(day 3\)](#)

Fixation of slice cultures (day 1) • TIMING 15 min

1. Remove the culture medium beneath the membrane by suction.
2. Add 1 ml of cold 4% PFA solution above and 1 ml beneath the membrane insert.

! CAUTION Use gloves to handle PFA, and wear a mask.

3. Wait 5 minutes. **? TROUBLESHOOTING**
4. Remove the PFA solution completely.
5. Wash once briefly by adding 1 ml of cold PBS above and 1 ml beneath the insert and then removing by suction.
6. Add 1 ml of cooled 20% MeOH/PBS solution above and 1 ml beneath the insert.
7. Wait 5 minutes. **? TROUBLESHOOTING**
8. Wash once briefly with PBS as in Step 5.

Permeabilization of slice tissue (day1) • TIMING Minimum 12 h

9. Add 1 ml of permeabilization solution (0.5% Triton X-100 in PBS) above and 1 ml beneath the insert.

10. Incubate overnight, or for at least 12 h, at 4 °C.

■ **PAUSE POINT** Slices can be kept in the permeabilization solution for up to 18 h.

?TROUBLESHOOTING

Blocking (day 2) • TIMING Minimum 4 h

11. Remove permeabilization solution.

12. Add blocking solution (20% BSA in PBS).

■ **PAUSE POINT** Can be left for 4 h at room temperature (22–24 °C) or overnight at 4 °C. Sections can be kept in the blocking solution at 4 °C for at least 2–3 d.

Cutting slices off membrane of culture plate inserts (day 2) • TIMING 5 min

13. To reduce the volume of antibody solutions needed, the slices are cut off the membranes of the culture plate inserts. Place the culture plate insert on a plastic cover (preferably a transparent plastic cover lying on a dark background to make the tissue easily visible).

14. Use forceps and scalpel to carefully cut the membrane piece together with the hippocampal slice out of the surrounding membrane. Keep 1–2 mm of distance to the tissue to avoid damage. (Optional: the slices can already be cut off just after the fixation to further limit the amounts of permeabilization and blocking solutions required).

▲ **CRITICAL STEP** Always keep the top side of the membrane facing up, and do not flip it around.

15. Place the cut-off membrane pieces (top sides facing up) onto the lid of a culture plate.

▲ **CRITICAL STEP** To avoid drying, always keep a droplet of 5% BSA/PBS solution on top of each slice.

Incubation with primary antibody (day 2) • TIMING Minimum 4 h or overnight

16. To avoid drying of the slices during the antibody incubations, build a 'wet chamber' by putting wet paper tissues into a box that can be tightly closed and is large enough to hold the culture dish covers of Step 15.
17. Prepare the primary antibody solutions in 5% BSA/PBS (50 μ l per slice).
18. Drop 50 μ l of the antibody solution onto each slice.
19. Carefully place the lid holding the slices into the wet chamber and close it.

■ **PAUSE POINT** The primary antibody can be incubated overnight at 4 °C or for 3–4 h at room temperature.

Washing off primary antibody (day 3) • TIMING 30 min

20. Fill the wells of a 12- or 24- well plate with 5% BSA/PBS (fill three times as many wells as you have slices to stain).
21. Put each stained slice into one well containing the 5% BSA/PBS washing solution.

▲ **CRITICAL STEP** Always keep the top side of the slice facing up.

22. To wash off excess antibody, put the plate onto a horizontal shaker for 5–10 min at moderate speed (be careful that the fluid movement does not cause the slice to flip over).
23. Transfer the slices to the next unused wells and repeat this washing twice more.

Incubation with secondary antibody (day 3) • TIMING Minimum 3 h

24. Prepare the secondary antibody solution (50 μ l per slice).

▲ **CRITICAL STEP** If you use fluorescent secondary antibodies, perform the following steps whenever possible in the dark, and keep the antibody-containing solutions away from light.

25. Put the slices back onto a fresh plate lid (as in Step 15).

26. Proceed as for primary antibody (Steps 16–19).

■ **PAUSE POINT** The secondary antibody can be incubated for 3–4 h at room temperature or overnight at 4 °C.

Washing off secondary antibody • TIMING 30 min

27. Wash off the secondary antibody as for the primary antibody (Steps 20–23) but using simple PBS solution (no BSA required).

Mounting of stained slice cultures (day 3) • TIMING 30 min

28. Put the washed slices, top sides facing up, onto a glass microscope slide.

29. Put a droplet of mounting medium directly on the slice.

▲ **CRITICAL STEP** Avoid drying out the slices.

30. Cover the slice immediately with a thin cover glass.

31. Seal the cover glass with nail polish.

■ **PAUSE POINT**

32. Store at 4 °C in the dark. The labeled slices can be kept for several months.

• **TIMING**

Day 1: fixation, 5 min PFA + 5 min MeOH; permeabilization, minimum 12 h (overnight).

Day 2: blocking, minimum 3 h; incubation with primary antibody, minimum 4 h or overnight.

Day 3: washing off primary antibody, 30 min; incubation with secondary antibody, minimum 3 h; washing off secondary antibody, 30 min; mounting sections, 5 min; sealing cover glasses, 5 min.

?TROUBLESHOOTING

Table 1 Troubleshooting advice.

Problem	Possible reason	Solution
Transgenic GFP signal is beaded or very weak	Fixation can destroy GFP signal (Steps 3 and 7)	Reduce fixation times (e.g., 3 min each for PFA and MeOH)
		Methanol fixation may not be required for each antibody. Try omitting methanol
		Use anti-GFP antibody to enhance the signal
Antibody does not penetrate deeply into the tissue	Permeabilization too weak (Step 10; especially in young slices, which are more dense)	Increase Triton X-100 concentration during the permeabilization step to 1–2% and/or prolong the incubation

ANTICIPATED RESULTS

Critical factors are the fixation of the slices and penetration of antibodies and reagents. Penetration of reagents can be enhanced by double fixation followed by permeabilization overnight. Unfortunately, fixations are not entirely predictable, even when using the same protocol, so one should plan on processing several copies of crucial data. Suboptimal fixation can lead to a blurred appearance of small structures such as active zones. Optimization of protocols for special needs is recommended.

This protocol should produce good-resolution labeling of cellular and subcellular structures ([Fig. 1](#)) and unambiguous identification of regions of interest, such as those that had been followed with live imaging before fixation.

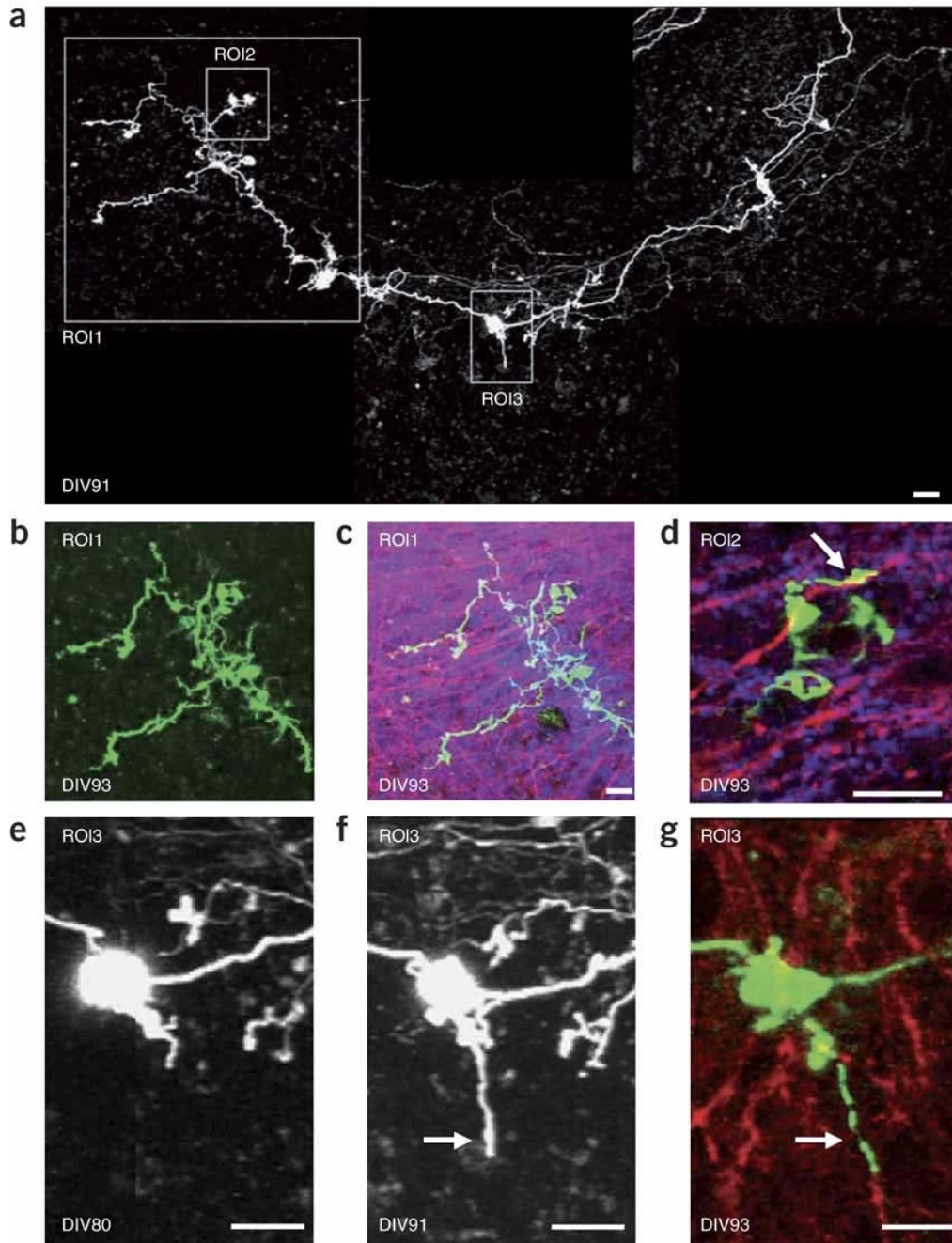


Figure 1. A slice from a Thy1-mGFP single-transgenic mouse shows mossy fiber projection expressing membrane-targeted GFP. After imaging, the slice was fixed and stained for Bassoon (active zone marker) and phospho-GluR1 (pyramidal neuron dendrite marker). Live imaging was done on *in vitro* day 80 (DIV80) and DIV91; fixation and staining were done on DIV93. (a) Low-magnification view of mossy fiber projection and regions of interest (mossy fiber terminal complexes; ROI1–3). (b) Maximum-intensity projection of the GFP signal in ROI1 after fixation. (c) Same as b, but with superimposed Bassoon (blue) and phospho-GluR1 (red) signals. (d) Single confocal plane of ROI2. Note process grown from the mossy fiber terminal between DIV91 and DIV93 (arrow), which exhibits a terminal bouton and contacts the same dendrite (phospho-GluR1) as its mossy fiber terminal of origin. (e,f) Live imaging of ROI3 (maximum-intensity projection). (g) Single confocal plane of ROI3 after fixation and staining (green, GFP; red, phospho-GluR1). Note process that grew from the mossy fiber terminal between DIV80 and DIV91 (arrows in f and g), extending along a phospho-GluR1-positive dendrite. Scale bars, 25 μ m.

5. REFERENCES

- Acsady L, Kamondi A, Sik A, Freund T, Buzsaki G (1998) GABAergic cells are the major postsynaptic targets of mossy fibers in the rat hippocampus. *J Neurosci.* 18(9):3386-403.
- Alsina B, Vu T, Cohen-Cory S (2001) Visualizing synapse formation in arborizing optic axons in vivo: dynamics and modulation by BDNF. *Nat Neurosci.* 4(11):1093-101.
- Amaral, D.G. & Lavenex, P (2007) in *The Hippocampus Book* (eds Andersen, P., Morris, R.G.M., Amaral, D.G., Bliss, T.V.P. & O'Keefe, J.) 37-114 (Oxford Univ.Press, New York).
- Aravamudan B, Broadie K (2003) Synaptic Drosophila UNC-13 is regulated by antagonistic G-protein pathways via a proteasome-dependent degradation mechanism. *J Neurobiol.* 15;54(3):417-38.
- Bagri A, Tessier-Lavigne M (2002) Neuropilins as Semaphorin receptors: in vivo functions in neuronal cell migration and axon guidance. *Adv Exp Med Biol.* 515:13-31.
- Bailey CH, Kandel ER (1993) Structural changes accompanying memory storage. *Annu Rev Physiol.* 55:397-426.
- Benediktsson AM, Schachtele SJ, Green SH & Dailey ME (2005) Ballistic labeling and dynamic imaging of astrocytes in organotypic hippocampal slice cultures. *J. Neurosci. Meth.* 141, 41–53.
- Berardi N, Pizzorusso T, Maffei L (2004) Extracellular matrix and visual cortical plasticity: freeing the synapse. *Neuron* 44(6):905-8.
- Biederer T, Sara Y, Mozhayeva M, Atasoy D, Liu X, Kavalali ET, Südhof TC (2002) SynCAM, a synaptic adhesion molecule that drives synapse assembly. *Science* 297(5586):1525-31.
- Bliss TV, Gardner-Medwin AR (1973) Long-lasting potentiation of synaptic transmission in the dentate area of the unanaesthetized rabbit following stimulation of the perforant path. *J Physiol.* 232(2):357-74.
- Bliss TV, Lomo T (1973) Long-lasting potentiation of synaptic transmission in the dentate area of the anaesthetized rabbit following stimulation of the perforant path. *J Physiol* 232(2):331-56.
- Bolshakov VY, Siegelbaum SA (1995) Regulation of hippocampal transmitter release during development and long-term potentiation. *Science* 22;269(5231):1730-4.

Brecht M, Fee MS, Garaschuk O, Helmchen F, Margrie TW, Svoboda K, Osten P (2004) Novel approaches to monitor and manipulate single neurons in vivo. *J Neurosci.* 24(42):9223-7.

Caroni P (1997) Overexpression of growth-associated proteins in the neurons of adult transgenic mice. *J Neurosci Methods* 71(1):3-9.

Chicurel ME, Harris KM (1992). Three-dimensional analysis of the structure and composition of CA3 branched dendritic spines and their synaptic relationships with mossy fiber boutons in the rat hippocampus. *J Comp Neurol.* 325:169-182.

Chklovskii DB, Mel BW, Svoboda K (2004) Cortical rewiring and information storage. *Nature* 431:782-788.

Colledge M, Snyder EM, Crozier RA, Soderling JA, Jin Y, Langeberg LK, Lu H, Bear MF, Scott JD (2003) Ubiquitination regulates PSD-95 degradation and AMPA receptor surface expression. *Neuron* 40(3):595-607.

Conchello JA & Lichtman JW (2005) Optical sectioning microscopy. *Nat. Meth.* 2, 920–931.

Crepel L (1971) Maturation of climbing fiber responses in the rat. *Brain Res.* 35, 272-276.

Dalva MB, Takasu MA, Lin MZ, Shamah SM, Hu L, Gale NW, Greenberg ME (2000) EphB receptors interact with NMDA receptors and regulate excitatory synapse formation. *Cell* 103(6):945-56.

Dan Y, Poo MM (2004) Spike timing-dependent plasticity of neural circuits. *Neuron* 44(1):23-30.

Dan Y & Poo MM (2006) Spike timing-dependent plasticity: from synapse to perception. *Physiol Rev.* 86(3):1033-48.

Danglot L, Triller A, Marty S (2006) The development of hippocampal interneurons in rodents. *Hippocampus* 16(12):1032-60.

Danzer SC, McNamara JO (2004) Localization of brain-derived neurotrophic factor to distinct terminals of mossy fiber axons implies regulation of both excitation and feedforward inhibition of CA3 pyramidal cells. *J Neurosci.* 15:11346-11355.

De Paola V, Arber S, Caroni P (2003) AMPA receptors regulate dynamic equilibrium of presynaptic terminals in mature hippocampal networks. *Nat Neurosci.* 6(5):491-500.

- De Paola V, Holtmaat A, Knott G, Song S, Wilbrecht L, Caroni P, Svoboda K (2006) Cell type-specific structural plasticity of axonal branches and boutons in the adult neocortex. *Neuron* 49: 861-875.
- De Simoni A, Griesinger CB & Edwards FA (2003) Development of rat CA1 neurons in acute versus organotypic slices: role of experience in synaptic morphology and activity. *J. Physiol.* 550, 135–147.
- Dudek SM, Bear MF (1992) Homosynaptic long-term depression in area CA1 of hippocampus and effects of N-methyl-D-aspartate receptor blockade. *Proc Natl Acad Sci U S A* 89(10):4363-7.
- Engel D, Jonas P (2005) Presynaptic action potential amplification by voltage-gated Na⁺ channels in hippocampal mossy fiber boutons. *Neuron* 45:405–417.
- Engert F, Bonhoeffer T (1999) Dendritic spine changes associated with hippocampal long-term synaptic plasticity. *Nature* 399(6731):66-70.
- Ehlers MD (2003) Activity level controls postsynaptic composition and signaling via the ubiquitin-proteasome system. *Nat Neurosci.* 6(3):231-242.
- Ehrengruber MU *et al* (1999) Recombinant Semliki Forest virus and Sindbis virus efficiently infect neurons in hippocampal slice cultures. *Proc Natl Acad Sci USA* 96, 7041–7046.
- Feng G, Mellor RH, Bernstein M, Keller-Peck C, Nguyen QT, Wallace M, Nerbonne JM, Lichtman JW, Sanes JR (2000) Imaging neuronal subsets in transgenic mice expressing multiple spectral variants of GFP. *Neuron* 28:41-51.
- Fischer M, Kaech S, Knutti D, Matus A (1998) Rapid actin-based plasticity in dendritic spines. *Neuron* 20(5):847-54.
- Gabrieli JD, Brewer JB, Desmond JE, Glover GH (1997) Separate neural bases of two fundamental memory processes in the human medial temporal lobe. *Science* 276(5310):264-6.
- Gahwiler BH (1981) Organotypic monolayer cultures of nervous tissue. *J Neurosci Meth.* 4, 329–342.
- Gahwiler BH, Capogna M, Debanne D, McKinney RA, Thompson SM (1997) Organotypic slice cultures: a technique has come of age. *Trends Neurosci.* 20:471-477.
- Galimberti I, Gogolla N, Alberi S, Santos AF, Muller D, Caroni P (2006) Long-term rearrangements of mossy fiber terminal connectivity in the adult regulated by experience. *Neuron* 50(5): 749-63.

Gan WB, Kwon E, Feng G, Sanes JR, Lichtman JW (2003) Synaptic dynamism measured over minutes to months: age-dependent decline in an autonomic ganglion. *Nat Neurosci.* 6(9):956-60.

Geiger JR, Jonas P (2000) Dynamic control of presynaptic Ca^{2+} inflow by fast-inactivating K^+ channels in hippocampal mossy fiber boutons. *Neuron* 28:927-939.

Geinisman Y, Berry RW, Disterhoft JF, Power JM, Van der Zee EA (2001) Associative learning elicits the formation of multiple-synapse boutons. *J Neurosci.* 21(15):5568-73.

Gil OD, Needleman L, Huntley GW (2002) Developmental patterns of cadherin expression and localization in relation to compartmentalized thalamocortical terminations in rat barrel cortex. *J Comp Neurol.* 453(4):372-88.

Gogolla N, Galimberti I, Caroni P (2007) Structural plasticity of axon terminals in the adult. *Curr Opin Neurobiol.* 17(5):516-24.

Gogolla N, Galimberti I, DePaola V, Caroni P (2006) Staining protocol for organotypic hippocampal slice cultures. *Nat Protoc.* 1(5):2452-6.

Gogolla N, Galimberti I, DePaola V, Caroni P (2006) Long-term live imaging of neuronal circuits in organotypic hippocampal slice cultures. *Nat Protoc.* 1(3):1223-6.

Gogolla N, Galimberti I, DePaola V, Caroni P (2006) Preparation of organotypic hippocampal slice cultures for long-term live imaging. *Nat Protoc.* 1(3):1165-71.

Gonzales RB, DeLeon Galvan CJ, Rangel YM, and Claiborne BJ (2001). Distribution of thorny excrescences on CA3 pyramidal neurons in the rat hippocampus. *J Comp Neurol.* 430:357-368.

Gruart A, Muñoz MD, Delgado-García JM (2006) Involvement of the CA3-CA1 synapse in the acquisition of associative learning in behaving mice. *J Neurosci.* 26(4):1077-87.

Grutzendler J, Kasthuri N, Gan WB (2002) Long-term dendritic spine stability in the adult cortex. *Nature* 420:812-816.

Guzowski JF, Setlow B, Wagner EK, McGaugh JL (2001) Experience-dependent gene expression in the rat hippocampus after spatial learning: a comparison of the immediate-early genes Arc, c-fos, and zif268. *J Neurosci.* 21(14):5089-98.

Henke K, Buck A, Weber B, Wieser HG (1997) Human hippocampus establishes associations in memory. *Hippocampus* 7(3):249-56.

Henze DA, Urban NN, Barrionuevo G (2000) The multifarious hippocampal mossy fiber pathway: a review *Neuroscience* 98:407-427.

- Henze DA, Wittner L, Buzsaki G (2002) Single granule cells reliably discharge targets in the hippocampal CA3 network in vivo. *Nat Neurosci.* 5:790-795.
- Holahan MR, Rekart JL, Sandoval J, Routtenberg A (2006) Spatial learning induces presynaptic structural remodeling in the hippocampal mossy fiber system of two rat strains. *Hippocampus* 16(6):560-70.
- Holtmaat AJ, Trachtenberg JT, Wilbrecht L, Shepherd GM, Zhang X, Knott GW, Svoboda K (2005) Transient and persistent dendritic spines in the neocortex in vivo. *Neuron* 45(2):279-91.
- Holtmaat A, Wilbrecht L, Knott GW, Welker E, Svoboda K (2006) Experience-dependent and cell-type-specific spine growth in the neocortex. *Nature* 441(7096):979-83.
- Ikegaya Y, Aaron G, Cossart R, Aronov D, Lampl I, Ferster D, Yuste R (2004) Synfire chains and cortical songs: temporal modules of cortical activity. *Science* 304:559-564.
- Ishida M, Saitoh T, Shimamoto K, Ohfune Y, Shinozaki H (1993). A novel metabotropic glutamate receptor agonist: marked depression of monosynaptic excitation in the newborn rat isolated spinal cord. *Br J Pharmacol.* 109:1169-1177.
- Isaac JT, Crair MC, Nicoll RA, Malenka RC (1997) Silent synapses during development of thalamocortical inputs. *Neuron* 18(2):269-80.
- Jefferis GS, Potter CJ, Chan AM, Marin EC, Rohlfsing T, Maurer CR Jr, Luo L (2007) Comprehensive maps of *Drosophila* higher olfactory centers: spatially segregated fruit and pheromone representation. *Cell* 128(6):1187-203.
- Johnston D, Amaral DG (1998) Hippocampus in „The synaptic organization of the brain“ (ed. Shepherd G.M.) Oxford Univ Press, N.Y:417-458.
- Kamiya H, Shinozaki H, Yamamoto C (1996) Activation of metabotropic glutamate receptor type 2/3 suppresses transmission at rat hippocampal mossy fibre synapses. *J Physiol.* 493:447-455.
- Kavalali ET, Klingauf J, Tsien RW (1999) Activity-dependent regulation of synaptic clustering in a hippocampal culture system. *Proc Natl Acad Sci U S A* 96:12893-12900.
- Kempermann G, Kuhn HG & Gage FH (1997) More hippocampal neurons in adult mice living in an enriched environment. *Nature* 386:493–495.
- Kempermann G, Kuhn HG & Gage FH (1998a) Experience-induced neurogenesis in the senescent dentate gyrus. *J Neurosci.* 18:3206–3212.

Kempermann G, Brandon EP & Gage FH (1998b) Environmental stimulation of 129/SvJ mice causes increased cell proliferation and neurogenesis in the adult dentate gyrus. *Curr Biol.* 8:939–942.

Kempermann G, Gast D & Gage FH (2002) Neuroplasticity in old age: sustained fivefold induction of hippocampal neurogenesis by long-term environmental enrichment. *Ann Neurol.* 52:135–143.

Kirov SA, Harris KM (2000) Dendrites are more spiny on mature hippocampal neurons when synapses are inactivated. *Nat Neurosci.* 2(10):878-83.

Kleim JA, Swain RA, Czerlanis CM, Kelly JL, Pipitone MA, Greenough WT (1997) Learning dependent dendritic hypertrophy of cerebellar stellate cells: plasticity of local circuit neurons. *Neurobiol Learn Mem.* 67:29–33.

Kleim JA, Barbay S, Cooper NR, Hogg TM, Reidel CN, Remple MS, Nudo RJ (2002) Motor learning-dependent synaptogenesis is localized to functionally reorganized motor cortex. *Neurobiol Learn Mem.* 77(1):63-77.

Knott GW, Quairiaux C, Genoud C, Welker E (2002) Formation of dendritic spines with GABAergic synapses induced by whisker stimulation in adult mice. *Neuron* 34:265-273.

Knott GW, Holtmaat A, Wilbrecht L, Welker E, Svoboda K (2006) Spine growth precedes synapse formation in the adult neocortex in vivo. *Nat Neurosci.* 9(9):1117-24.

Kobayashi K, Poo MM (2004) Spike train timing-dependent associative modification of hippocampal CA3 recurrent synapses by mossy fibers. *Neuron* 41:445-454.

Konur S, Yuste R (2004) Developmental regulation of spine and filopodial motility in primary visual cortex: reduced effects of activity and sensory deprivation. *J Neurobiol.* 59(2):236-46.

Korkotian E, Segal M (1999) Release of calcium from stores alters the morphology of dendritic spines in cultured hippocampal neurons. *Proc Natl Acad Sci U S A* 96 (21):12068-72.

Kozorovitskiy Y, Gross CG, Kopil C, Battaglia L, McBreen M, Stranahan AM, Gould E (2005) Experience induces structural and biochemical changes in the adult primate brain. *Proc Natl Acad Sci U S A* 102(48):17478-82

Kozorovitskiy Y, Hughes M, Lee K, Gould E (2006) Fatherhood affects dendritic spines and vasopressin V1a receptors in the primate prefrontal cortex. *Nat Neurosci.* 9(9):1094-5.

Kuhl PK (2004) Early language acquisition: cracking the speech code. *Nat Rev Neurosci.* 5:831–843.

Lamprecht R, LeDoux J (2004) Structural plasticity and memory. *Nat Rev Neurosci.* 5(1):45-54.

Larramandi LMH & Victor T (1967) Synapse on the Purkinje cell spines in the mouse. An electron microscopic study. *Brain Res.* 5, 247-260.

Laurienti PJ, Burdette JH, Maldjian JA, Wallace MT (2006) Enhanced multisensory integration in older adults. *Neurobiol Aging* 27(8):1155-63.

Lawrence JJ, McBain CJ (2003) Interneuron diversity series: containing the detonation--feedforward inhibition in the CA3 hippocampus. *Trends Neurosci.* 26:631-640.

Laxson LC, King JS (1983) The formation and growth of the cortical layers in the cerebellum of the opossum. *Anat Embryol (Berl)* 167(3):391-409.

Lee CK, Weindruch R, Prolla TA (2000) Gene-expression profile of the ageing brain in mice. *Nat Genet.* 25(3):294-7.

Lee EH, Hsu WL, Ma YL, Lee PJ & Chao CC (2003) Enrichment enhances the expression of sgk, a glucocorticoid-induced gene, and facilitates spatial learning through glutamate AMPA receptor mediation. *Eur J Neurosci.* 18, 2842-2852.

Lee WC, Huang H, Feng G, Sanes JR, Brown EN, So PT, Nedivi E (2006). Dynamic remodeling of dendritic arbors in GABAergic interneurons of adult visual cortex. *PLoS Biol.* 4:e29.

Lee SM, Tole S, Grove E, McMahon AP (2006) A local Wnt-3a signal is required for development of the mammalian hippocampus. *Development* 127(3):457-67.

Leggio MG et al. (2005) Environmental enrichment promotes improved spatial abilities and enhanced dendritic growth in the rat. *Behav Brain Res.* 163:78-90.

Lendvai B, Stern EA, Chen B, Svoboda K (2000). Experience-dependent plasticity of dendritic spines in the developing rat barrel cortex in vivo. *Nature* 404:876-881.

LeVay S, Wiesel TN, Hubel DH (1980) The development of ocular dominance columns in normal and visually deprived monkeys. *J Comp Neurol.* 191(1):1-51.

Li W, Luxenberg E, Parrish T, Gottfried JA (2006) Learning to smell the roses: experience-dependent neural plasticity in human piriform and orbitofrontal cortices. *Neuron* 21;52(6):1097-108.

Lichtman JW, Colman H (2000). Synapse elimination and indelible memory. *Neuron* 25:269-278.

Linkenhoker BA, Knudsen EI (2002). Incremental training increases the plasticity of the auditory space map in adult barn owls. *Nature* 419:293-296.

Linkenhoker BA, von der Ohe CG, Knudsen EI (2005). Anatomical traces of juvenile learning in the auditory system of adult barn owls. *Nat.Neurosci.* 8:93-98.

Lo DC, McAllister AK & Katz LC (1994) Neuronal transfection in brain slices using particle-mediated gene transfer. *Neuron* 13, 1263–1268.

Maguire EA, Gadian DG, Johnsrude IS, Good CD, Ashburner J, Frackowiak RS, Frith CD (2000) Navigation-related structural change in the hippocampi of taxi drivers. *Proc Natl Acad Sci U S A* 97(8):4398-403.

Majdan M, Shatz CJ (2006) Effects of visual experience on activity-dependent gene regulation in cortex. *Nat Neurosci.* 9(5):650-9.

Majewska AK, Newton JR, Sur M (2006) Remodeling of synaptic structure in sensory cortical areas in vivo. *J Neurosci.* 26(11):3021-9.

Malenka RC, Nicoll RA (1999) Long-term potentiation – a decade of progress. *Science* 285(5435):1870-4.

Malenka RC & Bear MF (2004) LTP and LTD: an embarrassment of riches. *Neuron* 44(1):5-21.

Martin LA, Tan SS, Goldowitz D (2002) Clonal architecture of the mouse hippocampus. *J Neurosci.* 22(9):3520-30.

Martin SJ, Grimwood PD, Morris RG (2000) Synaptic plasticity and memory: an evaluation of the hypothesis. *Annu Rev Neurosci.* 23:649-711.

Mataga N, Mizuguchi Y, Hensch TK (2004) Experience-dependent pruning of dendritic spines in visual cortex by tissue plasminogen activator. *Neuron* 44(6):1031-41.

McAllister AK (2007) Dynamic aspects of CNS synapse formation. *Annu Rev Neurosci.* 30:425-50.

McEwen BS (1999) Stress and hippocampal plasticity. *Annu Rev Neurosci.* 22:105-122.

McGaugh JL (2000) Memory--a century of consolidation. *Science* 287(5451):248-51.

McNaughton BL & Morris RG (1987) Hippocampal synaptic enhancement and information. *Trends Neurosci.* 10:408–415.

- Merzenich MM, Kaas JH, Wall JT, Sur M, Nelson RJ, Felleman DJ (1983a) Progression of change following median nerve section in the cortical representation of the hand in areas 3b and 1 in adult owl and squirrel monkeys. *Neuroscience* 10(3):639-65.
- Merzenich MM, Kaas JH, Wall J, Nelson RJ, Sur M, Felleman D (1983b) Topographic reorganization of somatosensory cortical areas 3b and 1 in adult monkeys following restricted deafferentation. *Neuroscience* 8(1):33-55.
- Merzenich MM, Nelson RJ, Stryker MP, Cynader MS, Schoppmann A, Zook JM (1984) Somatosensory cortical map changes following digit amputation in adult monkeys. *J Comp Neurol.* 224(4):591-605.
- Meshi D, Drew MR, Saxe M, Ansorge MS, David D, Santarelli L, Malapani C, Moore H, Hen R (2006) Hippocampal neurogenesis is not required for behavioral effects of environmental enrichment. *Nature Neurosci.* 9:729–731.
- Migliore M, Shepherd GM (2005) Opinion: an integrated approach to classifying neuronal phenotypes. *Nat Rev Neurosci.* 6(10):810-8.
- Milner B, Squire LR, Kandel ER (1998) Cognitive neuroscience and the study of memory. *Neuron* 20(3):445-68.
- Miyaguchi, K., Maeda, Y., Kojima, T., Setoguchi, Y. & Mori, N (1999) Neuron-targeted gene transfer by adenovirus carrying neural-restrictive silencer element. *Neuroreport* 10 2349–2353.
- Moita MA, Rosis S, Zhou Y, LeDoux JE, Blair HT (2003) Hippocampal place cells acquire location-specific responses to the conditioned stimulus during auditory fear conditioning. *Neuron* 37(3):485-97.
- Montgomery JM, Madison DV (2002) State-dependent heterogeneity in synaptic depression between pyramidal cell pairs. *Neuron* 33(5):765-77.
- Mori M, Abegg MH, Gähwiler BH, Gerber U (2004) A frequency-dependent switch from inhibition to excitation in a hippocampal unitary circuit. *Nature* 431:453-456.
- Moser MB, Trommald M, Andersen P (1994) An increase in dendritic spine density on hippocampal CA1 pyramidal cells following spatial learning in adult rats suggests the formation of new synapses. *Proc Natl Acad Sci U S A* 91(26):12673-5.
- Moser MB, Trommald M, Egeland T & Andersen P (1997) Spatial training in a complex environment and isolation alter the spine distribution differently in rat CA1 pyramidal cells. *J Comp Neurol.* 380:373–381.
- Mower GD (1991) The effect of dark rearing on the time course of the critical period in cat visual cortex. *Brain Res Dev Brain Res.* 58(2):151-8.

- Mulkey RM, Malenka RC (1992) Mechanisms underlying induction of homosynaptic long-term depression in area CA1 of the hippocampus. *Neuron* 9(5):967-75.
- Muller D, Toni N, Buchs PA (2000). Spine changes associated with long-term potentiation. *Hippocampus* 10:596-604.
- Muller D, Nikonenko I, Jourdain P, Alberi S (2002) LTP, memory and structural plasticity. *Curr Mol Med.* 2(7):605-11.
- Nägerl UV, Eberhorn N, Cambridge SB, Bonhoeffer T (2004) Bidirectional activity-dependent morphological plasticity in hippocampal neurons. *Neuron* 44(5):759-67.
- Naka F, Narita N, Okado N & Narita M (2005) Modification of AMPA receptor properties following environmental enrichment. *Brain Dev.* 27:275–278.
- Napper RM, Harvey RJ (1988a) Quantitative study of granule and Purkinje cells in the cerebellar cortex of the rat. *J Comp Neurol.* 274(2):151-7.
- Napper RM, Harvey RJ (1988b) Quantitative study of the Purkinje cell dendritic spines in the rat cerebellum. *J Comp Neurol.* 274(2):158-67.
- Neves G, Cooke SF, Bliss TV (2008) Synaptic plasticity, memory and the hippocampus: a neural network approach to causality. *Nat Rev Neurosci.* 9(1):65-75.
- Nicoll RA, Malenka RC (1995) Contrasting properties of two forms of long-term potentiation in the hippocampus. *Nature* 377(6545): 115-8.
- Nicoll RA & Schmitz D (2005) Synaptic plasticity at hippocampal mossy fiber synapses. *Nat Rev Neurosci.* 6:863–876.
- Nikonenko I, Jourdain P, Alberi S, Toni N, Muller D (2002) Activity-induced changes of spine morphology. *Hippocampus* 12(5):585-91.
- Nithianantharajah J, Levis H & Murphy M (2004) Environmental enrichment results in cortical and subcortical changes in levels of synaptophysin and PSD-95 proteins. *Neurobiol Learn Mem.* 81:200–210.
- Nithianantharajah J, Hannan AJ (2006) Enriched environments, experience-dependent plasticity and disorders of the nervous system. *Nat Rev Neurosci.* 7(9):697-709.
- O'Brien RJ, Xu D, Petralia RS, Steward O, Huganir RL, Worley P (1999) Synaptic clustering of AMPA receptors by the extracellular immediate-early gene product *Narp*. *Neuron* 23(2):309-23.
- O'Keefe J, Dostrovsky J (1971) The hippocampus as a spatial map. Preliminary evidence from unit activity in the freely-moving rat. *Brain Res.* 34(1):171-5.

- O'Keefe J, Nadel L (1978) *The Hippocampus as a Cognitive Map* (Clarendon, Oxford).
- O'Keefe J & Recce ML (1993) Phase relationship between hippocampal place units and the EEG theta rhythm. *Hippocampus* 3:317–330.
- Oray S, Majewska A, Sur M (2004) Dendritic spine dynamics are regulated by monocular deprivation and extracellular matrix degradation. *Neuron* 44(6):1021-30.
- Penttonen M, Kamondi A, Sik A, Acsady L, Buzsaki G (1997) Feed-forward and feed-back activation of the dentate gyrus in vivo during dentate spikes and sharp wave bursts. *Hippocampus* 7:437-450.
- Petersen JD, Chen X, Vinade L, Dosemeci A, Lisman JE, Reese TS (2003) Distribution of postsynaptic density (PSD)-95 and Ca²⁺/calmodulin-dependent protein kinase II at the PSD. *J Neurosci.* 23(35):11270-8.
- Pham TM et al. (1999) Changes in brain nerve growth factor levels and nerve growth factor receptors in rats exposed to environmental enrichment for one year. *Neuroscience* 94:279–286.
- Pleskacheva MG, Wolfer DP, Kupriyanova IF, Nikolenko DL, Scheffrahn H, Dell'Omo G, Lipp HP (2000). Hippocampal mossy fibers and swimming navigation learning in two vole species occupying different habitats. *Hippocampus* 10:17-30.
- Poirazi P, Mel BW (2001). Impact of active dendrites and structural plasticity on the memory capacity of neural tissue. *Neuron* 29:779-796.
- Polley DB, Steinberg EE, Merzenich MM (2006) Perceptual learning directs auditory cortical map reorganization through top-down influences. *J Neurosci.* 26: 4970–4982.
- Poo MM (2001) Neurotrophins as synaptic modulators. *Nat Rev Neurosci.* 2(1):24-32.
- Qin L, Marrs GS, McKim R, Dailey ME (2001). Hippocampal mossy fibers induce assembly and clustering of PSD95-containing postsynaptic densities independent of glutamate receptor activation. *J Comp Neurol.* 440:284-298.
- Ramírez-Amaya V, Bermúdez-Rattoni F (1999) Conditioned enhancement of antibody production is disrupted by insular cortex and amygdala but not hippocampal lesions. *Brain Behav Immun.* 13(1):46-60.
- Ramírez -Amaya V, Balderas I, Sandoval J, Escobar ML, Bermudez-Rattoni F (2001). Spatial long-term memory is related to mossy fiber synaptogenesis. *J Neurosci.* 21:7340-7348.

Rampon C et al (2000) Enrichment induces structural changes and recovery from nonspatial memory deficits in CA1 NMDAR1-knockout mice. *Nature Neurosci.* 3:238–244.

Rampon C et al (2000) Effects of environmental enrichment on gene expression in the brain. *Proc. Natl Acad Sci USA* 97:12880–12884.

Rassmusson DD (1982) Reorganization of raccoon somatosensory cortex following removal of the fifth digit. *J Comp Neurol.* 205(4):313-26.

Rassmusson DD, Nance DM (1986) Non-overlapping thalamocortical projections for separate forepaw digits before and after cortical reorganization in the raccoon. *Brain Res Bull.* 16(3):399-406.

Rassmusson DD (1988) Projections of digit afferents to the cuneate nucleus in the raccoon before and after partial deafferentation. *J Comp Neurol.* 277(4):549-56.

Recanzone GH, Merzenich MM, Jenkins WM, Grajski KA, Dinse HR (1992) Topographic reorganization of the hand representation in cortical area 3b owl monkeys trained in a frequency-discrimination task. *J Neurophysiol.* 67(5):1031-56.

Recanzone GH, Schreiner CE, Merzenich MM (1993) Plasticity in the frequency representation of primary auditory cortex following discrimination training in adult owl monkeys. *J Neurosci.* 13(1):87-103.

Reid CA, Fabian-Fine R, Fine A (2001) Postsynaptic calcium transients evoked by activation of individual hippocampal mossy fiber synapses. *J Neurosci.* 21(7):2206-14.

Rollenhagen A et al. (2007) Structural determinants of transmission at large hippocampal mossy fiber synapses. *J Neurosci.* 27(39):10434-10444.

Ross RS, Eichenbaum H (2006) Dynamics of hippocampal and cortical activation during consolidation of a nonspatial memory. *J Neurosci.* 26(18):4852-9.

Rosso SB, Sussman D, Wynshaw-Boris A, Salinas PC (2005) Wnt signaling through Dishevelled, Rac and JNK regulates dendritic development. *Nat Neurosci.* 8(1): 34-42

Sandi C, Davies HA, Cordero MI, Rodriguez JJ, Popov VI, Stewart MG (2003). Rapid reversal of stress induced loss of synapses in CA3 of rat hippocampus following water maze training. *Eur J Neurosci.* 17:2447-2456.

Sanes JR, Lichtman JW (1999) Development of the vertebrate neuromuscular junction. *Annu Rev Neurosci.* 22:389-442.

Sanes JR, Lichtman JW (2001) Induction, assembly, maturation and maintenance of a postsynaptic apparatus. *Nat Rev Neurosci.* 2(11):791-805.

- Sans N, Petralia RS, Wang YX, Blahos J 2nd, Hell JW, Wenthold RJ (2000) A developmental change in NMDA receptor-associated proteins at hippocampal synapses. *J Neurosci.* 20(3):1260-71.
- Scheiffele P (2003) Cell-cell signaling during synapse formation in the CNS. *Annu Rev Neurosci.* 26:485-508.
- Scheiffele P, Fan J, Choih J, Fetter R, Serafini T (2000) Neuroligin expressed in nonneuronal cells triggers presynaptic development in contacting axons. *Cell* 101(6):657-69.
- Schopke R, Wolfer DP, Lipp HP, Leisinger-Trigona MC (1991) Swimming navigation and structural variations of the infrapyramidal mossy fibers in the hippocampus of the mouse. *Hippocampus* 1:315-328.
- Schuett S, Bonhoeffer T, Hubener M (2001) Pairing-induced changes of orientation maps in cat visual cortex. *Neuron* 32(2):325-37.
- Schwegler H, Crusio WE (1995) Correlations between radial-maze learning and structural variations of septum and hippocampus in rodents. *Behav Brain Res.* 67(1):29-41.
- Scoville WB, Milner B (1957) Loss of recent memory after bilateral hippocampal lesions. *J Neurol Neurosurg Psychiatr.* 20:11-21.
- Segal M (2005) Dendritic spines and long-term plasticity. *Nat Rev Neurosci.* 6(4):277-84.
- Shapira M, Zhai RG, Dresbach T, Bresler T, Torres VI, Gundelfinger ED, Ziv NE, Garner CC (2003) Unitary assembly of presynaptic active zones from Piccolo-Bassoon transport vesicles. *Neuron* 38(2):237-52.
- Shapiro ML, Eichenbaum H (1999) Hippocampus as a memory map: Synaptic plasticity and memory encoding by hippocampal neurons. *Hippocampus* 9:365-384.
- Shatz CJ (1996) Emergence of order in visual system development. *Proc Natl Acad Sci U S A* 93(2):602-8.
- Shatz CJ (1997-1998) Form from function in visual system development. *Harvey Lect.* 93:17-34.
- Silva-Gomez AB, Rojas D, Juarez I, Flores G (2003) Decreased dendritic spine density on prefrontal cortical and hippocampal pyramidal neurons in postweaning social isolation rats. *Brain Res.* 983(1-2):128-36.

Sin WC, Haas K, Ruthazer ES, Cline HT (2002) Dendrite growth increased by visual activity requires NMDA receptor and Rho GTPases. *Nature* 419(6906):475-80.

Skaggs WE, McNaughton BL (1996) Replay of neuronal firing sequences in rat hippocampus during sleep following spatial experience. *Science* 271(5257):1870-3.

Skeberdis VA, Chevaleyre V, Lau CG, Goldberg JH, Pettit DL, Suadicani SO, Lin Y, Bennett MV, Yuste R, Castillo PE, Zukin RS. (2006) Protein kinase A regulates calcium permeability of NMDA receptors. *Nat Neurosci.* 9(4):501-10.

Smith DM, Mizumori SJ (2006) Hippocampal place cells, context, and episodic memory. *Hippocampus* 2006;16(9):716-29.

Song S, Sjöström PJ, Reigl M, Nelson S, Chklovskii DB (2005) Highly nonrandom features of synaptic connectivity in local cortical circuits. *PLoS Biol.* 3:e68.

Sorra KE, Harris KM (2000) Overview on the structure, composition, function, development, and plasticity of hippocampal dendritic spines. *Hippocampus* 10(5):501-11.

Speese SD, Trotta N, Rodesch CK, Aravamudan B, Broadie K (2003) The ubiquitin proteasome system acutely regulates presynaptic protein turnover and synaptic efficacy. *Curr Biol.* 13(11):899-910.

Staubli U, Lynch G (1990) Stable depression of potentiated synaptic responses in the hippocampus with 1-5 Hz stimulation. *Brain Res.* 513(1):113-8.

Stettler DD, Yamahachi H, Li W, Denk W, Gilbert CD (2006). Axons and synaptic boutons are highly dynamic in adult visual cortex. *Neuron* 49, 1-11.

Stewart MG, Davies HA, Sandi C, Kraev IV, Rogachevsky VV, Peddie CJ, Rodriguez JJ, Cordero MI, Donohue HS, Gabbott PL, Popov VI (2005) Stress suppresses and learning induces plasticity in CA3 of rat hippocampus: a three-dimensional ultrastructural study of thorny excrescences and their postsynaptic densities. *Neuroscience* 131(1):43-54.

Stickgold R (2005) Sleep-dependent memory consolidation. *Nature* 437(7063):1272-8.

Stoppini L, Buchs PA, Müller D (1991) A simple method for organotypic cultures of nervous tissue. *J Neurosci Methods* 37:173-182.

Sutherland GR, McNaughton B (2000) Memory trace reactivation in hippocampal and neocortical neuronal ensembles. *Curr Opin Neurobiol.* 10(2):180-6.

Svoboda K, Yasuda R (2006) Principles of two-photon excitation microscopy and its applications to neuroscience. *Neuron* 50(6):823-39.

Tailby C, Wright LL, Metha AB, Calford MB (2005) Activity-dependent maintenance and growth of dendrites in adult cortex. *Proc Natl Acad Sci U S A* 102(12):4631-6.

Tang YP, Wang H, Feng R, Kyin M & Tsien JZ (2001) Differential effects of enrichment on learning and memory function in NR2B transgenic mice. *Neuropharmacology* 41: 779–790.

Tashiro A, Dunaevsky A, Blazeski R, Mason CA, Yuste R (2003) Bidirectional regulation of hippocampal mossy fiber filopodial motility by kainate receptors: a two-step model of synaptogenesis. *Neuron* 38(5):773-84.

Teng E, Squire LR (1999) Memory for places learned long ago is intact after hippocampal damage. *Nature* 400(6745):675-7.

Tessier-Lavigne M (1995) Eph receptor tyrosine kinases, axon repulsion, and the development of topographic maps. *Cell* 82(3):345-8.

Tom Dieck S, Sanmarti-Vila L, Langnaese K, Richter K, Kindler S, Soyke A, Wex H, Smalla KH, Kampf U, Franzer JT, Stumm M, Garner CC, Gundelfinger ED (1998) Bassoon, a novel zinc-finger CAG/glutamine-repeat protein selectively localized at the active zone of presynaptic nerve terminals. *J Cell Biol.* 142:499-509.

Toni N, Buchs PA, Nikonenko I, Bron CR, Muller D (1999) LTP promotes formation of multiple spine synapses between a single axon terminal and a dendrite. *Nature* 402(6760):421-5.

Toni N, Teng EM, Bushong EA, Aimone JB, Zhao C, Consiglio A, van Praag H, Martone ME, Ellisman MH, Gage FH (2007) Synapse formation on neurons born in the adult hippocampus. *Nat Neurosci.* 10(6):727-34.

Trachtenberg JT, Chen BE, Knott GW, Feng G, Sanes JR, Welker E, Svoboda K (2002) Long-term in vivo imaging of experience-dependent synaptic plasticity in adult cortex. *Nature* 420:788-794.

Turner DA, Deupree DL (1991) Functional elongation of CA1 hippocampal neurons with aging in Fischer 344 rats. *Neurobiol Aging* 12(3):201-10.

Van Praag H, Kempermann G, Gage FH (2000) Neural consequences of environmental enrichment. *Nat Rev Neurosci.* 1(3):191-8.

Vaughn JE (1989) Fine structure of synaptogenesis in the vertebrate central nervous system. *Synapse* 3(3):255-85.

Vazdarjanova A, Guzowski JF (2004) Differences in hippocampal neuronal population responses to modifications of an environmental context: evidence for distinct, yet complementary, functions of CA3 and CA1 ensembles. *J Neurosci.* 24(29):6489-96.

- Von der Ohe CG, Garner CC, Darian-Smith C, Heller HC (2007) Synaptic protein dynamics in hibernation. *J Neurosci.* 27(1):84-92.
- Washbourne P, Bennett JE, McAllister AK (2002) Rapid recruitment of NMDA receptor transport packets to nascent synapses. *Nat Neurosci.* 5(8):751-9.
- West AE, Griffith EC, Greenberg ME (2002) Regulation of transcription factors by neuronal activity. *Nat Rev Neurosci.* 3(12):921-31.
- Whitlock JR, Heynen AJ, Shuler MG, Bear MF (2006) Learning induces long-term potentiation in the hippocampus. *Science* 313(5790):1058-9.
- Wonders CP, Anderson SA (2006) The origin and specification of cortical interneurons. *Nat Rev Neurosci.* 7(9):687-96.
- Xia Z, Storm DR (2005) The role of calmodulin as a signal integrator for synaptic plasticity. *Nat Rev Neurosci.* 6(4):267-76.
- Xu HT, Pan F, Yang G, Gan WB (2007) Choice of cranial window type for in vivo imaging affects dendritic spine turnover in the cortex. *Nat Neurosci.* 10(5):549-51.
- Yang Y, Fischer QS, Zhang Y, Baumgartel K, Mansuy IM, Daw NW (2005) Reversible blockade of experience-dependent plasticity by calcineurin in mouse visual cortex. *Nat Neurosci.* 8(6):791-6.
- Yoshikawa S, McKinnon RD, Kokel M, Thomas JB (2003) Wnt-mediated axon guidance via the *Drosophila* Derailed receptor. *Nature* 422(6932):583-8.
- Yoshimura Y, Dantzker JL, Callaway EM (2005) Excitatory cortical neurons form fine-scale functional networks. *Nature* 433:868-873.
- Yu X, Malenka RC (2003) Beta-catenin is critical for dendritic morphogenesis. *Nat Neurosci.* 6(11):1169-77.
- Yuste R, Bonhoeffer T (2001) Morphological changes in dendritic spines associated with long-term synaptic plasticity. *Annu Rev Neurosci.* 24:1071-89.
- Yuste R, Bonhoeffer T (2004) Genesis of dendritic spines: insights from ultrastructural and imaging studies. *Nat Rev Neurosci.* 5(1):24-34.
- Yuste R (2005) Fluorescence microscopy today. *Nat. Meth.* 2, 902–904.
- Zhou Q, Homma KJ, Poo MM (2004) Shrinkage of dendritic spines associated with long-term depression of hippocampal synapses. *Neuron* 44:749-57.

Zola-Morgan SM & Squire LR (1990) The primate hippocampal formation: evidence for a time-limited role in memory storage. *Science* 250:288-290.

Zuo Y, Lin A, Chang P, Gan WB (2005) Development of long-term dendritic spine stability in diverse regions of cerebral cortex. *Neuron* 46:181-189.

CURRICULUM VITAE

Personal Informations

Particulars

<i>Name</i>	<i>Ivan Galimberti</i>
<i>Date of birth</i>	<i>16.01.1979</i>
<i>Nationality</i>	<i>Swiss</i>
<i>Origin</i>	<i>Ascona, TI</i>
<i>Address</i>	<i>Reinacherstrasse 10, 4053 Basel</i>
<i>Email</i>	<i>Ivan.galimberti@fmi.ch</i>
<i>Telephone</i>	<i>+41 (0)61 331 47 67 (home), +41 (0)76 390 04 79 (mobile)</i>

General Interests

Sport *Running, biking, hiking and skiing*

Reading *Different kinds*

Cooking *Italian and asiatic food*

Schools, degrees and scientific results

Education

- 2003-present** **PhD thesis with Prof. Dr. Pico Caroni**
Structural plasticity of synaptic connectivity in the adult CNS. FRIEDRICH MIESCHER INSTITUTE, BASEL
- 1998-2003** **Studies of Natural Science,**
EIDGENÖSSISCHE TECHNISCHE HOCHSCHULE (ETH), ZÜRICH
- 1994-1998** **Highschool**
LICEO COLLEGIO PAPIO, ASCONA

Diplomas

- 2003** **Diplom in natural science, Dipl.Natw.ETH**
EIDGENÖSSISCHE TECHNISCHE HOCHSCHULE (ETH), ZÜRICH
- 1998** **Swiss Federal Matura Typ D**
LICEO COLLEGIO PAPIO, ASCONA

References

University of Basel **Prof. Dr. Pico Caroni**
pico.caroni@fmi.ch, +41 (0)61 69 766 53

ETH **Prof. Dr. Yves Barral**
yves.barral@bc.biol.ethz.ch, +41 (0)44 632 06 78

Publications

- 2007** Gogolla, N.¹, **Galimberti, I.¹** and Caroni, P. (2007). Structural plasticity of axon terminals in the adult. **Current Opinion in Neurobiology** 17: 1-9
¹equal contribution
- 2006** **Galimberti, I.¹** Gogolla, N.¹, Alberi, S., Santos, A.F., Muller, D., Caroni, P. (2006). Long- term rearrangements of hippocampal mossy fiber terminal connectivity in the adult regulated by experience. **Neuron** 50 (5):749-763
¹equal contribution
- Gogolla, N.¹, **Galimberti, I.¹**, De Paola, V., Caroni, P. (2006). Preparation of organotypic hippocampal slice cultures for long-term live imaging. **Nature Protocols** 1: 1165 - 1171
¹equal contribution
- Gogolla, N.¹, **Galimberti, I.¹**, De Paola, V., Caroni, P. (2006). Long-term live imaging of neuronal circuits in organotypic slice cultures. **Nature Protocols** 1: 1223 - 1226
¹equal contribution
- Gogolla, N.¹, **Galimberti, I.¹**, De Paola, V., Caroni, P. (2006). Staining protocol for organotypic hippocampal slice cultures. **Nature Protocols** 1: 2452 – 2456
¹equal contribution

Scientific communications

Abstract

Galimberti I, Gogolla N and Caroni, P. (2006) Long-term rearrangements of hippocampal mossy fiber terminal connectivity regulated by synaptic activity.
FENS Forum, Vienna, Abstract, vol.3, A225.6

Poster Presentations

FENS Forum (2006), Vienna, Austria

Neuronal Circuit meeting, (2007), Ascona, Switzerland

Talks

Bench to Bedside Symposium, University of Basel 2005
Life long growth of hippocampal mossy fiber terminals regulated by synaptic activity

Bench to Bedside Symposium, University of Basel 2007
Subtypes of principal neurons with distinct connectivities in the hippocampus

Ich erkläre, dass ich die Dissertation, **Structural plasticity of synaptic connectivity in the adult central nervous system**, nur mit der darin angegebenen Hilfe verfasst und bei keiner anderen Fakultät eingereicht habe.